nanomanufacturing

MDPI

Review

Synthetic Approach to Rice Waste-Derived Carbon-Based Nanomaterials and Their Applications

Shamroza Mubarik [1,*], Nawal Qureshi [1], Zainab Sattar [1], Aqeela Shaheen [1], Ambreen Kalsoom [2], Marryam Imran [1] and Farzana Hanif [1]

[1] Department of Chemistry, Government Sadiq College Women University, Bahawalpur 63100, Pakistan; nawalqureshi00@gmail.com (N.Q.); zainabsattar200@gmail.com (Z.S.); aqeela@gscwu.edu.pk (A.S.); maryam.imranbwp@gmail.com (M.I.); farzanawajid67@gmail.com (F.H.)

[2] Department of Physics, Government Sadiq College Women University, Bahawalpur 63100, Pakistan; kalsoom.ambreen@gscwu.edu.pk

* Correspondence: shamroza.mubarik@gscwu.edu.pk

Abstract: The utilization of biomass waste to produce valuable products has extraordinary advantages as far as both the economy and climate are concerned, which have become particularly significant lately. The large-scale manufacturing of agricultural waste, mainly rice by-products (rice husk, rice straw, and rice bran), empowers them to be the most broadly examined biomasses as they contain lignin, cellulose, and hemicellulose. Rice waste was first used to incorporate bulk materials, while the manufacturing of versatile nanostructures from rice waste at low cost has been developed in recent years and attracts much consideration nowadays. Carbon-based nanomaterials including graphene, carbon nanotubes, carbon dots, fullerenes, and carbon nanofibers have tremendous potential in climate and energy-related applications. Various methods have been reported to synthesize high-value carbon nanomaterials, but the use of green technology for the synthesis of carbon nanomaterials is most common nowadays because of the abundant availability of the starting precursor, non-toxicity, low fabrication cost, ease of modification, and eco-friendly nature; therefore, reusing low-value biomass waste for the processing of renewable materials to fabricate high-value products is remarkable. Carbon nanomaterials derived from rice waste have broad applications in various disciplines owing to their distinctive physicochemical, electrical, optical, mechanical, thermal, and enhanced biocompatibility properties. The main objective of this review and basic criteria of selecting examples and explanations is to highlight the green routes for the synthesis of carbon nanomaterials—i.e., graphene, carbon nanotubes, and carbon dots—from rice biomass waste, and their extensive applications in biomedical research (bio-imaging), environmental (water remediation), and energy-related (electrodes for supercapacitors, Li-ion battery, fuel cells, and solar cells) applications. This review summarizes recent advancements, challenges, and trends for rice waste obtained from renewable resources for utilization in the fabrication of versatile carbon-based nanomaterials.

Keywords: rice waste; carbon based nanomaterials; synthesis

Citation: Mubarik, S.; Qureshi, N.; Sattar, Z.; Shaheen, A.; Kalsoom, A.; Imran, M.; Hanif, F. Synthetic Approach to Rice Waste-Derived Carbon-Based Nanomaterials and Their Applications. *Nanomanufacturing* **2021**, *1*, 109–159. https://doi.org/10.3390/nanomanufacturing1030010

Academic Editor: Andres Castellanos-Gomez

Received: 17 June 2021
Accepted: 27 August 2021
Published: 18 November 2021

1. Introduction

Over the last few decades, the rapid speed of urbanization and industrialization has caused genuine ecological issues, particularly water contamination [1]. Energy deficiency, restricted accessibility, and the excessive usage of non-renewable assets combined with the rapid decline of the regular habitat are serious issues faced universally [2]. The difficulties of a worldwide temperature alteration and ecological contamination have driven researchers to utilize eco-friendly, clean, renewable resources to fabricate novel useful materials [3]. Therefore, it is necessary to develop novel materials from renewable sources that meet our day-to-day needs and at the same time are eco-friendly [4]. Among a wide range of carbon sources, biomass and its subordinates have pulled in broad consideration because of its abundant availability, low cost, and renewability [5]. Biomass is a natural material

derived from renewable sources of energy i.e., agricultural residues and by-products of forests. The overall production of biomass is assessed as approximately 150–200 billion metric tons a year [4].The conversion of biomass to fabricate novel nanomaterials for different applications is a favorable idea of 'waste to wealth' in the cutting-edge universe of nanotechnology [6]. Biomass waste utilization gives a solution to environmental problems and helps in lessening the negative effect of the wastes on the climate. The conversion of biomass waste to highly valued materials has incredible advantages regarding both economy and climate, which has acquired significant consideration in recent years [7]. Due to the increasing demand for carbon nanomaterials, scientists have put forth incredible attempts in the production of CNMs from biomass with great properties, for example, high electrical and thermal conductivities and great chemical stabilities [8]. Waste materials from domestic wastes to industrial residues cause adverse impacts on climate and human well-being [9]. Waste materials harm the environment; therefore these materials are frequently employed for the production of advanced materials at low cost using convenient green technologies that minimize harmful polluting substances during the synthesis of nanomaterials [10]. As for this part of defilement, we propose a basic methodology for transforming various biomass waste into the highly valued carbon nanomaterials [6]. Waste material with high carbon content can be recycled to get high valued materials at low cost [9]. Reusing low-valued natural waste materials to fabricate value-added products is remarkable, which has motivated analysts over the last 20 years [11]. Biomass is a nontoxic, feasible, and sustainable carbon-rich material essentially made up of hemicellulose, cellulose, and lignin, which has been broadly utilized as feedstock for the preparation of different highly valued carbon, for example, graphene, fullerene, carbon nano-fullerenes, and CNTs [8]. Various synthesis strategies have been employed for the production of carbon-based nanomaterials from biomass waste, but green synthesis strategies with either energy-saving responses or low-value waste materials are acquiring more attention [11].

Agriculture waste-derived carbon nanomaterials (CNMs) are a class of engineered nanomaterials (ENMs) having broad applications in various disciplines due to their extraordinary optical, electrical, mechanical, and thermal properties [12]. Moreover, around 7.6 billion tons of industrial wastes have been discovered to be produced or discarded each year. The most common agricultural biomass sources are sugarcane bagasse, corn straw, wheat stem, and rice residues. The rice industry produces a large amount of rice by-products that include rice husk (RH), rice bran rice straw (RS), rice husk ash (RHA), and broken rice [13]. Diverse assortments of paddy rice are made out of generally, 69% starchy endosperm, 20% rice husk or rice hull, and 11% grain/bran layers. Around 18–20% of the RH upon burning is changed to rice husk ash (RHA). In 2012, the yearly worldwide amount of rice husk and rice straw produced was 137 metric tons and 685 MT [14]. Rice by-products considered as agricultural waste are utilized as a precursor for the fabrication of highly valued nanomaterials; rice husk consists of 65–75% organic substances (i.e., cellulose, hemicellulose, and lignin), and 15–20% inorganic substances such as silica SiO_2. Therefore, the conversion of rice husk into various carbon and silica nanomaterials is of great significance. [15]. In the previous few decades, perhaps the most widely recognized and broadly considered biomass was rice husk. This is a result of the huge modeling of greater than 160 million tons of rice husk every year, and the majority of them were scorched or bagged in landfills, i.e., wasted [16]. Moreover, rice husk biomass consists of a 3D network of natural carbon (C) and silica (SiO_2), hence they could be utilized for manufacturing flexible carbon-based and silicon-based materials for different applications. At the beginning phase, rice husk biomass was straightforwardly put in for horticulture uses (litters, soil change, fertilizer, etc.) [17], the construction industry (composite materials and development materials), and conventional energy production (power and heat generation) [14]. Versatile chemical products were obtained from rice husk biomass, including dynamic silica, carbon, biofuel, and syngas due to its unique chemical composition and structure. These items have been applied in different fields including energy production and adsorption. With the increasing development of nanoscience and nanotechnology, enormous carbon-based

and silicon-based nanostructures (NSs) have been created from rice husks. By exploiting the interesting design and substance organization of rice husk biomass, an assortment of advanced practical nanostructures have been manufactured and designed. These rice husk-derived nanostructures are profoundly successful for energy-related (solar cell, Li-ion battery, triboelectric nano-generator, and supercapacitor electrode) applications; therefore, the rice husk-derived nanostructures (RH-NSs) have acquired much attention nowadays. To date, different strategies have been created to controllably synthesize and design practical nanostructures from rice husk biomass to fabricate silicon-based, carbon-based, and hybrid nanostructures (consisting of both silicon and carbon) according to their original compositions. As rice husk contains an organic component, i.e., lignin, hemicellulose, and cellulose [18], therefore, rice husks can be used as a natural, renewable, and abundant source for manufacturing promising carbon nanomaterials: namely, graphene, carbon dots, and carbon nanotubes [7]. Table 1 illustrates the various biomass sources used for the preparation of carbon nanomaterials—their synthesis method and applications.

Table 1. Carbon-based nanomaterials prepared from various biomass sources, their synthesis methods, and applications. In the future, continuous efforts for the production of carbon nanomaterials from biomass is of significant importance. This review discusses the synthesis of versatile carbon-based nanomaterials from rice residue i.e., rice husk and rice straw, and their promising application in various disciplines.

Biomass Waste	Synthesis Method	Carbon Nanostructure	Application	References
Hemp	Hydrothermal/ activation with KOH	Interconnected graphene carbon nanosheets	Supercapacitor	[19]
Rice husk	Combustion/chemical activation with KOH	Graphene sheets	Additives in polymer composites, electrochemical performance	[20–22]
Biochar from Wheat straw	Microwave CVD	MWCNTs	-	[23]
Sugarcane Bagasse	Microwave CVD	Graphitic flakes and MWCNTs	-	[24]
Rice husk	Microwave CVD	Thin graphene (2–6 layers) MWCNTs	-	[25]
Wood sawdust	Conventional Pyrolysis	CNTs	-	[26]
Rice straw	Conventional CVD	CNTs	-	[27]
Rice residue	Hydrothermal	C-dots	Fe^{3+} ions and tetracycline detection	[28]
Wheat straw	Hydrothermal	C-dots	Labeling, imaging, and sensing	[29]
Sugarcane bagasse char	Hydrothermal	C-dots	drug delivery	[30]
Rice husk	Pyrolysis	C-dots	Bio-imaging	[31]
Rice husk	Hydrothermal, Pyrolysis	GQDs	Fluorescent sensor	[31]
Rice grains	Pyrolysis	GQDs	-	[32,33]
Rice husk	KOH activation	Graphene oxide	Desalination membrane	[34,35]
Rice Straw	Microwave-assisted	Graphene oxide	Ni(II) Adsorption	[36]
Rice husk	Pyrolysis	Graphene oxide	-	[37]

2. Carbon-Based Nanomaterials

Carbon is the most flexible element in the periodic table [38] due to the huge number of bonds of distinctive type and strength that bond with itself or with numerous other elements [39]. Carbon naturally exists in two crystalline allotropic forms, diamond and graphite [40], and several low-dimensional allotropes of carbon derived from synthetic processes are graphene, carbon nanotubes, fullerenes [4]. Various nanomaterials have been discovered, but carbon-based nanomaterials especially have prime importance in nanotechnology [41]. With the discovery of various carbon-based nanostructures i.e., fullerenes

in 1985, carbon nanotubes in 1991, and graphene in 2004, carbon-based nanomaterials have gained much attention in nanotechnology [39]. Carbon nanostructures are being classified into 3D graphite, 2D graphene, 1D carbon nanotubes, and 0D fullerenes, but the major element carbon is the backbone of these structures [42,43]. Among these, graphene, fullerenes, carbon nanotubes, and carbon nanofibers are the dazzling stars and have the most promising applications in nanotechnology [44]. Figure 1 displays various forms of carbon allotropes.

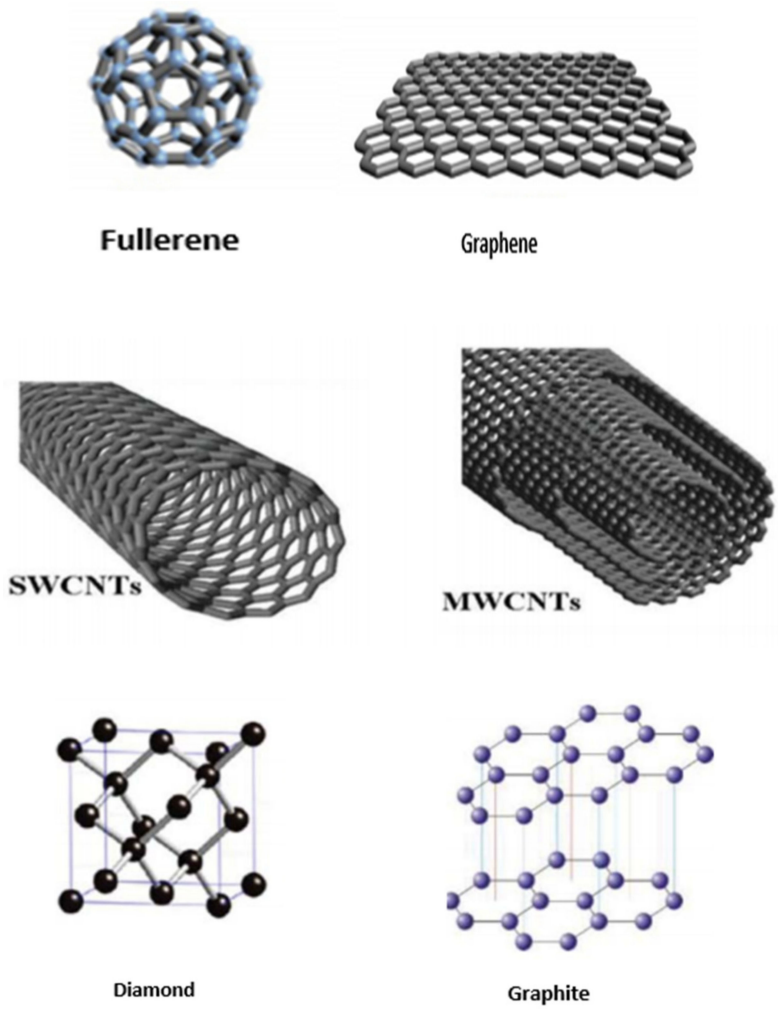

Figure 1. Representation of various allotropes of carbon: fullerene, graphene. Reprinted from Ref. [39]. Carbon nanotube (SWCNTs and MWCNTs), diamond, and graphite. Reprinted with permission from Ref. [45]. Copyright 2016 Taylor & Francis.

Due to their multifunctional nature, carbon-based nanomaterials are highly attractive biomaterials. Moreover, the incorporation of carbon-based nanomaterials into existing biomaterials enhances their functions. Therefore, carbon-based nanostructures have been found in different fields of biomedical research i.e., bio-imaging, tissue scaffold reinforcements, drug delivery, wastewater treatment, catalyst support, control air pollution, energy conversion, cellular sensors, hydrogen, and energy storage [46]. Table 2 illustrates the properties of natural and synthetically derived carbon-based nanomaterials.

Table 2. Properties of different carbon-based nanomaterials. Adapted from Refs. [39,47,48].

Carbon Material	Graphite	Graphene	Carbon Nanotube		Fullerene
			SWCNTs	MWCNTs	
Dimensions	3	2	1	1	0
Hardness	high	highest	high	high	high
Hybridization	sp^2	sp^2	sp^2	sp^2	sp^2
Tenacity	Flexible, non-elastic	Flexible, elastic	Elastic	Elastic	Elastic
Young modulus		856.4 ± 0.7(z) 964.0 ± 0.68(a)	1000	1000	
Thermal conductivity (Wm^{-1} K^{-1})	Anisotropic, 1500–2000, 5–10	4840–5300	3500–6600	600–6000	0.4
Electrical conductivity	−4000 p, 3.3 c	−2000	10^6–10^7	10^3–10^5	10^{-5}

Biomass waste-derived carbon nanomaterials, in comparison to those synthesized from other precursors, serve as a source of carbon, as a catalyst, or catalyst support for the fabrication of CNMs and possess superior qualities to the traditional carbon nanomaterials, for example, carbon content (graphitic degree), length, structure, and diameter [49]. Owing to their physicochemical properties i.e., great chemical stability, increased electrical conductance, manageable porosity, increased specific area, and impenetrable electroactive sites, these promising nanomaterials have acquired a lot of interest [4]. Biomass-derived carbon nanomaterials have more promising applications because they are eco-friendly, cost-effective, and possess distinctive properties including large surface for the functionalization of various functional groups and minerals [8]. Various methods are employed to synthesize carbon nanomaterials derived from biomass such as the physical activation method, chemical activation, and hydrothermal carbonization [50,51]. Rice husk is a natural and abundant source utilized for manufacturing promising carbon nanomaterials, e.g., carbon dots, graphene, carbon nanotubes, graphene quantum dots, and carbon quantum dots [7].

3. Graphene

Graphene is a hexagonal lattice structure comprising of a two-dimensional, one-atom thick carbon sheet. The sp^2 hybridized carbon atoms are packed in the form of a dense honeycomb network that acts as a building unit for several nanocarbons. When stacked, it forms a three-dimensional graphite; and when rolled or wrapped, it produces one-dimensional nanotubes and zero-dimensional fullerenes respectively [52].

Single-layer graphene was initially isolated in 2004 through a technique called micromechanical cleavage. Since then, the material has been in the limelight owing to its remarkable properties such as chemical inertness, quantum Hall effect, super hydrophobicity, ambipolar field effect, high carrier mobility, etc. [53]. Such unique characteristics opened doors for a lot of interesting physics and suggested the possible implementation of graphene in lots of advanced devices [52]. Despite the physicists' huge interest and successful experimentation of graphene, still, there is huge room for further experimentation and the widespread implementation of graphene. The fabrication of graphene is the cheapest compared to all other nanomaterials, and this explains its extended experimentation and widespread applications [54]. Graphene exists in various forms that fall into two major categories: that is, functionalized and non-functionalized graphene. The functionalized forms include graphene oxide (GO) and reduced graphene oxide, while the non-functionalized ones are pristine graphene, single-layer graphene, and graphene sheets, as shown in Figure 2. The next subsection discusses the synthesis of graphene from rice husk [55].

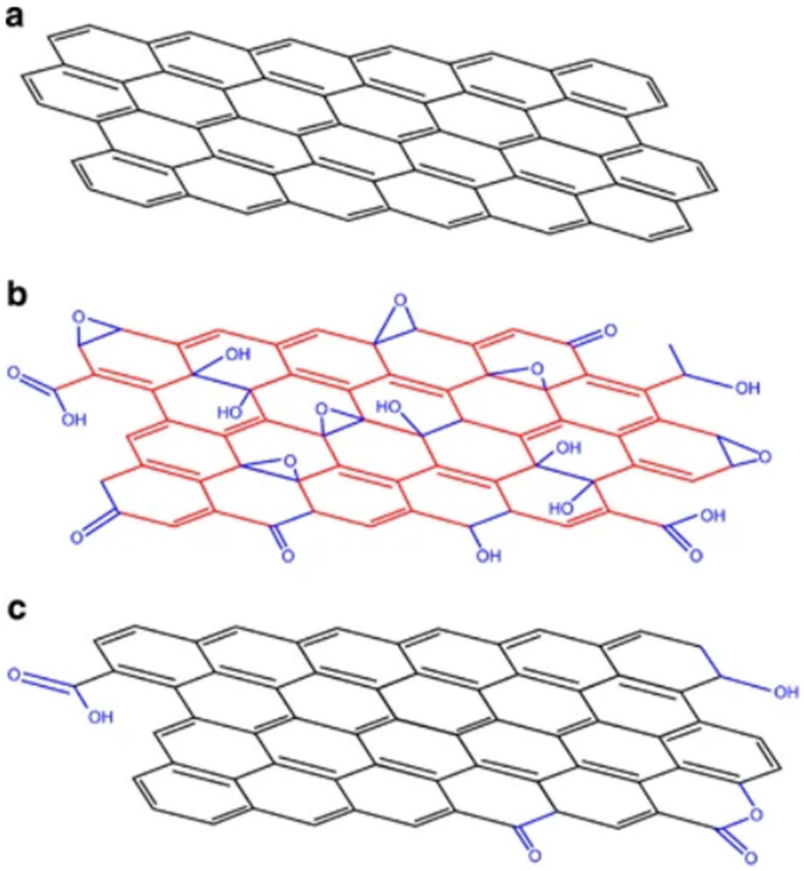

Figure 2. Structural modes of graphene: (**a**) single-layer graphene; (**b**) graphene oxide (GO); (**c**) reduced graphene oxide. Reprinted from Ref. [56].

3.1. Synthesis of RH-Derived Graphene

Annually, about 120 million tons of rice husks are being produced worldwide [57]. The majority of the rice-producing countries either burn or dump this material because of its difficult disposal and low commercial value [58]. This adversely affects the environment and ultimately human health [59]. That is why it must be utilized at its best. Due to its good composition and high availability, it has potential to be utilized as a precursor for the production of valuable nanomaterials such as carbon nanotubes, silica, porous carbon, and graphene [60]. Rice husk (RH), rice husk ash (RHA), and rice straw (RS) can be transformed to value-added graphene. The section below summarizes methods to synthesize graphene or graphene oxide (GO) from rice waste.

3.1.1. Chemical Activation

A common method of chemical activation involves treating carbonaceous substances with chemical activating agents such as $ZnCl_2$, KOH, H_2SO_4, etc. Then, the resulting material is carbonized at 400–900 °C. The procedure produces carbons with a large number of pores and a high specific surface area [61]. Graphene is produced by rice wastes using a variety of chemical activating agents. However, potassium hydroxide (KOH) is the most frequently employed chemical agent in producing carbon nanomaterials as it induces and enhances the porosity of the resulting CNMs [62]. Activation with KOH provides a continuous 3D network resulting in high volumetric capacitance [63]. It also enhances the purity and integrity of the graphene nanomaterial by efficient etching of impurities such as silica and disordered carbon [64].

Muramatsu et al. [20] proposed a novel approach toward the synthesis of corrugated graphene and crystalline graphene by the activation of rice husk with KOH, and basic calcination was performed at a temperature of 850 °C. Monolayer and bi-layer graphene

sheets with high crystallinity, nano-sized domains, and clean and active edges were synthesized. The nano-structured crystalline graphene comprises of a single layer or multilayer of graphene with clear and stable edges, while the corrugated graphene was a few nanometers having 200 to 300 carbon atoms, clear boundaries, and non-hexagonal carbon rings (pentagons and heptagons). XRD and Raman spectroscopy were the characterization techniques. This method proved that graphene can be produced at a low temperature and without the use of catalysts. In addition to KOH, Muramatsu et al. [20] used carbon black as a protective barrier against oxidation. However, later, Singh el al. [65] removed carbon black by updating the synthesis process and replacing carbon black with rice husk itself.

They produced graphene by a two-step process; firstly, the chemical activation of rice husk with KOH, and secondly, annealing it at 900 °C. Figure 3 illustrates the overall procedure of the synthesis. The TEM images revealed a few-layered graphene with the agglomeration of silica particles.

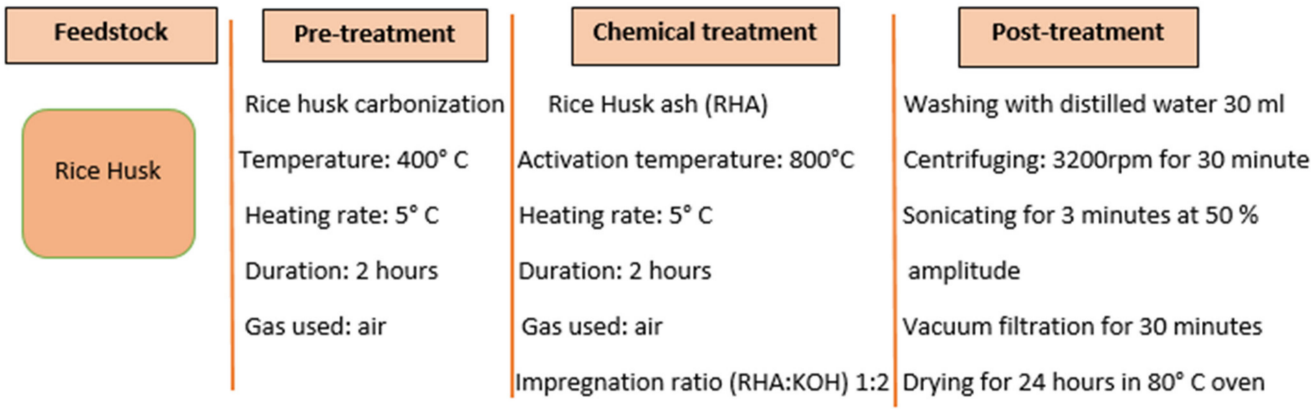

Figure 3. Flow chart of synthesis of graphene derived from rice husk. Reprinted from Ref. [60].

Uda et al. [66] also employed the same procedure for synthesizing graphene from rice straw ash (RSA) by the use of KOH with an impregnation ratio of 1:2.5 at 700 °C. FESEM (Field Emission Scanning Electron Microscopy), SEM (Scanning Electron Microscopy), EDX (Energy-Dispersive X-ray), AFM (Atomic Force Microscopy), and FETEM (Field Emission Transmission Electron Microscopy) were used for the characterization of graphene.

Othman et al. [67], prepared porous graphene by treating rice husk ashes at different stabilization temperatures. Rice husk was converted to solid residues called rice husk ash (RHA) at varying stabilization temperatures (100 °C, 200 °C, 300 °C, and 400 °C). The samples were denoted as GRHA100, GRHA200, GRHA300, and GRHA400 with respect to the pre-treatment temperature of each. Chemical activation using KOH at a 1:5 impregnation ratio yielded rice husk ashes-derived graphene (GRHA). The characterization was done using TEM, XRD, and Raman spectroscopy. A shematic illustration of the activation process of GRHA is shown in Figure 4. The stabilization temperature showed a major influence on the porosity of the as-synthesized GRHA. Increasing the temperature increased the number of volatiles released, with the formation of more micropores and resulting in enhanced BET-specific surface area and total pore volume (TPV) of GRHA. However, increasing the temperature increases surface properties but only to a limit; i.e., above the optimum temperature, a reduction of surface area occurs. The results clearly showed that GRHA obtained at a temperature of 200 °C exhibited the highest specific surface area; hence, 200 °C was considered the optimum stabilization temperature for GRHA.

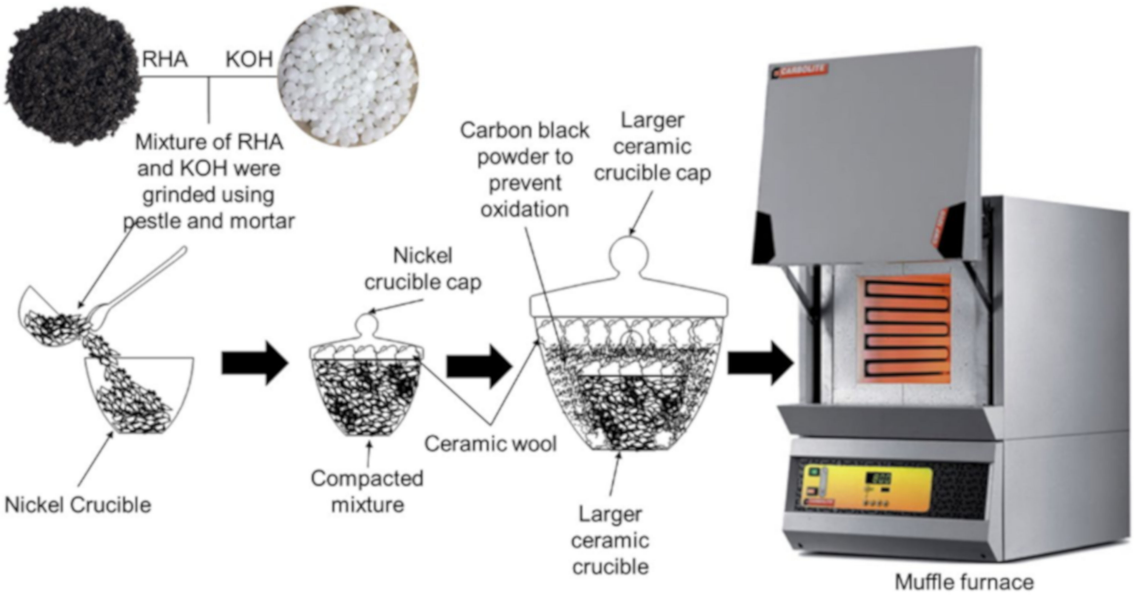

Figure 4. Schematic activation treatment process of GRHA. Reprinted with permission from Ref. [68]. Copyright 2020 Springer Nature.

Seitzhanova et al. [35] demonstrated the synthesis of graphene oxide by a four-step process: preliminary carbonization of rice husk reported in [21], desilication of carbonized rice husk (CRH) using NaOH, activation with KOH (carbon to KOH ratio: 1:4 and 1:5), activating it in air at 850 °C for 2 h, and finally, the exfoliation of the product by washing it with water until it becomes neutral (pH ≈ 7) and further drying at 105 °C. The resulted graphene layers had high carbon content and were also rich in inorganic matter. To remove this inorganic matter, the product was functionalized using H_2SO_4 at a controlled temperature followed by continuous stirring for 1 h or 24 h, centrifuging the mixture, washing until neutral pH, and then filtering it with PVDF membrane. The multilayer graphene produced was characterized using FTIR (Fourier transform infrared spectroscopy), Raman spectroscopy, SEM, thermogravimetric analysis (TGA), TEM, and elemental analysis.

Azizovna et al. [34] also performed the synthesis of graphene oxide (GO) using rice husk via KOH activation followed by alkaline desilication as reported earlier by Seitzhanova et al. [35]. GO was characterized using electron microscopy and Raman spectroscopy. Then, the prepared GO was used to develop a desalination membrane, which was capable of filtering out organic molecules, common salts, and small particles.

3.1.2. Microwave-Assisted Method

The science of microwave chemistry deals with the application of microwave radiations to chemical reactions [69]. The microwave-assisted method is used extensively for the direct carbonization of organic materials into valuable products under microwave radiation. Figure 5 displays a comparison between conventional heating and microwave heating methods. Microwave assisted strategy is a cheap method for synthesizing carbon-based nanomaterials including graphene, carbon dots, activated carbon [70].

Kumar et al. [71] developed a microwave furnace method to prepare graphene from rice husk. Rice husks were washed using distilled water with the aid of ultrasonication for 1 h and then dried in natural air for a day. Dried rice husk is ground into powder by means of a mechanical process using ferrocene Fe $(C_5H_5)_2$ as a catalyst. Ethanol is mixed with ferrocene with a magnetic stirrer at three distinct levels. Every 150 mL of ethanol is mixed with 20, 30, or 40 gm of ferrocene in three stages. The three resulting mixtures of ethanol and ferrocene (150 mL-20 gm, 150 mL-30 gm, 150 mL-40 gm) were mixed with rice husk powder at three different levels (50, 60, and 70 g). Then, the three mixtures were heated in a microwave furnace at three different temperatures (650 °C,

700 °C, 750 °C). The material was studied using XRD (X-ray diffraction), FESEM, FTIR, UV-Vis spectroscopy, Zeta Sizer, and EDX. Figure 6 clearly demonstrates the schematic mechanism of the microwave synthesis of graphene. Parametric investigation clearly showed that the effect of temperature for the suggested model was a more important factor than the other two variables. A Taguchi L9 array was used to determine the optimum combination of input variables that affect the crystalline size of graphene particles as an output variable. For obtaining minimum particle size, the suggested variable setting was rice husk 60 gm, ferrocene 30 gm, and 750 °C temperature.

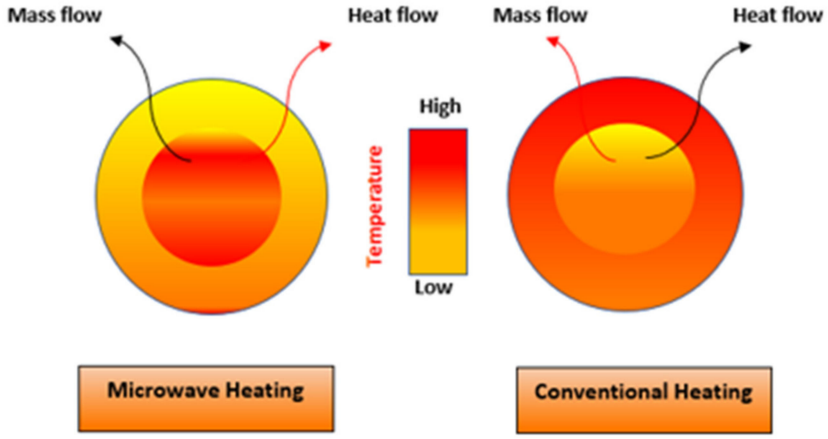

Figure 5. Schematic of microwave and conventional heating methods. Reprinted with permission from Ref. [71]. Copyright 2021 Elsevier.

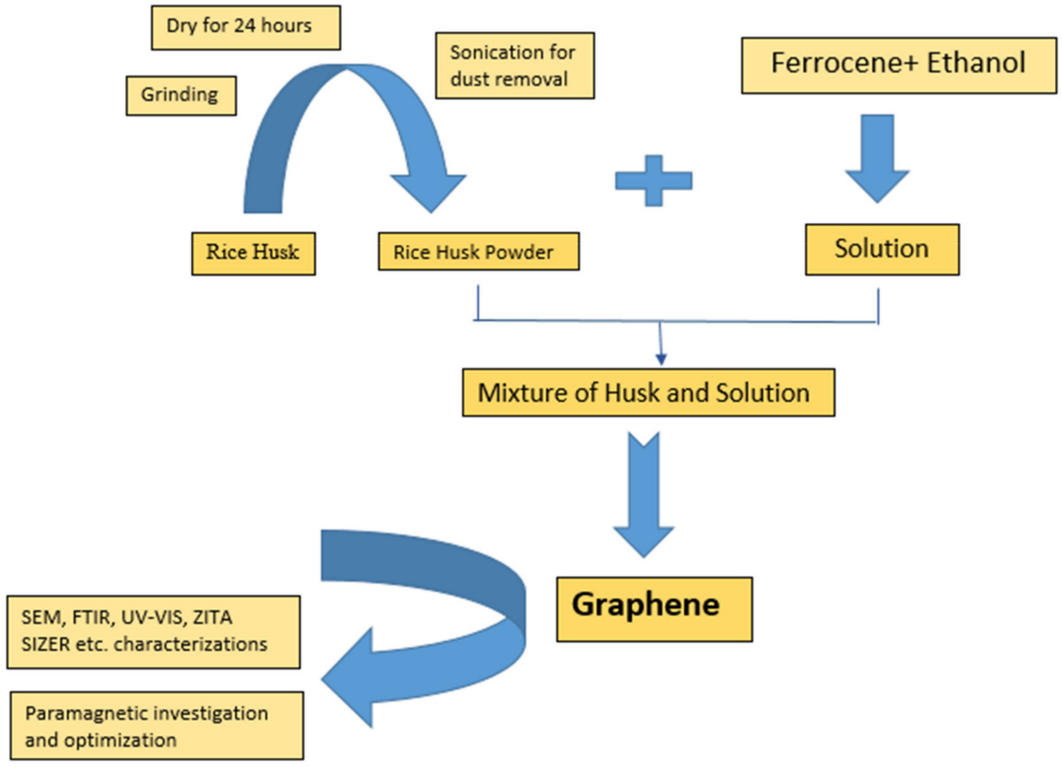

Figure 6. Schematic diagram of all steps included in the synthesis of graphene from rice husk by a simple microwave process. Reprinted from Ref. [60].

In another study, rice bran was used as a carbon source for graphene production. Rice bran comprises of fats, proteins, ash, and minerals and acts as a carbon source for

synthesizing GO. Hashmi et al. [72] reported the effective production of GO from agro waste at optimum conditions and relatively low temperature, in both individual and tri composite form (sugarcane bagasse, rice bran, and orange peel). The powdered rice bran, a carbonaceous precursor, along with ferrocene were placed at a temperature of 300 °C in a muffle kiln for 15 min, resulting in black-colored solid products that are kept for half an hour at room temperature. Then, the material was studied by SEM, HR-TEM (High-Resolution-Transmission Electron Microscopy), XRD, FTIR, TGA, and DTA (Differential Thermal Analysis) analysis techniques. This simple, rapid, single step, and green strategy for producing graphene oxide has showed that different kinds of solid carbonaceous agricultural wastes, without any sanitization as feedstock, can be used to produce value-added and high-quality GO.

The same strategy was adopted by Tohamy et al. [36], who synthesized GO by the oxidation of rice straw (RS), sugarcane bagasse (SCB), lignin (L), and mature beech pinewood sawdust (MW) individually, using ferrocene as a catalyst in a muffled atmosphere. Characterization was done using FTIR, TEM, SEM, EDS (Energy-Dispersive Spectroscopy) and Raman spectroscopy. Then, the rice straw-derived GO was applied in designing an adsorption method for wastewater treatment. RS-derived GO proved to be an efficient and cheap adsorbent for eliminating Ni (II) from contaminated water.

3.1.3. Pyrolysis

Pyrolysis is termed as the thermal decomposition of organic compounds at high temperature in either vacuum or inert atmosphere [70]; it brings about a change in chemical composition. Extreme pyrolysis, which mostly leaves carbon as a residue, is called carbonization [73]. Biomass pyrolysis is a very effective approach for the production of a broad range of value-added products. It involves heating, dehydration, degradation, and finally carbonization of the organic substance present in the biomass precursor. Figure 7 displays the basic pyrolysis procedure towards the synthesis of graphene using biomass waste.

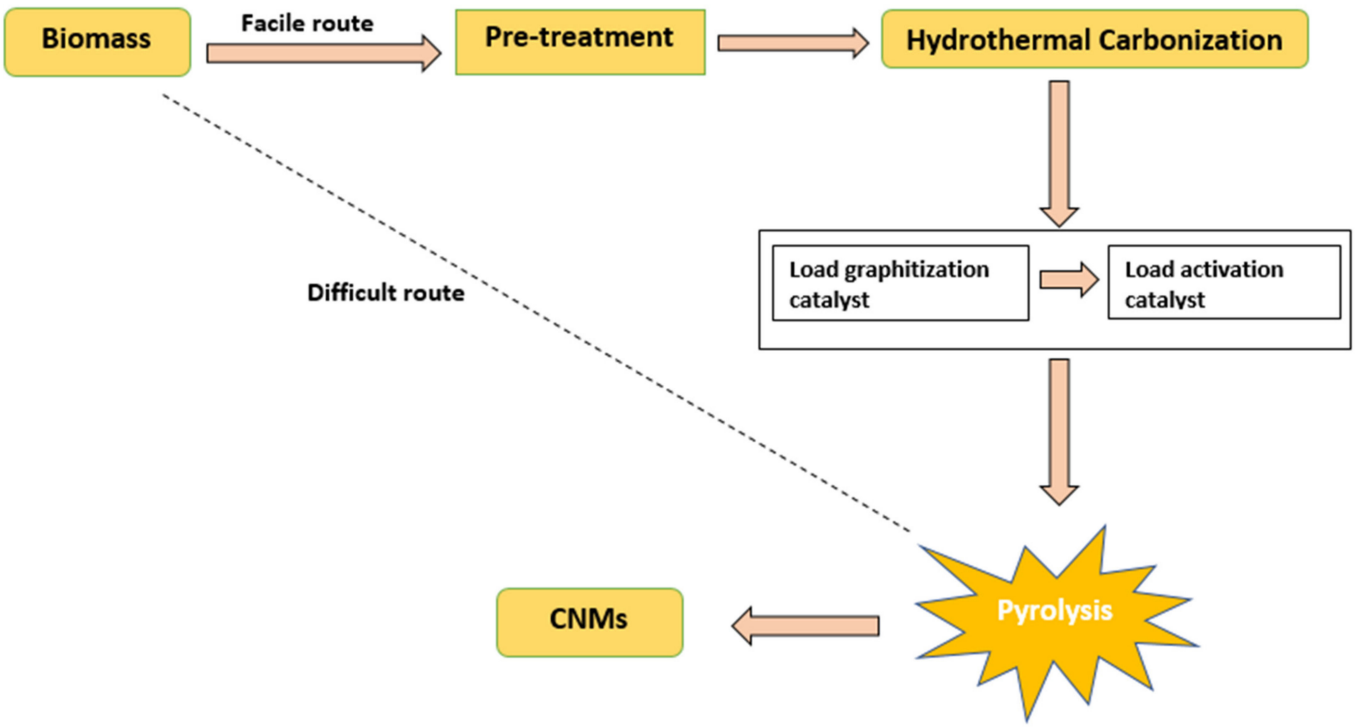

Figure 7. Synthesis of CNMs from biomass pyrolysis. Reprinted with permission from Ref. [8]. Copyright 2018 Royal Society of Chemistry.

Any carbonaceous waste material can be transformed to graphene oxide by optimizing the thermal heating conditions, bypassing the use of graphite and other harmful chemicals. Naik et al. [37] demonstrated the pyrolytic synthesis of graphene oxide from a non-graphitic carbonaceous source without the use of inert atmosphere. The agro waste materials including sugarcane bagasse, rice husk, and waste newspaper were chosen as a precursor of the production of graphene oxide nano-flakes. The precursors were subjected to pyrolysis (at optimum temperature) in the presence of a trace amount of air, leading to the decomposition of cellulosic structures (breakage of glycosidic bonds) to monomeric glucose as represented in Figure 8. This resulted in the aromatization and condensation of the monomeric glucose, in addition to oxidation simultaneously. Results indicated brown-blackish powders/flake-like structures of GO which were grounded, washed, and dried in an oven for a day. The nano-flakes were graphitic in nature. Graphene oxide nano-flakes were characterized using XRD, EDS, FESEM, TEM, and HR-TEM.

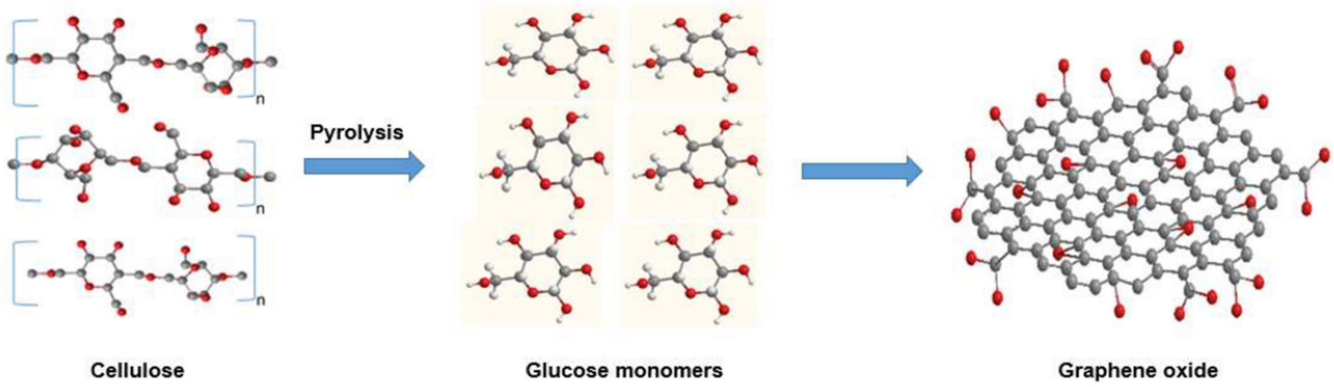

Figure 8. Mechanism for the formation of graphene oxide. Reprinted with permission from Ref. [37]. Copyright 2020 John Wiley and Sons.

3.2. Applications of RH-Derived Graphene

3.2.1. Desalination Membranes

Approximately 1.2 billion people worldwide are facing potable water shortage and its harmful effects on human health, energy, and food [74]. The development of novel water treatment methods must be done at low cost, with less energy and via an environment-friendly process. Desalination is considered as one of the most appropriate strategies for freshwater augmentation, as 97.5% of all water on the Earth is present in seas. Hence, seawater desalination provides a steady and infinite supply of high-quality water. It can enhance water availability more than what is available from the hydrological cycle [75]. Membranes for water desalination and purification are widely used to access worldwide challenges of environment contamination and the scarcity of aqueous bodies [76]. Highly permeable and highly selective next-generation membranes have been developed to limit the drawbacks of present-day membrane technologies. The use of biomass-derived nanomaterials in the seawater desalination is being employed frequently owing to the efficiency, low cost, and green process. Graphene can be used in membranes in any of its forms including pristine graphene, graphene oxide (GO), and reduced graphene oxide. Membrane-based desalination processes can be classified on the basis of pore size of membrane and rejection mechanism: reverse osmosis (RO), electrodialysis (ED), nanofiltration (NF), ultrafiltration (UF), and membrane distillation (MD) [77]. Seawater desalination is mainly done via reverse osmosis (RO) technology [78], which is a conventional pressure-driven membrane process that has proven useful due to its potent salt rejection and suitable energy requirements [79]. In reverse osmosis, water is filtered via a partially permeable membrane by applying an extrinsic positive hydraulic pressure that acts as a driving source. A large amount of water is passed through the membrane in comparison to the volume of organic molecules or dissolved salts. The core of RO is the semi-permeable membrane, which is a

selective barrier that separates pure water from seawater [80]. However, RO technology is limited due to the high capital cost and low desalination capacity [81]. Recently, forward osmosis (FO) has gained the attention of researchers. It is an emerging method involving the separation of effluents by an osmotic pressure [82]. Regarding water desalination, graphene is one atom thick, maximizing its permeability, and it has been proven to be cost effective. It removes the water contaminants using the nanoscale pores. In addition, its potential for size-selective transport and excellent mechanical stability makes it a perfect option for desalination membranes [83]. RH-graphenated membranes are generally meant for FO, RO, and NF [84].

These membranes have major advantages as compared to traditional membranes. First, the raw material, which is rice waste, is inexpensive, making the fabrication process quite cheap. Second, the production of graphene membranes, such as designing GO nanosheets-based GO membranes, is a facile and extensible process. In addition, modification of the charge-based selectivity of membranes can be achieved by the functionalization of graphene oxide with several functional groups [56]. Nanotechnology, when combined with a polymeric RO membrane, surprisingly opens up new pathways for wastewater treatment. For the development of desalination membranes, graphene oxide can be incorporated into freestanding membranes, which use GO as a separating layer directly through incorporated casted membranes where GO is impregnated into a polymer matrix or on the surface of membranes that utilize GO for surface modification [77].

Cohen-Tanugi and Grossman et al. [85] studied the salt rejection capability of nanosized graphene as a reverse osmosis (RO) membrane. This study was further validated by Wang and Karnik et al. [86], who showed that GO has the potential to increase the separation performance of the membranes [87]. Separation depends on the shape, charge, and size of particles. For achieving an ideal filtration efficiency, a membrane must be as selective as possible, as thin as possible for high water permeation, and as mechanically tough as possible for inhibiting membrane decay [56]. Nicolai et al. [80] employed an MD simulation strategy for membrane development and illustrated that it is possible for freestanding GO membranes to exhibit 100% efficiency for salt rejection in the RO process. Fathizadeh et al. [88] modified polyamide membranes with nitrogen-modified graphene oxide (N-GOQD) for preparing a novel reverse osmosis film that exhibited excellent salt rejection of 93%. Azizovna et al. developed a graphene oxide-based membrane, which consists of a thin GO layer on the hydrophilic polyvinylidene fluoride (PVDF) membrane, for desalination. The membrane has pore sizes ranging between 8 and 50 nm and is capable of filtering common salts, organic molecules, and small particles.

3.2.2. Removal of Ni (II)

Water contamination by natural organic matter or the leakage of heavy metals is a global issue that must be addressed [89]. Impure water causes liver sicknesses, nasal ulceration, cancer, and dermatitis [90]. A variety of techniques have been formulated for the purification of water including electro-coagulation, ion exchange, cementation, distillation, precipitation, adsorption, and reverse osmosis [91]. Out of all these purifying strategies, adsorption is frequently employed, as it is cost-effective and has high adsorption potential for metal ions. Adsorbents such as zeolites, diatomite, ceramics, and ferric hydroxide in granular form have been used [92]. However, these adsorbents have a number of limitations, including high cost, self-contamination, high power requirements, and a reduced removal of metal ions [93,94]. Carbon nano-sorbents, namely, graphene, carbon nanotubes, graphene oxide, and carbon dots have been used extensively in the purification of water due to their large surface area [95]. Among these, GO has emerged as a promising absorbent candidate and is widely applicable. It versatile applicability is because of its structure; it possesses reactive oxygen containing functional groups including carbonyl (–C=O), phenol, and carboxyl (–COOH) groups at the edges of the sheet, while epoxy (C–O–C) and hydroxyl (–OH) groups are on the basal plane, thereby imparting hydrophilic properties to graphene oxide. Graphene oxide exhibits excellent water dispersion and

versatile surface modification [96]. Tohamy et al. [36] demonstrated a facile adsorption method for the effective removal of nickel (II) ion by using rice straw-derived GO, sugarcane bagasse-derived GO, mature beech pinewood sawdust-derived GO, and lipid-derived GO. The results proved the ability of GO from agro residues to be a cheap adsorbent for the removal of Ni (II) ions from wastewater. The adsorption of nickel ion on the GO surface depends on the initial concentration of Ni (II), contact time, and temperature. It was observed that the adsorption and removal of Ni (II) by rice straw decreases with temperature increase. This observation suggested that the interaction between rice straw and metal ions is exothermic in nature [97]. This can be justified by the thickness of the boundary layer, which is reduced at elevated temperature. High temperature causes an increase in nickel's tendency to leave the surface of GO into the solution, as they are linked through weak adsorption interactions, i.e., physical adsorption. Increasing the initial concentration of Ni(II) decreases the percentage of Ni(II) removed. This depends on the number of exchangeable sites in graphene oxide and also the ratio of Ni (II) to GO. As the ratio of Ni(II) to GO increases, the active exchangeable sites on GO become saturated, lacking enough surface area for accommodating excess Ni(II) in the solution and resulting in the reduction in nickel ion removal [98]. The effect of contact time was evaluated at different times: 15, 30, 45, 60, 75, and 90 min. The adsorption of Ni(II) by RS-GO was observed to be rapid at the beginning due to the availability of a large number of active sites [99]. The rate of removal becomes slow with no noticeable increment in adsorption by RS-GO above 30 min because of the leaching process. Hence, the optimum time for rice straw-derived GO for the efficient removal of nickel metal ion is 30 min at 25 °C. Oxygen-containing functional groups played a vital role in Ni (II) adsorption on GO. The greater the O-containing groups, the more adsorption capacity [100].

3.2.3. Gas Storage

The ongoing burning of fossil fuels in transportation sectors has attracted the attention of researchers to design alternative energy sources. Natural gas (NG) is one of the promising energy sources owing to its widespread availability and environment-friendly nature. Natural gas comprises primarily of methane, ≈87–96%, but commonly including varying amounts of other higher alkanes, and sometimes a small percentage of carbon dioxide, nitrogen, hydrogen sulfide, or helium [101]. It possesses the highest heating value per unit mass in comparison to the other hydrocarbon fuels. Despite its uses, its storage and transportation is a big issue [102]. In the past, natural gas was stored and transported in cryogenic condition (−161.5 °C) and large upfront capital such as in liquefied natural gas (LNG). Storage in the form of compressed natural gas (CNG) requires high pressure (≈250 bar) and more space [103]. Finally, adsorbed natural gas (ANG) technology revolutionized the transportation and storage of NG. It uses highly porous adsorbents for the safe absorption of NG at room temperature and relatively low pressure (3–4 MPa). ANG displays a high volumetric capacity for the storage of natural gas [104,105]. Conventional carbon-based nanomaterials are considered as effective energy storage materials for the storage of gases such as CO_2, CH_4, and H_2, owing to their large surface area. The formation of composites of CNMs with metals or metal oxides of noble metals, rare-earth metals, metalloids, and alkaline-earth metals increases the capacity of gas storage by CNMs [106–108]. Carbon-based adsorbents including activated carbon, graphene, carbon nanofibers, etc. have been used frequently as NG adsorbents. These are considered the most suitable medium for NG storage owing to their high specific surface area, regenerative capacity, and micro-porosity. Among carbon-based adsorbents, graphene-related adsorbents are widely developed for gas adsorbates (preferably CH_4) because of their high iso-steric heat of adsorption, despite the smaller surface area and porosity compared with activated carbons. The smaller specific surface area (SSA) of graphene-related adsorbents is enlarged by physical or chemical treatment. Highly porous graphene derived from various agro wastes has been employed for CH_4 adsorption. To date, there has been very limited research on

the graphene-like materials derived from agricultural waste for gas adsorption, especially with respect to the stabilization conditions on the resultant graphene properties [68].

Othman et al. [68] reported the synthesis of GRHA at various stabilization temperatures and studied the adsorption of CH_4 by each. It was concluded that an optimum stabilization temperature is necessary to yield GRHA having high SSA and abundant micro-pore volume. The degree of gas adsorption depends on the synthesis conditions of the graphene-like materials. SSA and total pore volume are contributing factors toward the maximum adsorption performance of the GRHA. Increasing the optimum temperature (200 °C) causes a subsequent decrease in the SSA and micro-pore volume. These results were similar to the previous study reported by Hayashi et al. [109], in which the adsorption of gas by the graphene-like material is directly proportional to the pressures [110]. In this case, the adsorption capacity approaches a limit at pressures near 30 bar as the monolayer of the sorbent is almost saturated with CH_4 molecules. For the adsorption or storage process to occur, high-pressure diffusion of the targeted gas into the internal structure of CNMs is necessary [111]. The change in pore structure with respect to temperature should be attributed to the thermal properties, morphology change, and activation degree of GRHA with temperature. The adsorption mechanism between GRHA200 and CH_4 molecules was found to be van der Waals forces of attraction [112]. GRHA200 possesses a wider hysteresis loop, which shows the co-existence of both micropores and mesopores in excess. These interlinked micropores and mesopores are responsible for gas adsorption as reported by Durá et al. [113] GRHA200 exhibited the largest SSA of 1556.3 m^2/g and TPV of 1.1269 cm^3/g, with the largest micro-pore volume distribution of 0.5782 cm^3/g.

Othman et al. [114] demonstrated the synthesis of activated carbon nanofibers (ACNFs) incorporated with graphene-based materials called gACNFs. GRHA/ACNFs exhibited the highest SSA, of 384 m^2/g, with ahigh micro-pore volume of 0.1580 cm^3/g, which is up to 88% of the total pore volume. It was concluded that GRHA/ACNFs happen to be better adsorbents for CH4 compared to pristine ACNFs and reduced graphene oxide (rGO/ACNF).

3.2.4. Bactericidal Action

The research on the antimicrobial activity of graphene or its derivatives showed that the 2D structure inactivates and physically damages the bacterial cells. The crystal structure with sharp and clean edges of graphene or GO sheets having higher edge-to-weight ratios is responsible for the bactericidal action. Studies have shown that graphene sheets envelop bacterial cells, isolating them from their environment, thereby blocking the transport of nutrients inside the cells and inhibiting growth. [115–117]. Sheets wrapping bacterial cells were much larger in size than the cells themselves [118].

4. Carbon Nanotubes

Carbon nanotubes have attracted much attention in various scientific fields [119]. Carbon-based nanomaterials such as CNTs have been synthesized early in 1958 [120], but CNTs were firstly observed by Radush- Kevich and Lukyanovich in 1952 [121] and then in 1976 were observed by Oberlin et al. [122]. Carbon nanotubes were the most scrutinized material before the discovery of graphene. CNTs were discovered by Iijima [123] and separated abundantly by Ebbesen and Ajayan [124]. Carbon nanotubes are cylindrical carbon nanostructures made up of a hexagonal network of sp^2 hybridized carbon atoms [125]. CNTS are categorized as single-walled carbon nanotubes (SWNTS) which consist of a single layer of graphene sheet, and multi-walled carbon nanotubes (MWCNT) which consist of more than one layer of graphene sheets or a single graphite sheet rolled up to make multilayers of the graphene sheet [126–128]. The diameter of an SWCNT is a few nanometers, while MWCNTs have a diameter of several tens of nanometers [129]. Carbon nanotubes possess strong electrical, mechanical, optical, thermal, and electrochemical properties [130]. Owing to the high electrical conductivity, chemical stability, large surface area, and mechanical strength, carbon nanotubes show distinctive properties [131]. CNTs

have a wide range of applications in sensors, electronics, semiconductors, supercapacitors, gas storage materials, catalysis, and biomedical research [128].

4.1. Synthesis of RH-Derived Carbon Nanotubes

The rich carbon content (45–55 wt %) of biomass waste is utilized for the production of high esteemed carbon nanomaterials [45]. Rice husk is a good starting precursor to synthesize highly valued carbon materials because it is considered a low-cost, cheap, renewable raw material that can be easily obtained in bulk amount [132]. Nowadays, CNTs are mostly prepared by three techniques: arc discharge [123], laser ablation [133], and chemical vapor deposition [134,135]. Other methods such as pyrolysis [136], flame synthesis [137], and electron or ion beam irradiation [138] methods are also used to prepare carbon nanotubes. However, CVD is the most common method to prepare carbon nanotubes, because this process requires a low temperature of 600–900 °C and ambient pressure [139,140]. Here, we will discuss the synthesis of carbon nanotubes from rice residue via three methods: chemical vapor deposition, microwave oven technique, and pyrolysis.

4.1.1. Chemical Vapor Deposition (CVD)

Chemical vapor deposition is a technique to produce the required product as a thin film by exposing the substrate to one or more volatile precursors, which interact with the substrate or decompose on the surface of the substrate [141]. Fathy (2017) [27] reported a method to fabricate carbon nanotubes bundles through two processes. First, pretreated rice straw was treated hydrothermally with the impregnation of iron and/or nickel metals as a catalyst for 2 h at a temperature of 250 °C to yield hydro-char, which is then utilized as a substrate. Then, camphor (gaseous carbon source) is decomposed by CVD under flowing nitrogen gas. The CVD unit comprises two separate chambers fixed on a work area. A clear picture of the CVD experimental setup is shown in Figure 9. Carbon nanotubes bundles are obtained via the carbonization of hydrothermally treated rice straw via the chemical vapor deposition of camphor supported with ferrocene or a ferrocene–nickel nitrate catalyst (RS-H/Fe-Ni) in the presence of gas-phase carbon discharged from heating camphor under flowing nitrogen gas. Various bundles of CNTs–Fe-Ni were synthesized over the pyrolysis RS-H/Fe–Ni support. It was seen that the carbonized RS-H/Fe-Ni support was completely covered by a carbon nanotube layer that was homogeneously distributed. Little amounts of small outer diameters of coiled bundles of CNTs and a large amount of outer diameter straight CNTs bundles were produced by the bottom growth mechanism over RS-H/Fe. CNTs created over the carbonized RS-H/Fe–Ni were observed to be well-graphitized when contrasted with those developed over RS-H/Fe. In this way, the mixture of nickel with ferrocene builds the graphitization degree as well as the amount of CNTs.

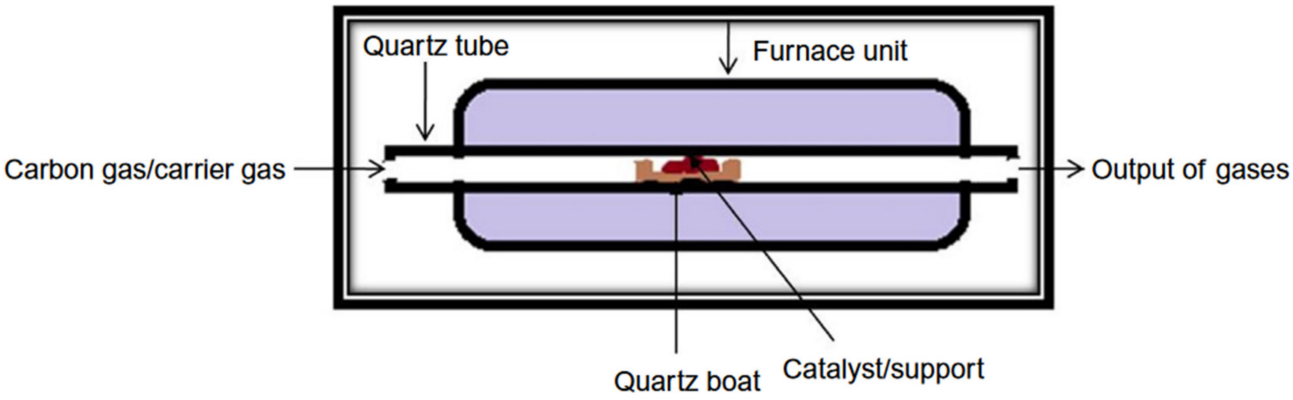

Figure 9. Schematic representation of the experimental setup used for the catalytic decomposition of hydrocarbons. Reprinted with permission from Ref. [11]. Copyright 2020 Elsevier.

Good quality CNTs are obtained when RS-H/Fe-Ni is thermally treated without flowing any inert gases. The obtained CNTs morphology was characterized by using Scanning Electron Microscopy (SEM) and Transmission Electron Microscopy (TEM), whereas the thermal and electronic properties of CNTs were estimated by Raman spectroscopy and thermogravimetric analysis. Flowchart diagram of the synthesis of CNTs from pre-treated rice straw is shown in Figure 10 CNTs with external diameters of 22–66 nm were obtained, and the yield of CNTs was found to be 44%.

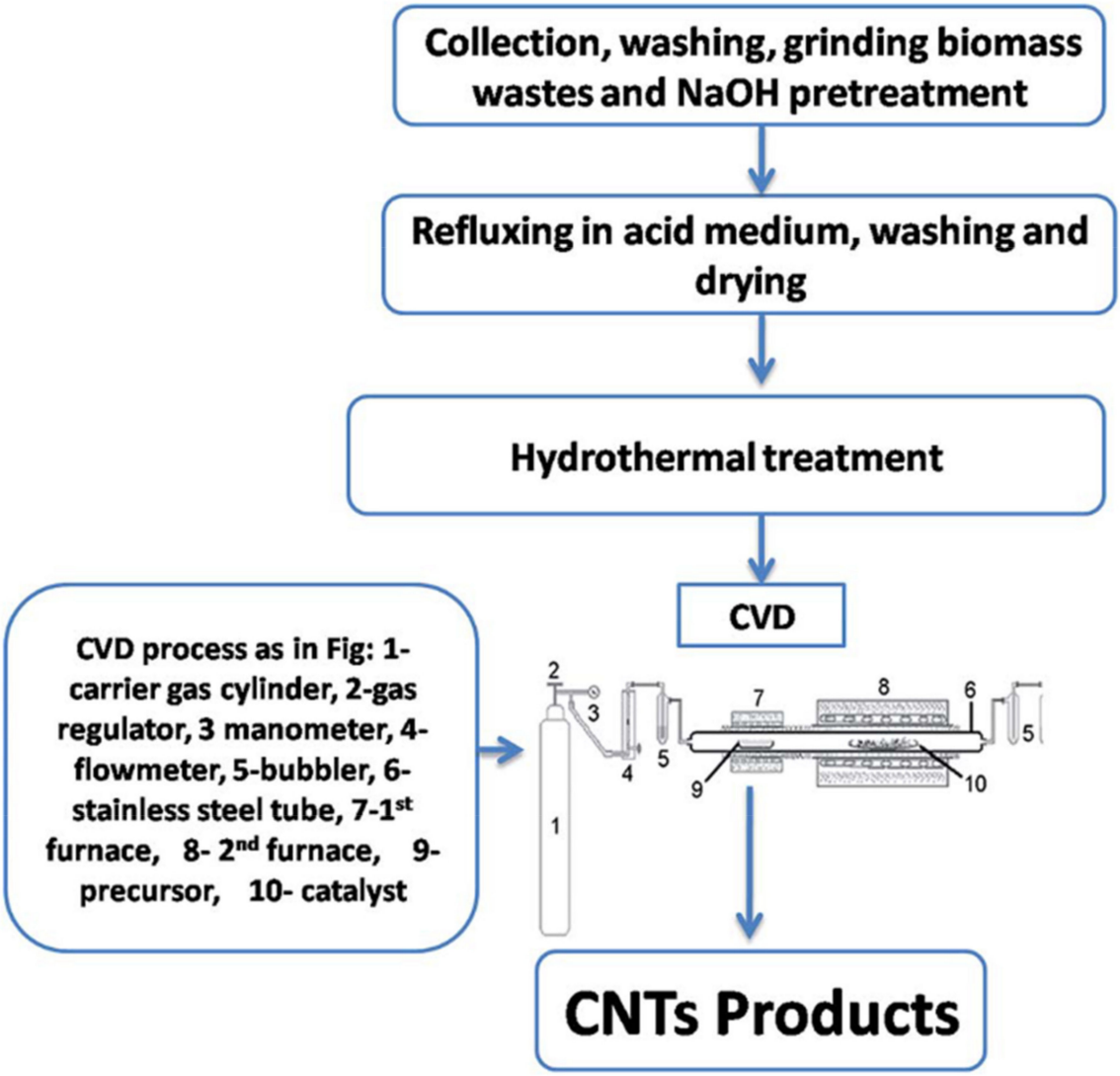

Figure 10. Flow chart diagram for the synthesis of CNTs from pretreated rice straw through CVD. Reprint from Ref. [27].

4.1.2. Microwave Oven Technique

Agricultural residues comprised of highly carbonaceous lignin, cellulose, and hemicellulose are frequently employed as carbon precursors for the fabrication of carbon-based nanomaterial [142]. Asnawi et al. (2018) [143] reported a method to synthesize carbon nanotubes by the use of the microwave oven technique. Rice husk, a biomass waste from paddy rice, contains lignin and cellulose, which is a good source of carbon that is widely utilized as a precursor for the fabrication of carbon nanotubes by the use of the microwave oven technique [139,140]. Nowadays, the microwave irradiation technique has been utilized frequently because it tends to develop high-energy-density plasma to fabricate carbon nanomaterials namely carbon nanotubes, nano-walls, and nanofibers [11]. To activate a plasma carbon source, an economical microwave oven and catalyst is used. Prepared

CNTs were characterized by FESEM; Figure 11 show the spherical and tubular structures of carbon nanotubes.

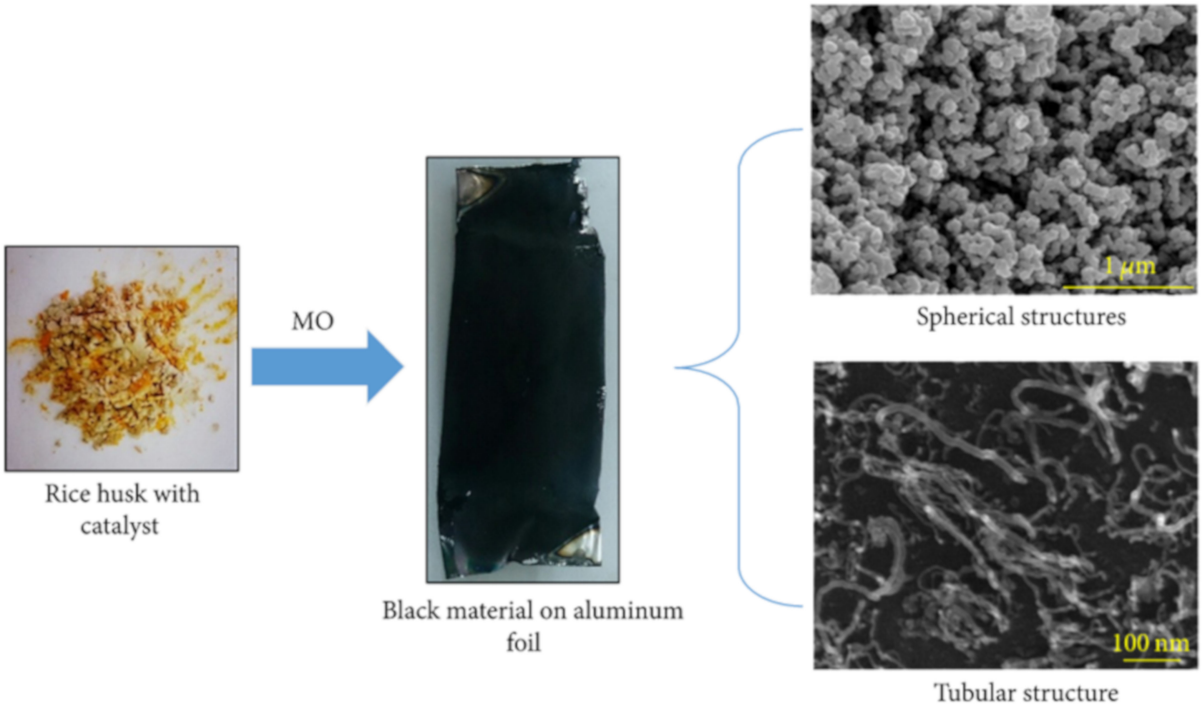

Figure 11. Conversion process of RHs into soot-like material on aluminum foil top including spherical and tubular structures of CNTs. Reprint from Ref. [143].

Later, Wang et al. (2015) [25] reported a microwave plasma irradiation (MPI) method to synthesize graphenated-CNT (g-CNTs) under the H_2 and argon flow from rice husk (RH). Without any purification, rice husk waste was used to fabricate g-CNTs by a one-step microwave plasma irradiation technique. The resulted nano-sized carbons were fiber-like graphenated-carbon nanotubes (g-CNTs) made of graphene developed on the sidewalls of CNTs: two to six-layered graphene sheets and several micrometers long CNTs having a breadth of 50–200 nm. The dissociation of RHs to form nanocarbons depends on the pressure and temperature.

4.1.3. Pyrolysis Technique

Lotfy et al. (2018) [144] reported a novel strategy to fabricate carbon nanotubes of various sizes and shapes from hydrothermally treated rice straw followed by pyrolytic decomposition in a vertical bed reactor for 60 min at a temperature of 830 °C without the flow of any outside gases (e.g., N_2, Ar, or H_2). In this approach, first hydro-char and intermediate carbon source were produced hydrothermally from rice straw, and then, the impact of pulping i.e., alkaline, sulfite, and neutral on rice straw hydro-chars for the generation of carbon nanotubes was evaluated. In this methodology, rice straw (a carbon source) and its pulps were hydrothermally treated followed by pyrolytic decomposition (in a closed stainless-steel reactor) for the preparation of carbon nanotubes. Distinctive pulping processes were utilized for the modification of un-pulped rice straw for the preparation of carbon nanotubes, i.e., (RS-AP) alkaline pulping, and rice by-products were exposed to alkali treatment, which results in the efficient removal of hemicellulose and lignin components, yielding an amorphous surface having maximum cellulose content in the fibrous structure. In sulfite pulping (RS-SP), rice straw was pulped with sodium sulfite. Rice straw in neutral pulping (RS-NP) was pulped with a mixture of sodium sulfite and sodium carbonate. Pure carbon nanotubes produced from untreated rice straw and treated rice straw with alkaline, sulfite, and neutral pulp were denoted as RS-CNTs, RS-AP-CNTs,

RS-SP-CNTs, and RS-NP-CNTs, respectively. The subsequent carbon nanotubes were studied using TEM, SEM, and FTIR. TEM reports showed that rice straw significantly affected the size and shape of obtained CNTs. Rice straw pretreated with acid, base, and neutral pulping produces RS pulps of different chemical composition. The carbon precursor type, catalyst support, temperature, growth time, and strategy to be utilized for the synthesis significantly affect the quality, yield, morphology, and porosity attributes of CNTs [44].

Various morphologies of CNTs (e.g., shape, size, thickness of bundles, and length of CNTs) were produced over Fe-Ni/Al_2O_3 catalyst. From the pyrolysis of un-pulped rice straw hydro-char, multi-walled CNTs of RS-CNTs and RS-NP-CNTs of diameter 15 to 40 nm and from 4 to 8 nm and 14.6–47.9 nm have moderately higher surface regions (188 m^2/g) than others, whereas needle-like CNT bundles of RS-AP-CNTs and RS-SP-CNTs of diameter 2.5 to 6.8 nm and from 4 to 8 nm gave the best methylene blue color adsorption limit (283.3 mg/g). Subsequently, both RS-AP-CNTs and RS-SP-CNTs are made out of few CNTs and graphene nano-sheets. Therefore, CNTs can be regarded as a pleating of graphene sheets which can be grown in between graphene nano-sheets to yield three-dimensional CNTs–graphene nano-sheets. The yield of carbon obtained from un-pulped RS (raw) which exhibited multi-walled CNTs was ≈80% when contrasted with the treated pulped rice straw, which gave values of 50, 40, and 65%, respectively. Thus, hydro-char obtained from untreated rice straw produced well-structured CNTs (having large surface area) of different shapes than treated (pulped-RS).

4.2. Potential Application of RH-Derived CNTs

4.2.1. Water Purification

Adsorption is a facile and environment-friendly technique for the removal of organic and inorganic contaminants from water bodies. Activated carbons (ACs), due to their thermal stability and chemical inertness, are considered to be an excellent option for the adsorptive removal of contaminants. However, the recycling and regeneration of activated carbons is a difficult process. The use of activated carbons for the removal process leads to slow sorption kinetics. Activated carbon fibers (ACFs), the second-generation carbonaceous sorbents, have been developed [145], and carbon nanotubes can be regarded as the contracted form of activated carbon fibers [146]. The extraordinary potential of CNTs to act as an adsorptive medium is related to its functional and structural properties [147]. Carbon nanotubes have proven to be excellent sorbents for water purification owing to their suitability in the removal of organic, biological, and inorganic water pollutants and their extraordinary wastewater treatment potential [148]. Figure 12 shows a schematic illustration of the CNT-based wastewater treatment.

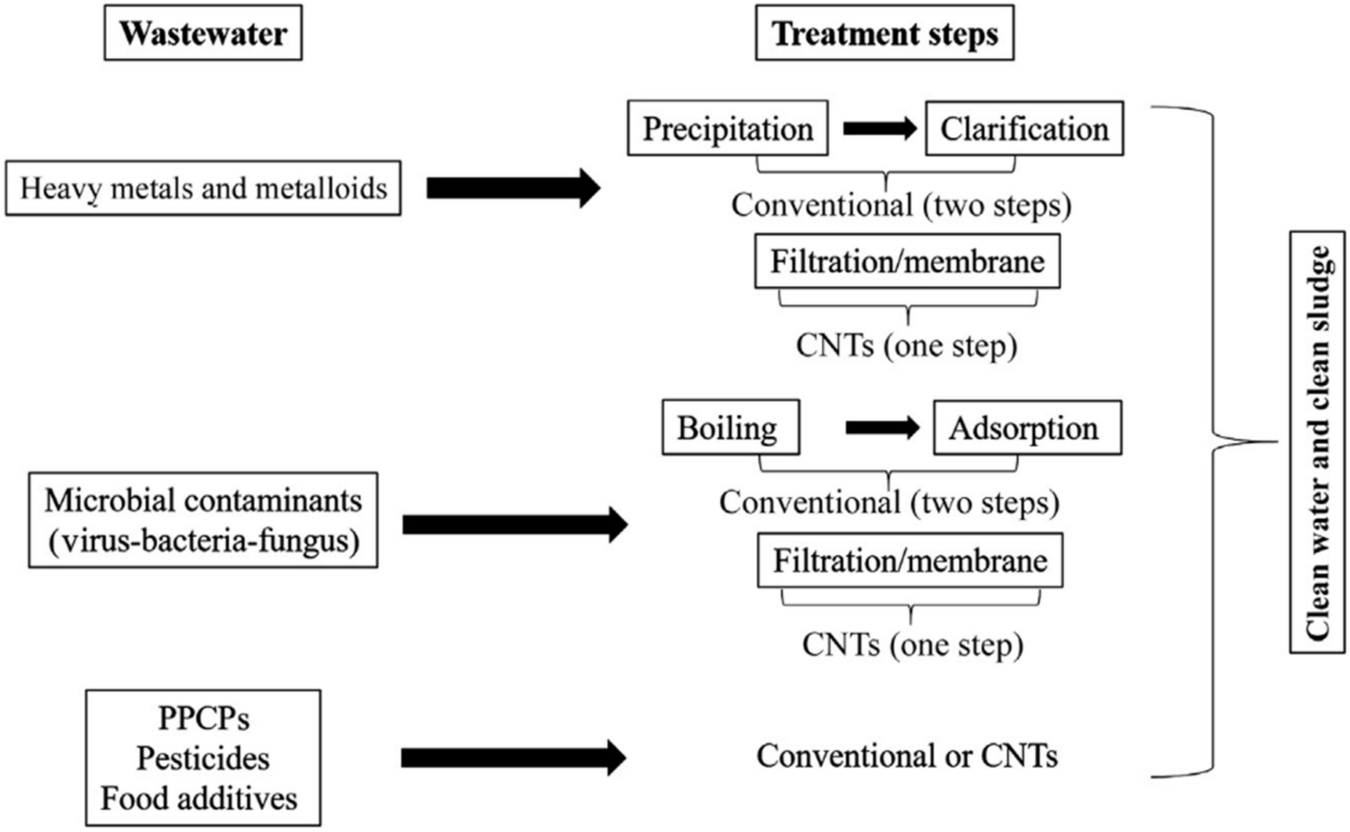

Figure 12. Roles of CNT-based materials in treating wastewater and achieving clean sludge. Reprinted with permission from Ref. [149]. Copyright 2019 Elsevier.

Removal of Chemical Contaminants

Removal of Emerging Organic Contaminants:

The natural balance of the ecosystem is being disturbed by rapid urbanization and industrialization. Almost all environmental compartments are being contaminated by pollutants. Organic pollutants in aqueous systems are a result of human activities and animal and/or plant decay [150]. More than one billion people lack clean water resources, leading to severe health issues globally [151]. Every year, about 200 million die as victims of water-borne infections [152]. These pollutants occur as dissolved materials or particulate matter. Common organic contaminants include Natural Organic Matter (NOM) namely polysachharides, lipids, carbohydrates, proteins, fulvic acids, and humic acids, and Synthetic Organic Compounds (SOCs) such as dyes, pesticides, and pharmaceuticals [118]. Organic acids possess affinity toward hydrophobic organic micropollutants (OMPs) such as personal care products (PCPs) and polycyclic aromatic hydrocarbons (PAHs), leading to water deterioration [153]. The release of herbicides, personal care products, pesticides, and pharmaceuticals are the several types of organics expelled into natural water by humans, causing adverse health effects to aquatic life and mankind. The adsorption efficiency of CNMs for the removal of these effluents depends on the chemical nature of organic wastes to be removed, the physiochemical properties of NMs (e.g., pore size and pressure of surface charges), and water solution chemistry such as ionic strength and pH [154–156]. The pollutants having aromatic rings in their structure develop π–π interactions with carbon nanomaterials, which favors the removal process of these pollutants from water [157].

CNTs or CNT membranes are being used extensively for removing aqueous organic pollutants. The low-pressure membranes [158] such as reverse osmosis (RO) and (nanofiltration) NF membranes were being used for the removal of organic pollutants [159,160], but these membranes possess low water permeability, which is a major drawback in their application in wastewater treatment [161,162]. High-permeability membranes such as

novel functionalized-CNT (f-CNT) membranes are being widely employed for organic contaminant removal. Water transport and rejection mechanism of f-CNT membranes is clearly demonstrated in Figure 13.

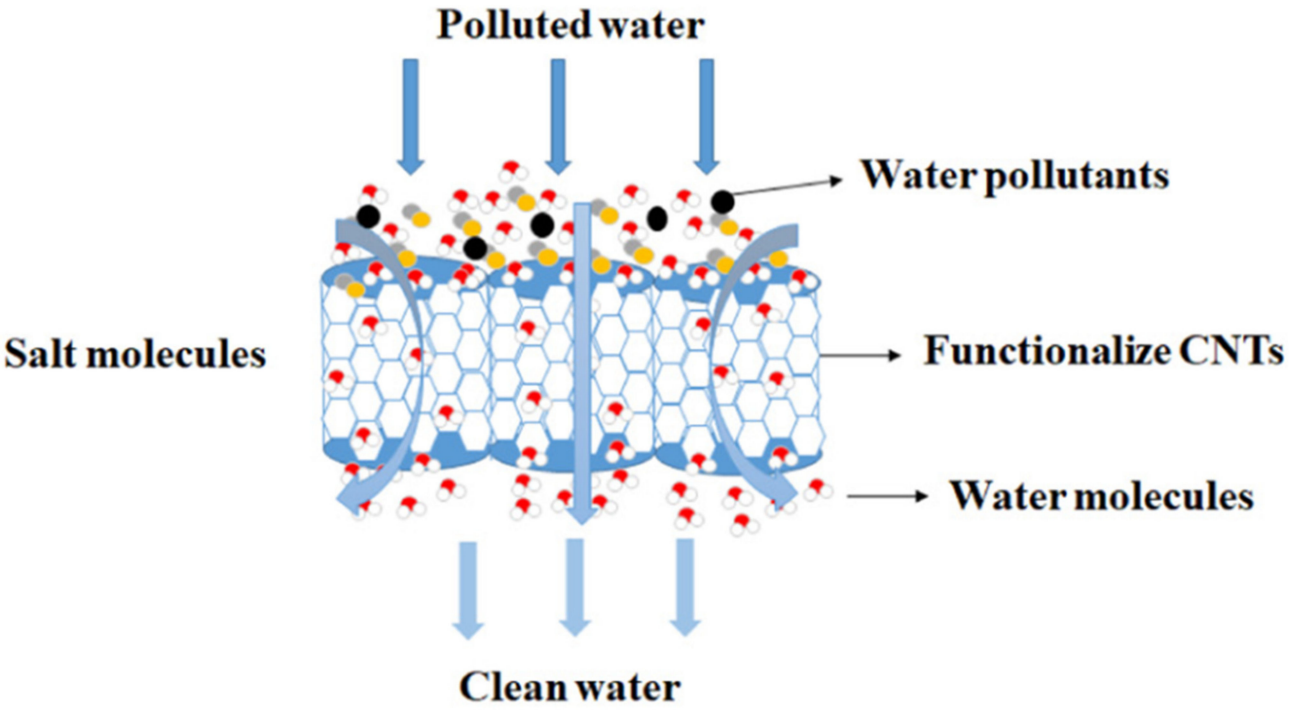

Figure 13. Water transport and rejection mechanism of current state-of-the-art f-CNT membranes. Reprinted with permission from Ref. [163]. Copyright 2019 Elsevier.

f-CNTs exhibit high absorption affinity for various organic pollutants. These membranes interact with the organic contaminants, and the removal mechanism occurs due to the electrostatic interactions, π–π electron–donor acceptor (EDA) effect, hydrogen bonding, hydrophilic–hydrophobic effect, Van der Waals interactions, and chemical adsorption between the organics and membranes [164]. The outer surface of CNTs is hydrophobic in nature, thereby facilitating the binding of non-polar organic compounds [165,166]. Modifying the CNTs surface by the attachment of various functional groups makes it hydrophilic, thereby increasing the removal efficiency of polar organic compounds such as phenols [167]. Functionalization with oxygen functional groups reduces the adsorption of non-polar contaminants such as naphthalene [168]. Increasing the pH value and oxygen-containing functional groups on the surface of CNTs ultimately decreases the adsorption capacity of the f-CNT membrane for NOM. This decrease is attributed to a decrease in π–π interactions and an increase in electrostatic repulsion [169]. It was reported by researchers that a high removal of NOM through f-CNTs is only possible when the specific surface area of CNTs is high [170], and π–π interactions exist between NOM and the aromatic rings of f-CNTs [171]. There exists a competition between different organic pollutants in aqueous bodies for the CNT surfaces. This diminishes the adsorption of the target organic chemical [172]. That is why there is a great need to fabricate CNT membranes for the selective adsorption of different organic pollutants by modifying their surface properties. Nowadays, NOM responsible for competitive adsorption is being removed by the pre-coagulation of wastewater effluents. Wang et al. [173] and Wang et al. [174] investigated the removal of pharmaceutical and personal care products (PPCP) by the use of CNT nanocomposite membranes with 95% removal efficiency.

Among synthetic organic matter, organic micro-pollutants (OMPs) are regarded as the most serious threat for mankind [175,176]. Drinking water containing OMPs, even in extremely low concentrations such as parts per trillion (ppt) or parts per billion (ppb),

drastically affects living organisms [177,178]. The most commonly occurring OMPs include solvents, pesticides, personal care products, surfactants, polycyclic aromatic hydrocarbons (PAHs) [179], endocrine-disrupting compounds, phthalate asters [180], polybromodiphenyl ethers (PBDEs), bisphenol A (BPA) [181], alkyl phenols (APs) [182], organochlorine pesticides (OCPs), polychlorinated biphenyls (PCBs), micro-cystins, and pharmaceutical products [183]. π–π electron donor–acceptor interactions are considered the most important pathways for removing various OMPs from wastewater using CNTs. Generally, OMPs contain π electrons that can link with CNTs by forming π bonds, as each carbon atom in CNTs also has one π electron. However, the strength of the π–π interaction is determined by the nature of functional groups present on the benzene rings of organic micro-pollutants [184]. The electrostatic interactions present on the surface of CNTs and OMPs are the reason behind the adsorption of OMPs. Owing to the variations from pH at a point-of-zero charge, the surface of CNTs becomes charged, creating electrostatic forces on their surface. In the same way, protonation or deprotonation occurred at varying pH conditions, which leads to the formation of positive and negative charges on the surfaces of OMPs. The oxygen-containing functional groups on the surface of CNTs react with $–NH_2$, –NH, and –OH by forming hydrogen bonds, leading to the adsorption of organic micro-pollutants onto carbon nanotubes [185]. Hydrophobic interactions are involved in eliminating a variety of hydrophobic organic micro-pollutants [186,187]. The highest adsorption of OMPs is achieved at zero net charge density of carbon nanotubes, which results in stronger hydrophobic interactions. The aggregation of CNTs decreases the nano-curvature of their wall. CNTs' structural aggregation leads to a reduction in their external surface, resulting in the production of various sorption sites inside the CNTs' channels. This makes the adsorption process of synthetic organic compounds on aggregated CNTs a difficult process [147].

Pesticides, Organic dyes and Oil spills:

Among the most alarming OMPs, pesticides are of great significance. Pesticides have also been employed as plant growth promoters or plant regulators. Approximately 4.6 million tons of pesticides are sprayed each year. These pollutants contain hazardous substances such as arsenic, lead, and mercury. More than 220,000 people are killed every year due to pesticide contamination, https://en.wikipedia.org/wiki/Pesticide (accessed on 9 August 2021). According to the WHO, around three million cases of pesticide poisoning are reported every year. Organophophorous and organochlorine are the most important classes of pesticides [188]. About 99% of pesticides harm the non-target species due to the domestic wastes and runoff from lawns and gardens [189]. They can enter the ecosystem through industrial wastes, agricultural wastes, landfills leaching, leakage of storage tank, or septic and sewer leakage [190]. Pesticides can damage reproductive systems and sex hormones. In addition, the widespread use of weedicide, pesticide, and herbicide rapidly decreases the density of shrubs and plants, leading to deforestation [164]. CNTs possess great potential to remove pesticides from wastewater. CNTs markedly influence the amount of pesticides to plants. Rocha et al. [191] investigated the electronically sorted (i.e., metallic or semiconducting types) SWCNTs for removing 2,4-dichlorophenoxyacetic acid, 1-pyrenebutyric acid, and diquat dibromide from water and reported that semiconducting SWCNTs showed more pesticide adsorption ($\approx$70.6%) as compared to metallic SWCNTs. The high pesticide removal of semiconducting SWCNTs can be attributed to less electron density around it. Thus far, information regarding pesticide removal using CNTs is not as vast as the material on other organic effluents.

Organic dyes are generated and expelled into the surrounding environment from various industrial units (e.g., food, paper, pharmaceutical, textile, plastic, and cosmetic industries) [192,193]. The discharge of colored wastewater dyes into water bodies without pre-treating them contaminates water and affects the ecosystem and living beings. Mostly, organic dyes, even at low concentrations, pose high toxicity. Moreover, these dyes owing to their complex aromatic morphology are stable to oxidizing agents, biodegradation, heat, and photodegradation. CNMs have been used widely for the removal of organic dyes from water by adsorption. Among all CNMs, graphene and CNTs possess excellent

adsorption ability for organic dyes. CNTs, as compared to traditional adsorbent materials such as activated carbon, zeolites, polymers, and clays, possesses excellent adsorption potential for organic dyes [188]. Functionalized CNTs with enhanced adsorptive sites and mesopores, especially oxidized MWCNTs, have proven to be the most effective for the removal of methyl orange and methylene blue from water bodies [194]. In addition, Ma et al. [195], synthesized alkali-activated carbon nanotubes for removing methylene blue and methyl orange from wastewater. Rajabi et al. [196] experimented and compared the adsorption potential of CNTs and f-CNTs under varying pH, temperatures, and contact times. The enhanced adsorption of f-CNTs in comparison to pristine CNTs is due to the addition of functional groups. MWCNT-COOH-cysteamine, synthesized by modifying CNTs, was capable of enhancing the elimination of Amido black 10B (AB 10B) from water. The adsorption rate showed an increment of 80% for MWCNT-COOH and 162% for MWCNT-COOH-cysteamine as compared to pristine CNTs [197]. Duman et al. successfully fabricated a MWCNT-κ-carrageenan-Fe_3O_4 nanocomposite to remove crystal violet dye. In addition, Jahangir et al. reported the elimination of Blue 29 (RB 29) from water by SWCNTs [198].

Oil–water emulsions, produced from sewage waste, crude oil production, and oil refineries, are rapidly being disposed of in water bodies. Oil spill management in water is much more difficult as compared to a land spill, as oil spreads more rapidly in water over a large area with sea wind and waves. These oil spills pose a great threat to water bodies and aquatic life. Different filtration techniques have been employed for the efficient removal of oil spills from water including ultrafiltration (UF), microfiltration (MF), and nanofiltration (NF). These techniques have the benefit of low energy consumption and efficient water treatment; however, these are based upon the size-exclusion separation of oil particles [199,200].

Nanofiltration, especially using carbon-based nanomaterials, is commonly being used for wastewater treatment. Among carbon-based materials, CNTs are reported to be an efficient material for controlling oil spills in an aquatic environment because of their significant oil adsorption capacity [188]. This is due to their large surface area (provides more active sites), enhanced porosity, chemical inertness, super-hydrophobicity, easy recyclability, high selectivity, and high stability [201]. Gu et al. [202] reported the effective separation of an array of surfactant-stabilized water-in-oil emulsions. A CNTs–polystyrene composite membrane with super hydrophobicity was developed, which showed a high oil rejection rate (>99.94%). CNTs provide robustness to the membrane, making it durable and resistant for oil removal. The mechanical properties of the membrane, including tensile strength and Young's modulus, were also improved [202]. Chen et al. [203] designed a CNT/YSZ composite membrane, incorporating CNTs inside the porous channels of an Y_2O_3–ZrO_2 (YSZ) membrane. A 100% rejection efficiency of oil droplets was reported by the insertion of CNTs in the YSZ membrane. The soft lipophilic layers developed on CNTs ensure sufficient adsorption along with size-exclusion separation in comparison to size-exclusion separation for YSZ membranes.

Removals of inorganic contaminants and heavy metals:

For a long time, the drinking water has been treated through traditional chemical coagulation and disinfection procedures that eliminated natural organic matter and microbes such as bacteria and viruses from the water [118]. However, in the present decade, the rapidly growing industries, extensive use of antibiotics, widespread utilization of chemicals in agriculture, and several other human activities have introduced new contaminants such as pesticides, dyes, and heavy metals in drinking water [204,205]. Such contaminants and their products with organic matter are hazardous for human health. Disinfecting water through chlorination produces carcinogenic by-products. Plus, the ozone or ultraviolet disinfection methods are costly [206]. Absorption-based contaminants removal offers a reliable solution for these issues that is able to eliminate organic matter, heavy metals, microbial contaminants, and other harmful by-products [207]. Using activated carbon and polymers as absorbents is common, and the process is relatively easier to implement, but

they are not much more efficient in absorbing heavy metals [208] and some other chemical contaminants. The increasing research interest in nanotechnology has led to the production of several carbon-based nanomaterials such as graphene, carbon nanotubes, and carbon dots [209]. Their characteristics such as high surface area, high microbial disinfection capacity, easy physical and chemical modification, and ability to remove both organic and inorganic wastes make them a highly interesting material for novel water treatment procedures. Carbon nanotubes (CNTs) act as potential water-disinfecting agents. The high porous structure, high surface area, low density, and interactions with water contaminants make CNTs one of the most reliable procedures for water purification [210]. GAC filters are commonly used to eliminate heavy metals from water, but they have slow absorption rates and absorb metals in low concentrations [211]. Recent studies have proved that carbon nanotubes (CNTs) are highly efficient in removing high concentrations of heavy metals from water [212]. The researchers suggest that SWNT successfully absorbs Zn^{2+}, Cd^{2+}, Pb^{2+}, and Cu^{2+} from contaminated water [213]. The point on which all of these researchers agree is that CNTs have much more absorption capacity when it comes to heavy metals than any other traditional absorbent kept under similar experimental conditions [214]. Figure 14 describes various pathways adopted by f-CNTs for removal of heavy metals. The capacity of CNTs to absorb heavy metals depends on the surface area, porosity, pH value of the aqueous media, purity, presence of functional groups, and site density [215].

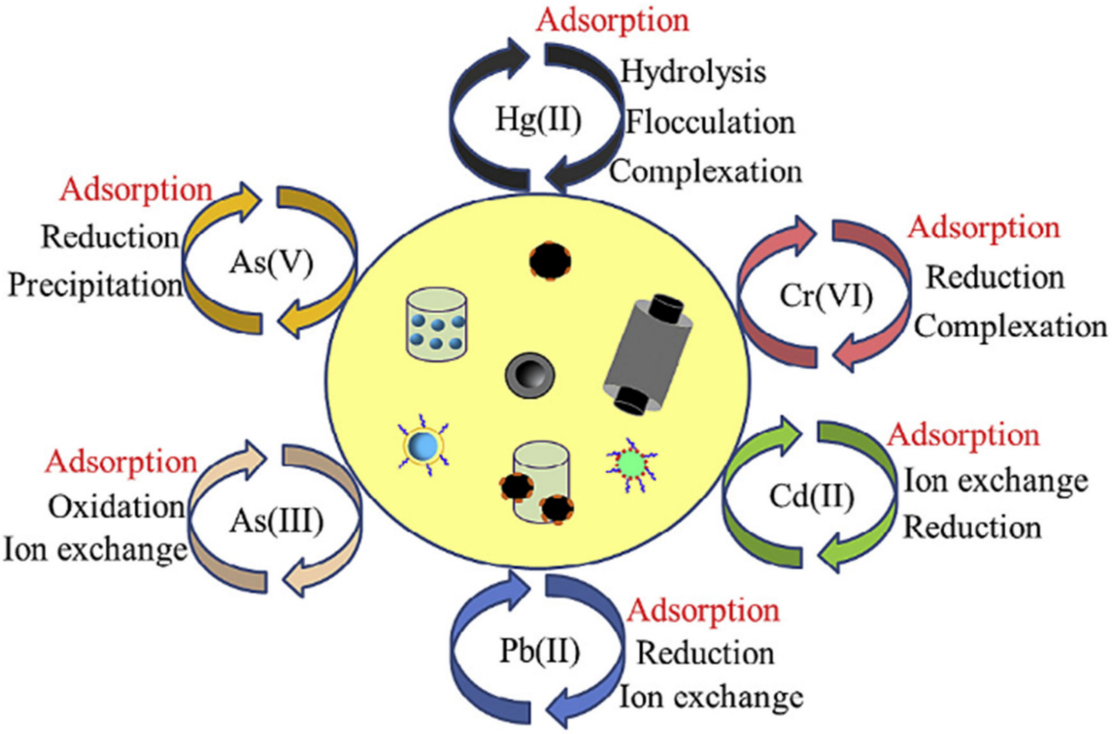

Figure 14. Pathways for aqueous heavy metal removal by functionalized carbon nanomaterials. Reprinted with permission from Ref. [216]. Copyright 2018 Elsevier.

The sites on CNTs for heavy metal absorption are the internal surface, outside sites, interstitial channels, and grooves. The site where the highest concentration of heavy metals can be absorbed is the interstitial channel site [149].

Surface modification is one way to further enhance the heavy metal absorption effectiveness in carbon nanotubes. The oxidative modification [217] and functionalization of CNTs with magnetic or non-magnetic metal oxides or sulfur-containing groups make the CNT-based absorbents highly effective in the removal of metal or a metalloid contaminant from drinking water [218].

Researchers have implemented f-CNTs or f-CNT membranes for eliminating inorganic contaminants including heavy metals and arsenic from water [219,220]. Owing to the large surface area, hollow tubular structure, high porosity, presence of functional groups on the surface of f-CNTs, and the desirable interactions between water effluents and f-CNTs, the high adsorption of arsenic and heavy metals onto CNT membranes is achieved [215,221–223].

The implementation of CNTs as absorbents in water removal systems is often hindered by the difficulty in separating nanoparticles after the absorption process. One workable solution is the use of metal oxide nanocomposites, which can then easily be separated through a magnetic field [118].

Gupta et al. [224] developed an MWNT/nano-Fe_3O_4 nanocomposite, where the iron oxide clusters were accumulated on MWNT nanomaterials. Testing has shown that this nanocomposite has far more absorption capacity for Cr^{3+} in water than that of activated carbons. Similarly, another such nanocomposite, that is, MWNT/Al_2O_3, was synthesized for an efficient absorption and removal of Pb^{2+}. Such studies reveal that a controlled growth of metal oxides over nanoparticle sheets surprisingly increases their absorption capacities [118].

Bahgat et al. [223] reported that the adsorption of metal ions on the surface of f-CNT can be attributed to the presence of several sorption sites on functionalized CNTs for the heavy metal binding. Plasma-functionalized CNT membranes were used to adsorb zinc ions. An excess of oxygen groups present on the functionalized CNT surface act as binding sites for zinc ions, deprotonating the functional groups and thereby increasing the reactive binding sites for eliminating cationic metal ions by the application of surface complexation. The adsorption capacities of f-CNT were higher compared to those of pristine CNTs. This high adsorption can be ascribed to the electrostatic interaction between the negatively charged carbon nanotubes and divalent metal ions [220].

The removal of pollutants by the use of carbon nanomaterials and nanocomposites depends a lot on the water chemistry, such as the pH of the solution, presence of different functional groups, contact time, and mixing rate [216]. The pH of the solution offers a key role in the adsorption of heavy metals [225]. The removal of cations is favorable at alkaline pH due to the enhanced negative charges on functionalized CNT surfaces, whereas at acidic pH, removal efficiency is not effective due to the protonation of functional groups on f-CNT (Ihsanullah et al., 2016a [215], 2016b [222], 2016c [221]). The effect of pH on removal capacity was also demonstrated by Vuković et al. [226]. Functionalized MWCNTs were employed to remove cadmium from water, and it was reported that the adsorption capacity was highly dependent upon pH conditions.

Additionally, the competitive behavior of cations and anions on the CNTs also affects the metal ion removal process. For instance, the adsorption of lead by f-CNTs is highly efficient when sodium dodecylbenzene sulfonate (SDBS) is present. This is because of the complexation between cations (Pb^{2+}) and anionic surfactant (DBS^{-}). However, in the presence of benzalkonium chloride (BKC), lead adsorption and removal reduces as both the positive and negative ions compete for the CNTs surface to get adsorbed [227]. The binding mechanism between functionalized carbon nanotubes and heavy metals is different depending upon the charges (both positive and negative); for example, the adsorption of Cr(III) with nitrogen-doped magnetic CNTs is due to chemical adsorption, whereas with acid-modified CNTs, the adsorption mechanism is due to electrostatic interactions between Cr(III) and CNTs [228].

It was reported by researchers that the diameter of CNTs has no influence on the adsorption of inorganic pollutants, and indeed, the adsorption mechanism depends on the natureof the functional groups present on the CNT surface instead of its size.

Removal of Biological Contaminants/Microbial Decontamination

Pathogenic microbiological contaminants, namely bacteria, viruses, and protozoa, are considered as major disease-causing organisms in human beings. They are commonly

found in drinking water and wastewater effluents [118,229]. For many decades, adsorption methods have been used to remove microbial contaminants [207]. Traditional adsorbents, including polymers and activated carbon, can be utilized for the removal of microorganisms; however, these are not productive enough to get high-purity water [118]. CNTs, both MWCNTs and SWCNTs, have shown strong antimicrobial potential. In water, SWCNTs have the ability to absorb 27–36 times more *Bacillus subtilis* spores as compared to powdered activated carbon [148]. The functional and morphological properties of carbon nanotubes and their high affinitive interactions with microbiological pollutants makes them best fit for this purpose. CNTs, due to their larger specific surface areas than all other adsorbents, can deactivate a broad range of microbes [149], including viruses (e.g., MS2 bacteriophage), bacteria (e.g., *Escherichia coli*, *Micrococcus lysodeikticus*, *Streptococcus mutans*, and *Salmonella*), and protozoa (e.g., *Tetrahymena pyriformis*) [163]. They have the potential to adsorb bacterial or viral spores with superior efficiency [230]. SWCNTs possess preferential affinity and selectivity for several bacterial species, which has proven beneficial in the selective removal of pathogenic over non-pathogenic species [118]. For instance, in a mixture of bacterial cultures of *Escherichia coli* and *Staphylococcus aureus*, the removal of *S. aureus* was 100 times more than that of *E. coli* within 5–30 min of contact time [231]. This rapid microbiological removal rate and selectivity for microbes is a desirable feature for developing sensors, filters, and water purification devices [148]. The geometry of CNTs and their diameter plays a vital part in the inactivation of microorganisms from wastewater. A small diameter means a higher surface area, and a higher surface area provides a higher contact area with the microbes, thereby increasing microbial interactions and adsorption capacity [232]. MWCNTs, due to their large diameter, which reduces their chances to invade the nucleus, are considered less bactericidal as compared to rod-shaped short SWCNTs. It was reported by Kang et al. [233] that single-walled carbon nanotubes inactivated *Escherichia coli* by penetrating inside their cell walls. Chemically modified CNTs such as CNT–metal oxide nanocomposites and polymeric CNTs exhibit more removal tendency than pristine CNTs. The direct contact of microbes with functionalized CNTs badly affects the integrity of the cell wall as well as the structure and metabolic activity of bacterial specie e.g., *E. coli*, which is mainly ascribed to the penetration of CNTs into their cell walls. The microbial inactivation ability of metal as well as metal oxide nanocomposites, mainly silver (Ag) and silver nanoparticles (AgNP), has also been proven to be very effective. Nanoscale silver particles deposited on CNTs showed great antimicrobial action against both Gram-negative and Gram-positive bacteria [234]. Ihsanullah et al. (2015a [215], 2015b [235], 2015c [236]) employed a wet chemistry strategy to fabricate three different kinds of Ag-doped CNT membranes using different quantities of silver (1, 10 and 20 wt %), and 100% of *E. coli* bacteria were killed by all the three membranes. The removal efficiency of nanometer-sized Ag-CNTs is attributed to the harmful effects of silver nanoparticles impregnated on CNTs [163]. However, antibacterial agents such as Ag can lead to bacterial resistance, thus limiting this mode of modification of CNTs. Ahmed et al. [237] reported the excellent antibacterial action of poly-N-vinyl carbazole-SWCNT nanocomposites (PVK-SWCNT) on bacterial species (Gram negative and Gram positive. A similar nanocomposite of SWCNT in poly(L-lysine) and poly(lactic-co-glycolic acid) polymers inactivates approximately 90% of bacterial species in water [238].

As with bacteria, viruses can also be adsorbed and removed efficiently by carbon nanomaterials. Commercial membrane filters impregnated with CNTs are capable of removing all viral cells from an influent containing 10^7–10^8 plaque-forming units [230,239]. The degree of removal of viruses depends largely on the thickness of the CNT layer [240]. Another important mechanism of CNMs' toxicity in microbes is the production of reactive oxygen species (ROS) such as H_2O_2 and O_2, which cause toxicity inside the microbial cells [241–243]. ROS bring about the oxidation of fatty acids present in the cell membrane, consequently damaging the permeability of the cell and important functions. According to Kang et al. [233], the working of genes responsible for detoxifying ROS, including catalase and superoxide dismutase, was markedly suppressed in the presence of SWNT

and MWNT. In addition, activation of the pathways of DNA damage and repair systems was also observed.

Small-diameter nanotubes (SWCNT) influence the bacterial cells to produce more stress-related gene products in comparison to large-diameter carbon nanotubes (MWCNT) [233]. Kang et al. performed gene expression experimentations and reported that metabolic pathways that are responsible for lipid recycling, membrane damage, and repair, namely glycolysis, fatty acid biosynthesis, and fatty acid beta-oxidation pathways, were up-regulated in the presence of single-walled carbon nanotubes but not expressed in MWNT presence. It was explained that the high expression of the fatty acid biosynthesis pathway leads to the production of new lipid molecules to be added into the bacterial cells for repairing membrane damage done by the nanomaterial or for cell growth. The up-regulation of fatty acid beta-oxidation pathways is responsible for the uptake of fatty acids from surrounding media; this showed that a greater amount of lipids from the membranes was being eliminated to the media because of cell death/membrane injury due to SWNT. The up-regulation of glycolysis suggests that the bacterial cells need to process more energy to overcome the stress induced by SWCNT and also because the by-products of this reaction (Acetyl-CoA) are commonly employed for the production of fatty acids for repairing the membrane [118].

4.2.2. Supercapacitors

Owing to the fossil fuel energy depletion and serious environmental issues, energy shortage has become a major problem faced by mankind. Renewable energy sources such as solar energy, geothermic energy, and wind energy can fulfill the energy crisis completely; however, they are limited due to geographical locations and available time [244]. Batteries, conventional capacitors, fuel cells, and electrochemical supercapacitors are the numerous energy storage devices. Among these, supercapacitors, also called electrochemical capacitors or ultra-capacitors, are the most efficient and appropriate energy storage devices (ESDs). These possess extremely high power density, superior specific capacitance, low cost, fast charge and discharge rates, broad operating temperature range, and long life cycle as compared to batteries and conventional capacitors [245,246]. Supercapacitors (SCs) are considered as green energy storage devices. SCs have been proven useful in the fields of portable electronics, transportation, memory storage, and power system [247,248].

Supercapacitors store charges by the development of a double layer at the electrode–electrolyte interface [249]. SCs, on the basis of the charge storage process, can be classified as electric double-layer capacitors (EDLC)s, pseudo-capacitors and hybrid supercapacitors [250]. EDLC store charges electrostatically by the absorption or desorption of electrolyte at the electrode interface [251]. Common electrode materials for EDLC include carbon-based materials such as graphene, activated carbon, carbon nanotubes, and carbon cloth [252]. However, EDLC exhibits much lower energy density in contrast to batteries [253].

Carbon-based materials are preferred as the electrode materials for supercapacitors due to their large surface area, excellent mechanical flexibility, high thermal and chemical stability, and high conductivity [254]. Among various carbon-based materials, carbon nanotubes (CNTs), both SWCNTs and MWCNTs, are of particular interest for electrode material owing to the excellent electrical conductivity and distinctive tubular porous structures, which favors fast ion and electron transportation [255]. However, the electrical performance of CNTs is limited due to their relatively small surface area. The electrical performance is controlled by several factors, such as specific surface area, pore size distribution, electrical conductivity, and pore size. The optimization of these factors, at the time of synthesis or post-treatment of CNTs, can lead to an enhanced supercapacitive performance. The structural properties such as diameter, length, and pore size play an important role in the EDLC, while pseudo-capacitance was observed in CNT-based supercapacitors due to the catalysts, functional groups, and impurities [256]. Pseudo-capacitors store energy through Faradic redox reactions that are fast and reversible [257]. Pseudo-capacitors display much

higher specific capacitance than EDLCs [246]. Electrode materials for pseudo-capacitors are various transition metal oxides and conducting polymers.

The first CNT-based supercapacitor electrode was developed by Niu et al. [258]. The electrode consists of irregular entangled and cross-linked CNTs, having various functional groups on the surface of MWCNT by functionalizing with nitric acid. This functionalized MWCNT exhibits a specific surface area of 430 m^2g^{-1}, with a gravimetric capacitance of 10^2 Fg^{-1} and an energy density of 0.5 Wh kg^{-1} using 38% sulfuric acid as the electrolyte. Most (90%) of the residue was removed, but the remaining residue would affect the overall performance.

Pure CNT electrodes show both characteristics of EDLC and pseudo-capacitance. The high specific capacitance of the pure CNT-based electrode is found to be around 100 Fg^{-1} [259,260]. Frackowiak et al. [261] studied the effects of diameters, elemental composition, structures, and micro-texture of CNT on capacitance [262]. Capacitance showed an increment by increasing the surface area. It was concluded that the most suitable CNTs for maximum capacitance are those with several edge planes. The rigid and straight CNTs show moderate performance despite the relatively high surface area. Higher surface area does not always show higher capacitance. This is because capacitance also depends on the pore size and its size distribution. The surface area is hardly accessible if it consists of micropores (2 nm).

Ahn et al. [263] also investigated these factors affecting the overall performance of supercapacitors fabricated using SWCNTs. Several factors, such as temperatures for annealing, binder composition, charging time, discharging current density, and current collector, have been optimized to get the desired performance of the supercapacitor. The change in specific capacitance of the electrode at different temperatures was studied. From the entire analysis, a maximum specific capacitance of 180 Fg^{-1} with a large power density of 20 kW kg^{-1} at an energy density of 6.5 Wh kg^{-1} was observed. It was reported that the capacitance of the CNTs that have a smaller diameter (33 nm) is higher than that of those with larger diameters (200 nm) owing to the enhanced specific surface area in smaller-diameter CNTs.

Jung et al. [264] developed anodic aluminum oxide (AAO) template-based CNTs with a uniform diameter (50 nm) using Co catalyst [265]. The AAO template leads to an enhanced capacitance by the formation of uniform diameter and length. The specific surface area of the electrode is observed to be 360 m^2/g with a specific capacitance of around 50 Fg^{-1}.

Heating is also a key factor that improves the graphitization of CNTs and removes amorphous carbon. Li et al. [266] showed that the specific capacitance was increased by oxidization up to 650 °C due to an increase in surface area. However, it decreases with further increase in temperature due to the decrease in surface area. This is because at high temperature, the average pore diameter decreases and saturates. At the same time, heating caused a reduction in the equivalent series resistance, resulting in an increment of the power density because of the improvement on graphitization.

The capacitance of CNT-based supercapacitors can also be improved by functionalization, chemical activation, and heat and surface treatment. Chemical activation of MWCNTs with KOH can lead to a highly developed microporous structure that increased capacitance to almost seven times in some cases. Functionalization with carboxyl groups led to a 3.2 times increment in capacitance owing to the enhanced hydrophobicity of MWCNTs in aqueous electrolyte. However, alkyl groups decrease the capacitance. In fact, longer alkyl groups cause a complete disappearance of capacitance due to the complete block of proton access to the CNTs' surfaces by intense hydrophobicity. Fluorine functionalization along with heat treatment also increases the specific capacitance of CNTs. The fluorination of SWCNT walls changed the nonpolar SWCNTs to the polar forms by producing dipole layers on the walls, resulting in more solubility in deionized water. Before heating, fluorinated samples show lower capacitance than raw samples due to the increased micropore area and decreased average pore diameter. However, after heating, the specific capacitance

was found to be higher than that of raw samples because of the additional redox reaction due to the residual oxygen gases existing on the surface of the electrodes. Plasma surface treatment with NH_3 also gives high capacitance values because of the increase in the total surface area and wettability of MWCNTs [260].

5. Carbon Dots

Fluorescent carbon nanomaterials have attracted a large amount of research interest in the last decade due to their excellent optical properties and incredible biocompatibility [267]. Carbon-based nanomaterials such as carbon dots (CDs), graphene, carbon quantum dots (CQDs), and graphene quantum dots (GQDs) are being deployed in a myriad of devices, bio-imaging agents, and biosensors. However, the widespread implementation of these materials is yet to occur. CDs were first derived in 2004 by Scrivens during the purification of single-walled carbon nanotubes produced by arc discharge procedures [268]. Since then, a number of synthesis methods have been introduced, including supported routes [269], combustion/heating, electrochemical synthesis [270], acidic oxidation, laser ablation, arc discharge, plasma treatment, hydrothermal methods, and microwave/ultrasonic methods. Carbon dots are quasi-spherical and discrete carbon nanostructures that are less than 10 nm size. Figure 15 shows the structure of carbon dots. On the contrary, GQDs comprise one to ten graphene layers with lateral dimensions of 100 nm. They have applications in in vivo nano-biotechnology due to high tissue transparency and low autofluorescence [271]. Although CDs and GQDs are both fluorescent quantum-confined carbon materials, they differ when it comes to their physical and chemical properties. The reason for this difference lies in their different spatial geometry [272]. The following subsection discusses the synthesis of carbon dots.

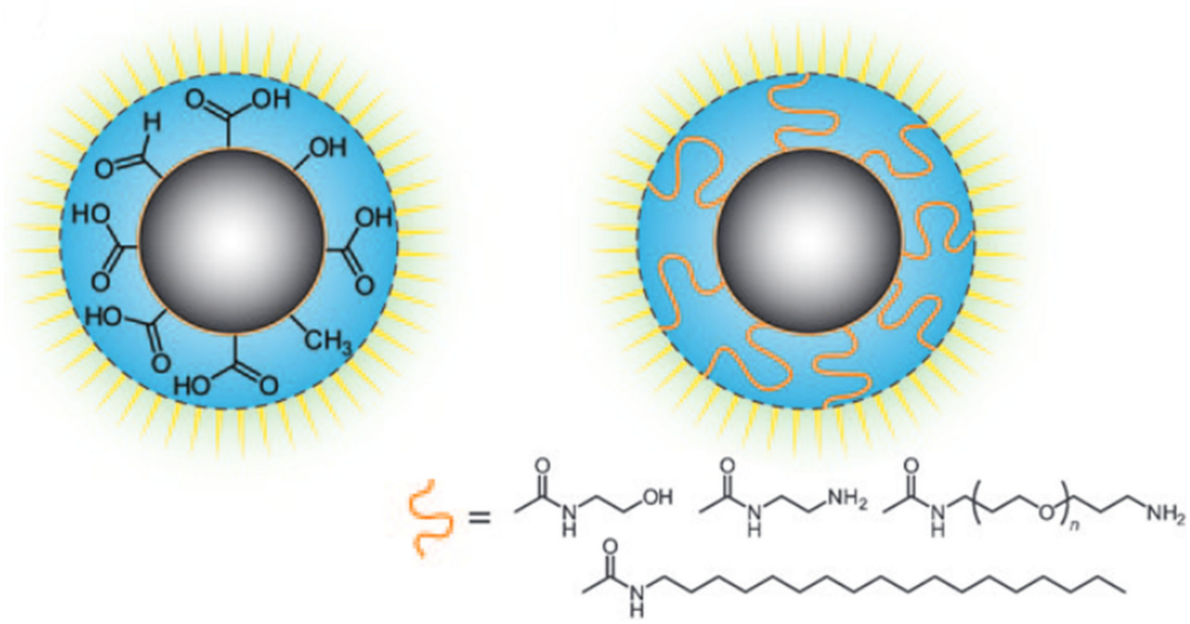

Figure 15. Structural illustration of CQDs. Reprinted with permission from Ref. [273]. Copyright 2020 American Chemical Society.

5.1. Synthesis of RH-Derived Carbon Dots (CDs, CQDs, GQDs)

The synthesis of rice waste-derived carbon dots has attracted much attention from researchers and much work is being done to explore the more efficient utilization of rice waste for the synthesis of carbon dots. Some of the synthesis approaches for fabricating carbon dots (CDs), carbon quantum dots (CQDs), and graphene quantum dots (GQDs) have been discussed in the following section.

5.1.1. Thermal Calcination

Thermal calcination is a novel route that is a facile, fast, low-cost, and green method to detect metal ions with high sensitivity and selectivity. Chaudhry et al. [147] developed a thermal calcination strategy followed by the pyrolysis of edible seeds including rice, pearl millet, wheat, and sorghum seed. These seeds are the principle cultivating crops that are an easily accessible, universally used, and cost-effective resource for the synthesis of highly luminescent CQDs, making this process unique. Under a nitrogen atmosphere, thermal calcination was carried out at 400 °C for two hours in a muffle furnace. CQDs were successfully synthesized: namely, CQD_1 (sorghum), CQD_2 (millet), CQD_3 (rice), and CQD_4 (wheat). Then, the black powders were cooled at room temperature and ground. They exhibit excellent luminescence properties and controlled stability. The material was studied using HR-TEM, SAED (selected area electron diffraction), and XRD, and its chemosensing potential was investigated for the identification of Cr^{3+} ions from water. The complete synthesis process is summarized in Figure 16. The use of any external template is not required for the sensitivity and stability of NPs, making it cheap and beneficial for practical applicability. Studies revealed that the activity of CQDs was tested by the fungus *Echinodontium taxodii*. When nanoparticles are present, the relative colonial size of the fungus did not show any reduction, which successfully proved the biocompatibility of the nanoparticles.

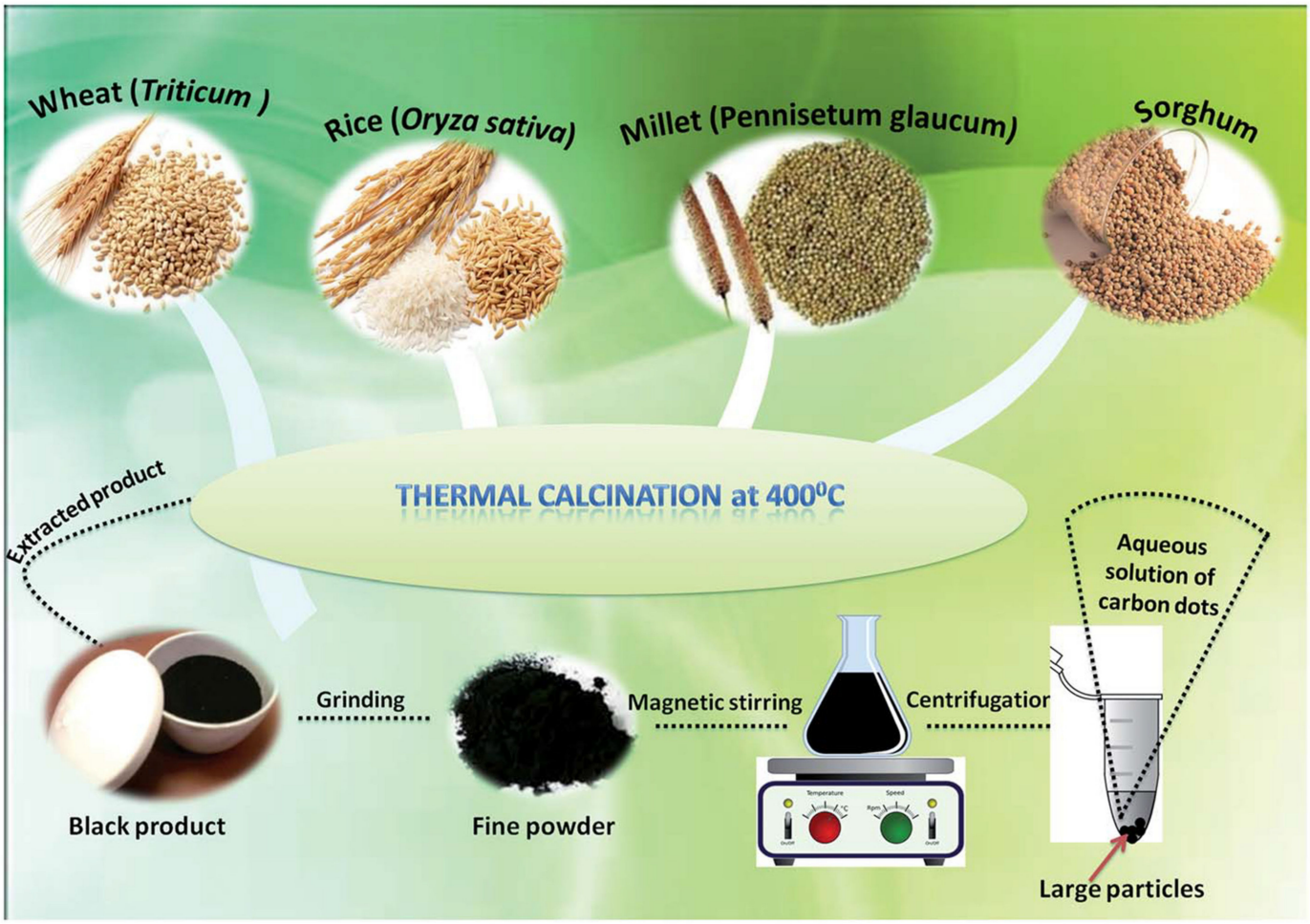

Figure 16. Complete illustration for the synthesis of CQDs. Reprinted with permission from Ref. [147]. Copyright 2016 RSC Publishing.

Zhu et al. [273] synthesized Si-CQDs from rice husk pyrolysis under nitrogen atmosphere at a temperature of 700 °C for 2 has represented in Figure 17. The as-synthesized Si-CQDs, with 8.1% quantum yield, showed blue luminescence color.

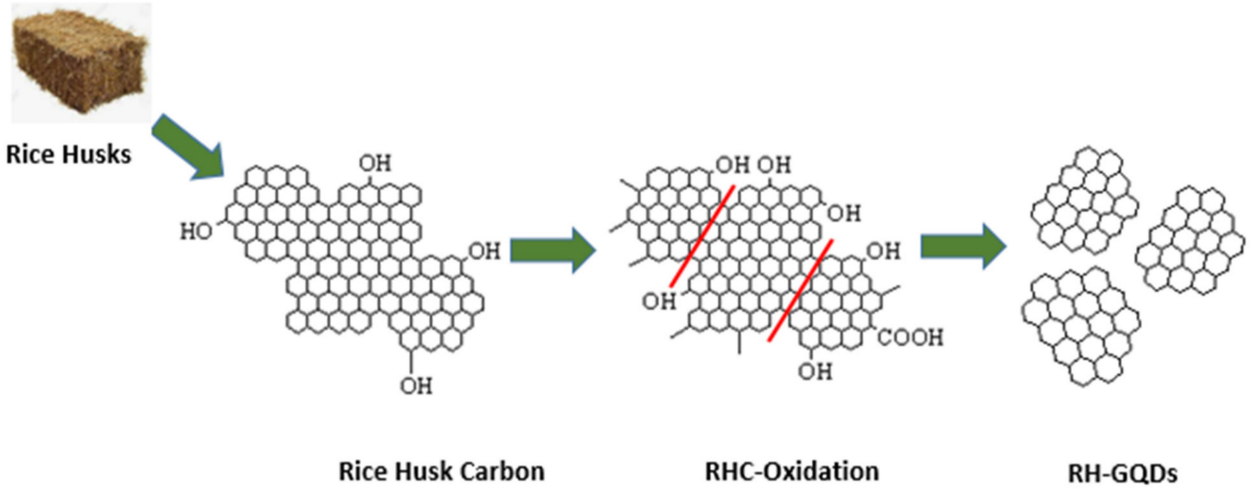

Figure 17. Bottom–up approaches for the preparation of biomass derived GQDs by acidic oxidation. Reprinted with permission from Ref. [273]. Copyright 2020 American Chemical Society.

5.1.2. Microwave Hydrothermal

Rice straw, as a vital by-product of rice crops, is a conventional material having low cost and huge quantity. The major 40 constituents of rice straw are lignin, cellulose, hemicelluloses, and rice carbon content, which acts as a basic source of carbon-based nanomaterials [274,275]. The strong hydrogen bonding inside the structure of cellulose as well as hemicelluloses inhibits their dissolution in conventional solvents: namely, water, tetrahydrofuran, and ethanol. Thus, the direct application of hydrothermal carbonization to rice straw is limited [276]. Ionic liquids (ILs) are green alternatives for traditional solvents having high stability, good recyclability, and the potential to dissolve oligosaccharides biopolymers including chitin, cellulose, and starch. Liu et al. [274] reported an unprecedented approach for highly photoluminescent heteroatom-doped carbon dots by the application of a microwave–hydrothermal method to rice straw in a mixture of solvents, i.e., water and ionic liquid (1-allyl-3-methylimidazolium chloride, AMIM-Cl, (Figure 18). The IL acts as a reaction media to solvate the cellulose of straw, and it also acts as a nitrogenous source for the heteroatom-doped carbon dots produced. The as-synthesized CDs were used as an efficient label-free fluorescent sensor for the determination of Fe (III) ions with high sensitivity and selectivity and low detection limit (LDL) of 200 nM. The IL-CDs were studied using TEM, UV/Vis, FTIR, and AFM analysis techniques.

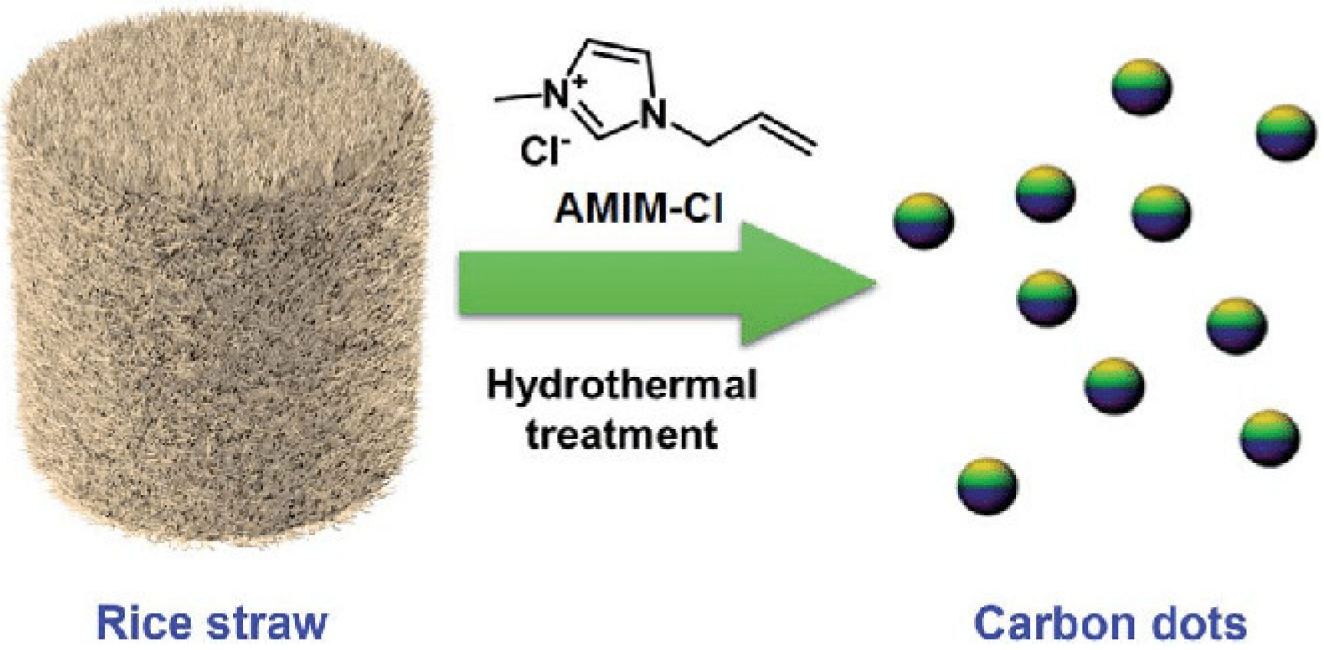

Figure 18. Schematic Illustration for the ionic-liquid-promoted microwave–hydrothermal synthesis of CDs using straw as starting materials. Reprinted from Ref. [274].

5.1.3. Hydrothermal Carbonization/Acid Oxidation

Mandal et al. [277] demonstrated the production of water-soluble carbon quantum dots (CQDs) by carbonizing rise straw biomass as a source of carbon. The as-prepared CQDs were highly luminescent, stable, and in the form of a black powder [278,279]. These CQDs synthesized in the water phase were highly specific for the bacterial cell membrane. Then, Mandal et al. demonstrated a fluorescence measurement method by using these CQDs as a fluorescence marker for the fast detection of bacteria only and their counting within the shortest time from any sample of environment.

A facile synthesis method of carbon dots was demonstrated by Thongsai et al. [280] by employing the hydrothermal treatment as illustrated in Figure 19. This yielded brown-colored solid carbon dots that have a 3% quantum yield, diameter of 4–5 nm, and showed blue emission with exceptional photostability. XPS characterizations and FT-IR spectroscopy reported the existence of hydrophilic functional groups on the external surface of CDs. These functional groups show strong forces of interactions with small molecules, making the carbon dots an excellent chemical probe. In addition, these interactions are also the basic cause for the emission characteristics of the CDs [281,282]. DLS (dynamic light scattering) and TEM analysis techniques were used to identify the morphology and size of the CDs. UV-vis and fluorescence spectroscopy were employed to detect the optical properties of the carbon dots. The as-synthesized carbon dots have the potential to detect alcohol vapors at room temperature. These CDs were also used as a sensing probe in an optical electronic nose system to distinguish between ethanol, methanol, and other volatile organic compounds.

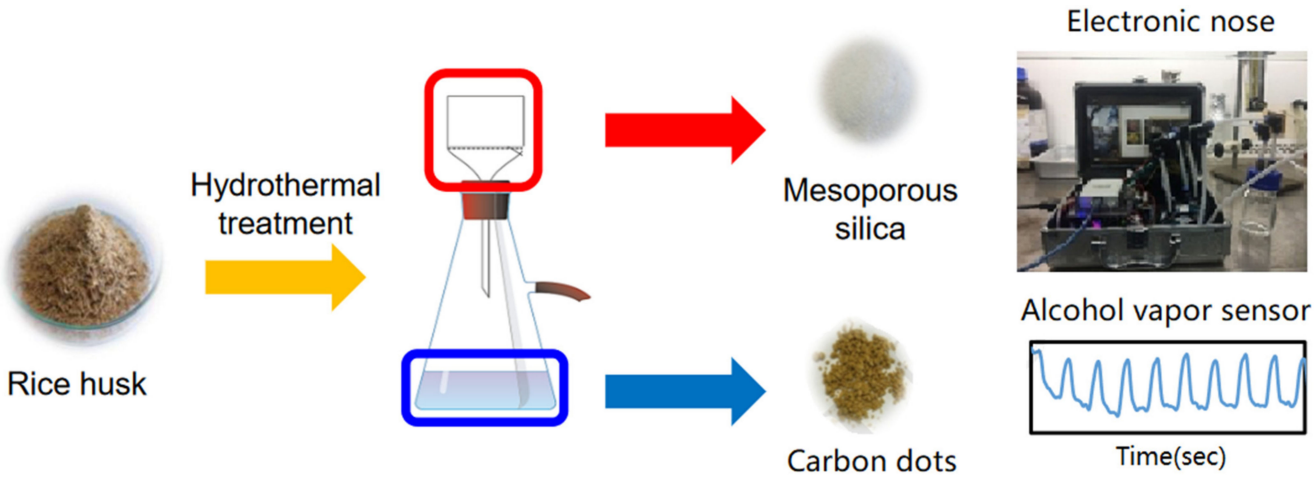

Figure 19. Schematic representation for synthesis of carbon dots from rice husk. Reprinted with permission from Ref. [280]. Copyright 2019 Elsevier.

Abidin et al. [283] developed RH-derived CQDs and demonstrated the effect of introducing functional groups on RH-derived CQDs. Rice husks were pretreated for easy carbonization of rice husk during the hydrothermal process. For obtaining enhanced purification, carbon quantum dots were dialyzed against deionized water in Visking tubing (Cellulose 10 M) for one day. FTIR, UV-Vis, HRTEM, XRD, thermogravimetric analysis, and XPS analysis techniques were employed to characterize CQDs. Functionalization yields clearer spherical CQDs due to the binding of functional groups: $–NH_2$ (from EDA), and –COOH (from ascorbic acid) to the structure of carbon quantum dots [284]. Due to the presence of functionalizing agents, the functionalized CQDs were observed to be smaller in size than the non-functionalized CQDs. This can be attributed to alkaline (protonation of CQDs) or acidic (deprotonation of CQDs) condition. The as-synthesized functionalized N-CQD and CCQD were used as in the sensing for cadmium ion and its removal from water.

Wang et al. [285] reported the synthesis of high-yield carbon quantum dot-grafted silica nanoparticles (silica–C NPs) using rise husk as the precursor. The strategy is summarized in Figure 20. In addition, the production of carbon quantum dots from RHs by the removal of silica was also carried out. The water-rinsed rice husks (5 g) were subjected to pyrolysis in a tube furnace under nitrogen atmosphere (700 °C for 2 h), resulting in the synthesis of RHA containing both silica and carbon. RHA is treated with 1.0 M NaOH at 100 °C for 2 h for the removal of silica. Then, RHA, containing carbon content only, was subjected to oxidation by using H_2SO_4 and HNO_3 in two steps; each step was followed by ultrasonication, resulting in a black dispersion. This is followed by vacuum filtration by the use of a 0.22 mm microporous membrane and then washed several times with deionized water. The black-colored sample was again dispersed in 30 mL of deionized water and transferred to a 40 mL Teflon-lined autoclave. The dispersion is treated hydrothermally at a temperature of 200 °C for 10 h. Then, it is cooled to room temperature and refiltered. RH-CQDs were reported successfully in the resulting filtrate. Further drying the filtrate at a temperature of 40 °C in a vacuum oven yields a solid powder of CQDs.

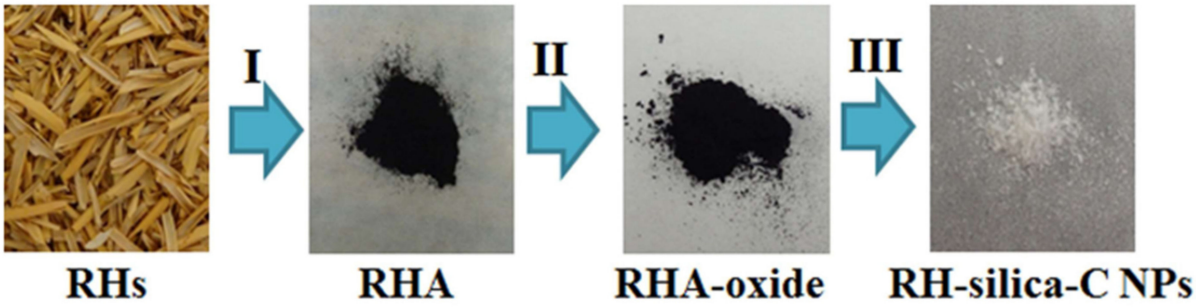

Figure 20. Transformation from RHs to RHA and to RH–silica–CNPs (i. Pyrolysis under nitrogen atmosphere, ii. Oxidation, iii. Carbon grafting, framework cutting, and oxygen-containing group reduction). Reprinted with permission from Ref. [285]. Copyright 2017 The Royal Society of Chemistry.

Wongso et al. [286] synthesized CQDs from the same procedure as described in the previous study (Wang 2017) but with some modifications. CQDs were fabricated without the use of functionalizing agents, and the process was modified by the addition of NaOH to vary pH value from 0 to 14. The mechanism involves intercalation followed by exfoliation. Intercalation is initiated when RHA is dispersed in a mixture of sulfuric acid and nitric acid. Afterwards, exfoliation is started by washing RHA with DI water, yielding carbon quantum dots. The material was studied using HR-TEM and EDX techniques. Changing pH conditions does not affect the crystal structure of the samples, but it alters the size of CQDs and the number of oxygen functional groups on their surface. Distinctive sizes arise due to the existence of NaOH having the ability to react with nitric acid and give $NaNO_3$. When HNO_3 is completely treated with NaOH (assumed at pH neutral), the excess NaOH acts as an oxidant to increase the intercalation process of RHA. Photoluminescence spectroscopy revealed that varying the pH of synthesis broadens the emission wavelength of carbon quantum dots from green photoluminescence to cyan–orange photoluminescence. Both carbon and silica were completely used in this study, which is in agreement with previous studies. A methodological bibliography of rice waste-derived carbon nanomaterials is represented in Table 3.

Table 3. Methodological bibliography of carbon-based nanomaterials from rice biomass.

Precursor/ Raw Material	Synthesis Method	Reaction Conditions	Chemical Agents	Final Product	Characterization Technique	References
Rice Husk	Chemical Activation	400–900 °C	KOH	Few-layered graphene	TEM	[65]
Rice Straw	Chemical Activation	700 °C	KOH	Graphene	FESEM, SEM, EDX, AFM, and FETEM	[66]
Rice Husk	Chemical Activation	850 °C/2 h	NaOH, KOH	Multilayered graphene Oxide	FTIR, Raman, SEM, TGA, and TEM	[35]
Rice Husk	Microwave-Assisted Synthesis	650–750 °C	Ethanol, ferrocene catalyst	Graphene	RD, FESEM, FTIR, UV-Vis, Zeta Sizer, and EDX	[67]
Rice Bran	Microwave-Assisted Synthesis	300 °C/15 min	Ferrocene	Graphene Oxide	SEM, HR-TEM, XRD, FTIR, TGA/DTA	[72]
Rice Straw	Microwave-Assisted Synthesis	N/A	Ferrocene catalyst	Graphene Oxide	FTIR, SEM, TEM, EDS, Raman	[36]

Table 3. *Cont.*

Precursor/ Raw Material	Synthesis Method	Reaction Conditions	Chemical Agents	Final Product	Characterization Technique	References
Rice Husk	Pyrolysis	300–400 °C/10 min, Inert atmosphere	N/A	Graphene Oxide Nanoflakes	XRD, EDS, FESEM, TEM, HR-TEM	[37]
Rice Straw	Chemical Vapor Deposition	800 °C/120 min Heating rate 10 °C/min	Ethanol, ferrocene, or ferrocene nickel nitrate catalysts, camphor substrate, N_2 gas	Small outer diameter coiled bundles of CNTs Large outer diameter straight bundles of CNTs-	SEM, TEM, Raman, TGA	[27]
Rice Husk	Microwave-Assisted Synthesis	600 W power, 2.45 GHz frequency/38 min	Ferrocene catalyst, ethanol	Spherical and tubular structures of carbon nanotubes	FESEM	[143]
Rice Husk	Microwave-Assisted Synthesis	N/A	H_2 and Ar gas	Fiber-like Graphenated carbon nanotubes (g-CNTs)	N/A	[25]
Rice Straw	Pyrolysis	830 °C/60 min	Urea solution, Fe, Ni, and Co catalysts supported on alumina	Carbon nanotubes on Fe-Ni/Al_2O_3	TEM, SEM, FTIR	[144]
Rice	Thermal Calcination	400 °C/2 h, N_2 atmosphere	N_2 atmosphere	Carbon Quantum Dots	HR-TEM, SAED, XRD	[147]
Rice Husk	Thermal Calcination	700 °C/2 h, N_2 atmosphere	N/A	Blue luminescent Si-CQDs	N/A	[273]
Rice Straw	Microwave Hydrothermal	N/A	Ionic liquid (as a solvent)	Heteroatom-doped carbon dots (IL-CDs)	TEM, UV-Vis, FTIR, AFM	[274]
Rice straw	Hydrothermal Carboniza-tion/Acid Oxidation	N/A	HNO_3	Water-Soluble CQDs	N/A	[277]
Rice Husk	Hydrothermal Carbonization	200 °C/6 h	HNO_3	Blue luminescent CDs	FTIR, XPS, DLS, TEM, UV-Vis, Flourescence	[280]
Rice Husk	Hydrothermal Carbonization	190 °C/2 h	EDA, ascorbic acid (functional-izing agents)	Functionalized N-CQDs and CCQDs	FTIR, UV-Vis, HR-TEM, XRD, TGA, XPS	[283]
Rice Husk	Hydrothermal Carbonization	200 °C/10 h, N_2 atmosphere	H_2SO_4, HNO_3	Carbon quantum dot grafted silica nanoparticles (silica–C-NPs)	N/A	[285]

5.2. Applications of RH-Derived Carbon Dots

Energy deficiency, ecological disintegration, and expanding client requests have driven researchers to create minimal effort, superficial, low-cost, green courses for the creation of novel advanced nanomaterials from sustainable resources. These biomass-derived nanomaterials have broad applications in the storage of hydrogen, biomedicine, sorption materials, heavy metal detection, supercapacitors, and so on [2]. Various applications of graphene quantum dots, carbon quantum dots, and carbon dots will be discussed here.

5.2.1. Bioimaging

Biomass is acquiring a lot of consideration as a raw material due to its low cost, high carbon content, sustainability, and simple transformation into graphene quantum dots (GQDs) [2]. The GQDs are biocompatible, highly radiant, dispersible in several solvents, and non-poisonous for incorporation onto gadgets of bio-imaging i.e., supercapacitors, batteries, light-emitting diodes, and photovoltaics [287–292]. GQDs derived from rice husk are readily dispersible in water with enhanced photoluminescence and have incredible biocompatibility; hence, they are broadly applied for biomedical applications, especially in bio-imaging [2]. To culture different living cells HeLa cells, MCF-7 cells, HepG2 cells, and biomass-derived CQDs are frequently employed [273]. Wang et al. [31] investigated the biomedical applications of rice husk-derived graphene quantum dots; they are best fit for the bio-imaging of Hela cells, which is the most commonly used and oldest immortal human cell line used in cancer research [293]. In order to explore the ability of RH-GQDs as real bio-probes, their biocompatibility was examined by analyzing the toxicity and cell viability of HeLa cells pretreated with different quantities of RH-GQDs. After incubating for a day or two, RH-GQDs showed less toxicity on Hella cells at low concentrations. At higher concentrations (100 μg/mL), they showed cell viability greater than 90%. After treatment on HeLa cells, no damage to cellular morphology was noticed. These outcomes demonstrated that the rice husk-derived GQDs have exceptional biocompatibility, making them suitable for biomedical applications. Moreover, the in vitro bio-imaging of HeLa cells treated with RH-GQDs (having cell viability almost 100%) was examined using a fluorescent microscope. The cells joined with RH-GQDs displayed solid blue photoluminescence in cytoplasm, and the internal cell morphology could be examined. The glow of HeLa cells/RH-GQDs was consistent and reproducible, proposing the attainability of using the water-dispersible graphene quantum dots in cell imaging. The fluorescent RH-GQDs can viably enter the cytoplasm of cells for imaging with great biocompatibility; hence, they are considered to be excellent fluorescent bio-probes.

Since biocompatibility is vital for biomedical applications, rice husk-derived carbon dots (CDs) were subjected to cytotoxicity tests utilizing MTT assay on MCF-7 breast cancer cells. First, 80 μg/mL of carbon dots was used, and cells were exposed for about 72 h. After incubation, CDs showed incredible biocompatibility and a cell viability more prominent than 80%. Therefore, CDs derived from rice husk are declared as great biocompatible nanomaterials to be employed in different biomedical applications such as bio-sensing, cell imaging, and nanomedicine [280].

N-CQDs (nitrogen-doped carbon quantum dots) synthesized from rice husk are used extensively in cell imaging owing to their high stability, cellular compatibility, and less toxicity. Multicolored N-CQDs were utilized in in vitro fluorescent bio-imaging by Qi et al. (2019) [28]. The cytotoxicity of carbon quantum dots was studied using the CCK-8 assay with HepG2 cells (human hepatoma HepG2 liver cells). The cytotoxicity of N-CQDs was less than that of CQDs; however, the cell viability of N-CQDs was more prominent than 85%, indicating the lower toxicity and excellent biocompatibility of the N-CQDs. Intracellular regions of HepG2 cells treated with N-CQDs showed solid green fluorescence. N-CQDs due to their strong biocompatibility can be used effectively for the imaging of Fe^{3+} ions and tetracycline in liver cells [28].

5.2.2. Removal of Cadmium

Metal ions are significantly important because of their existence in a biological system and climate. Therefore, metal ions are considered as potential analytes because they carry a positive charge; therefore, they had a high chance of associating with the oxidized surface of the CNPs [294]. Fluorescent CQDs have broad applications in the detection and removal of metal ions owing to their extensive absorption spectra and variable emission wavelength [295]. Cadmium (Cd^{2+}) is a heavy metal that causes environmental contamination and affects human well-being [296]. Abidin et al. (2020) reported a detection and removal mechanism of cadmium ions using CQDs derived from rice husk [297]. The functionalization of GQDs upgrades the cooperation with metal particles and adjusts the bandgap [298]. f-CQDs, with an ideal measure of ascorbic acid and EDA (functionalizing agents) are used for the adsorption and removal of cadmium ions from water. Cadmium nitrate solution of various concentrations was prepared for testing the capacity of functionalized CQDs in the detection of metal ions, and their removal was assessed by estimating the difference in concentration before and after the addition of functionalized CQDs in the solution of cadmium nitrate at various contact times. The photoluminescent intensity (PL) of functionalized CQDs diminishes with an increased quantity of cadmium solution blended with carbon quantum dots. The quenching of the CQDs structure occurred upon the expansion of heavy metal ions. The interaction among Cd^{2+} ions and CQDs prompts electron transfer from the carbon dots to heavy metal ions. The electrostatic association among positively charged metal ions and negatively charged CQDs assumes a significant part in measuring PL quenching [283]. The greater the pH value, the greater the adsorption limit with regard to both amino and carboxyl-functionalized CQDs to eliminate Cd^{2+} ions. For carboxyl-functionalized CQDs, when pH was varied from 2 to 8, the percentage of cadmium removal increases gradually from 75 to 76%. Whereas, for amino-functionalized CQDs, the cadmium removal expanded from 75.8 to 76.8%. At a pH value of 10, a higher removal of cadmium was seen [299]. Hence, increased pH results in higher cadmium removal. At a higher pH, the Cd^{2+} and Cd $(OH)^{+}$ ions trade hydrogen to assemble electrostatic interactions with amine and carboxyl groups in carbon dots. In addition, hydrogen bonding between the functional groups on CQDs and Cd $(OH)^{+}$ ions may occur, resulting in stable colloids in solution. Consequently, cadmium ion removal gets simpler at higher pH conditions. Amino-functionalized CQDs can eliminate a higher percentage of cadmium in contrast to carboxyl-functionalized CQDs because the functionalization agent EDA for amino-functionalized CQDs is higher contrasted with ascorbic acid for carboxyl-functionalized CQDs during the synthesis of CQDs. Great adsorption sites are present for collaboration among negatively charged carbon quantum dots and the positively charged metal ions. Hence, the binding energy of metal–CQDs gets stronger. Metal clusters formed at this point will finally diffuse across the surface of CQDs, promoting simple elimination of the metal particles [300]. Meanwhile, the decreased potential of cadmium solution improves the capacity of CQDs to eliminate cadmium ions from water [301]. Yang and Li et al. [302] have demonstrated that the performance of CQDs in Cd removal was excellent; in the initial 20 min of contact time, 85% of cadmium removal was accomplished. The impact of NaCl solution on the removal of cadmium was observed with the increase in sodium chloride concentration; by utilizing both amino and carboxyl-functionalized CQDs, the percentage removal of cadmium diminishes as a result of the decreased adsorption limit of CQDs with expanding salt concentration [283].

5.2.3. Detection of Bacteria

In microbiology, biotechnology, clinical determination, and sanitation, the quick and sensitive detection of bacteria is critical. As a result of slow detection speed and the muddled system of the traditional detection method such as plate count, the fast and productive detection of microbes is not possible. Fluorescence measurement methods are being used nowadays for sensing microbes. For rapid detection of bacterial count and its imaging, bacterial sensors have been developed by Mandal et al. employing specific

water-soluble CQDs, which are utilized due to their high-density consolidation of surface carboxylation [277]. Results revealed that the fluorescence signals of the bacterial cells coupled with CQDs < 100 nm were seen 30–40 min later after the addition of the CQDs solution to the bacterial culture broth, and signals for bacterial cells coupled with >100 nm CQDs were invisible 30–40 min after the cell was cultured. A lot of radiant bacterial cells were seen under a fluorescent magnifying instrument. Rice straw-derived water-soluble CQDs of size < 100 nm bind on the specific bacterial cell surface; this shows that the free carboxylic acid (functional group) of smaller-sized water-soluble CQDs binds more rapidly to the amine groups, i.e., proteins, peptides, and amino acids present on the surface of bacterial cells rather than other microbial organisms [303–308]. A single bacterial cell membrane carries many proteins, but only one protein binds to many water-soluble CQDs conjugates. This fluorescence technique detects bacterial count in the shortest time, which is at least 20–30 times lower than ordinary bacterial counting methods. It is inferred that a profoundly iridescent, specific bacterial surface and stable water-soluble CQDs have the capacity for quick and sensitive fluorescence detection of bacteria.

5.2.4. Fluorescent Probes for Setecting Fe^{3+} and Tetracycline

Rice waste contains a lot of carbohydrates and proteins, which can be used as a source of carbon and nitrogen for the production of CQDs. N-CQDs derived from rice residue by one-step hydrothermal treatment were used as a fluorescent probe in the detection of Fe^{3+} and tetracycline, as shown in Figure 21. N-CQDs were observed by a fluorescence microscope; by observing fluorescent quenching, the sensitive and selective detection of Fe^{3+} ions and tetracycline (TCs) was evaluated [28].

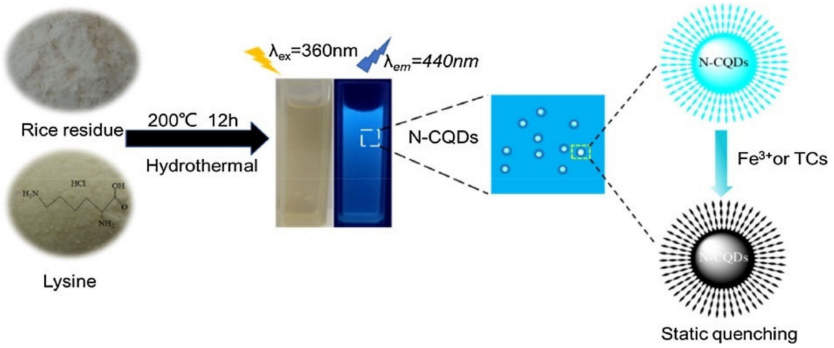

Figure 21. Fluorescent carbon dots produced by hydrothermal process used for detecting Fe^{3+} and tetracycline. Reprinted with permission from Ref. [28]. Copyright 2019 Elsevier.

Iron particles (Fe^{3+}) assume a significant part in the natural framework and are present in all body tissues, particularly in the liver, lungs, and spleen. Any variation in Fe^{3+} content can lead to infections, for example, paleness, Alzheimer's sickness, Parkinson's illness, cancer, diabetes, and hemochromatosis [309]. Consequently, the identification of Fe^{3+} ions is significant for the early analysis of these infections. Fluorescence spectrometry is an emerging strategy with high selectivity, affectability, and broad linear range for the fast and efficient testing of heavy metal ions. N-CQDs can be utilized as a fluorescent probe for the detection of Fe^{3+} ions with enhanced sensitivity and selectivity. Research conducted by Zhang et al. (2014) [310] revealed that the N-CQDs probe happened to be cell-permeable and was able to detect Fe^{3+} and tetracycline (antibiotic medication) in the living organisms. Quenching of the fluorescence of N-CQDs is due to the association of Fe^{3+} ions with the phenolic hydroxyl groups present on the surface of N-CQDs. With the increase in Fe^{3+} concentration, fluorescence was quenched dramatically. N-CQDs can be used as a sensor for the detection of Fe^{3+} with a 0.7462 mM limit of detection (LOD) [28].

GQDs are utilized in different organic and clinical fields owing to their low toxicity, phenomenal biocompatibility, enhanced dissolution, and uncommon electronic and optical properties. Ion sensing by the use of GQDs has pulled in much consideration nowadays.

Wang [33] synthesized GQDs from rice husk. Then, the specific quenching of RH-GQDs was examined with various metal ions. Fe^{3+} ions showed an obvious luminescence quenching in contrast to other metal ions as the RH-GQDs exhibited highly selective quenching of Fe^{3+}. This makes GQDs promising sensors for the detection of Fe^{3+} ions. The quenching process demonstrated that integrated GQDs were profoundly specific and delicate toward Fe^{3+} ions and accordingly utilized for Fe^{3+} detection. Different concentrations of Fe^{3+} solution with other metal ion solutions were prepared. Samples were studied by a fluorescence spectrophotometer. The scattering displayed intense blue luminescence. Different heavy metal ions were blended with the RH-GQD dispersion and examined, but the most obvious and best quenching was seen by Fe^{3+} ions. Other metal ions were unable to exhibit significant quenching. Hence, RH-GQDs quenching is exceptionally specific toward Fe^{3+} ions and in this manner conceivably appropriate for detecting Fe^{3+} ions. The quenching percentage was observed for Fe^{3+} ions at low concentrations (below 0.3 mM), but when the concentration was increased above 0.3 mM, the quenching decreases.

Antibiotic medications tetracyclines (TCs) are broadly utilized as anti-toxins in veterinary and humans. These antibiotics can aggregate in food items due to their unreasonable growth, which is a danger to human health [310]. Excessive use of tetracycline causes teeth yellowing, damage of the liver, and other allergic reactions. Various methods are available for the detection of tetracyclines, but a simple, quick, cheap, delicate, and selective method is fluorescence. N-CQDs are being significantly applied as probes for Fe^{3+} ions and antibiotic tetracycline (TCs) detection with great accomplishment [28]. For this purpose, N-CQDs prepared from rice husk were blended with specific amounts of organics such as BSA, lysine, tetracycline, EDTA, cysteine, glycine, erythromycin, chlortetracycline (CTC), vitamin C, terramycin (OTc), and glucose, and studied by fluorescence spectroscopy. Due to their structural compatibility to TC, both terramycin and chlortetracycline approach the binding sites and decrease the sensor fluorescence. By adding TCs into N-CQDs, the fluorescence diminished significantly. This shows that with an increase in tetracycline concentrations, the fluorescence intensity of nitrogen-doped CQDs diminishes. The detection limit of tetracycline was found to be 0.2367 mM and the linear range was 3.32–32.26 mM. Therefore, N-CQDs are considered as low-cost, specific eco-friendly sensors for recognizing antibiotic medication analogs, showing their incredible guarantee for applications in environmental monitoring.

5.2.5. Detection of Volatile Organic Compounds (VOC) and Alcohol Vapors

Carbon dots produced from rice husk precursors are amazing fluorophores for applications that demand great photostability. Carbon dots are considered as sensitive probes with excellent binding properties because of their great photostability, high polarity, and increased surface area to be used in sensing applications. CDs derived from rice husk can be incorporated into an optical–electronic nose to be utilized for the detection of alcohol vapors and VOCs by observing changes in optical absorptivity [280]. The diagrametical representation of the strategy is shown in Figure 22. These volatile organic compounds are commonly utilized in labs and industries. Long exposure to VOCs causes serious health issues. Therefore, estimation of VOCs in surroundings is of great interest. The electronic nose is a quick and steady instrument that has the potential to reproduce the olfactory system of humans. It is broadly utilized in the detection of gases and vapors [311–313]. In addition to alcohol vapor detection, the CDs are also used to recognize the other VOCs such as ketone, dichloromethane, diethyl ether, hexane, toluene, and various ratios of ethanol and methanol. The presence of various types of functional groups on the surface of carbon dots and their stable optical properties allow them to be utilized for detecting heavy metal ions, biomolecules, and chemical compounds [314]. CDs are particularly employed for polar VOCs detection because of their huge surface area as well as the hydrophilic functional groups that act as binding sites for VOCs. Thongsai et al. (2019) detected alcohol (ethanol and methanol) vapors and VOCs using an optical electronic nose system. The sensor response relative to the changes in the light intensity transmitted through

the carbon dot film was estimated. Observations showed that the carbon dots displayed strong stability and high sensitivity toward alcohol. The effect of solvation of VOC on the CDs prompted a change in optical absorptivity. Due to various polar interactions, different sensitivities of carbon dots toward different VOCs were observed. The carbon dot-incorporated optical electronic nose provides a facile sensor for alcohol vapors and VOC that works at room temperature. This system can be utilized to detect and distinguish volatile organic compounds based on polar–polar interactions. Moreover, carbon dots can also detect various other solvent vapors such as diethyl ether, acetone, dichloromethane, hexane, and toluene.

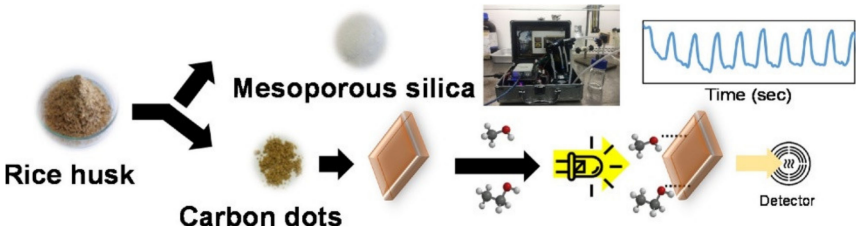

Figure 22. Graphical representation of synthesis of carbon dots from rice husk and their applications in VOC and alcohol vapors. Reprinted with permission from Ref. [280]. Copyright 2019 Elsevier.

6. Conclusions and Future Perspectives

The emerging worldwide energy crisis and climate change have imperiled the survival and evolution of human culture; therefore, demands for innovative technologies that provide materials of high performance and superior properties have increased. In this regard, nanotechnology has arisen as an amazing asset for the scientific community to develop advanced high-yield engineered nanomaterials. Various technologies have been developed for manufacturing CNMs, but green synthesis methods using low-value waste materials are acquiring more interest because of their abundant availability, ease of modification, low toxicity, renewability, unique structural, and biodegradable properties; therefore, developing modern technologies for the fabrication of carbon-based nanomaterials via simple, eco-friendly, low cost, sustainable routes through the utilization of low-valued biomass waste (natural and abundant renewable source), especially agricultural residues, has been in increasing demand for researchers. This review focuses on rice residue, an agricultural biomass waste that contains high carbon and silica content, for use as starting precursors to fabricate versatile highly valued carbon nanomaterials such as graphene, carbon nanotubes, and carbon dots and their broad range of energy-related, biomedical, and environmental applications. These versatile rice residues-derived nanomaterials could be joined in different ways to create innovative systems with remarkable physicochemical, electrical, optical, mechanical, and bio-compatibility properties in contrast to their pure and isolated forms.

Rice husk when used as a raw material for the synthesis of carbon-based nanomaterials requires its essential pre-treatment that leads to additional reaction conditions and requirements. This serves as a limitation for the use of rice husk. As a consequence of this limitation, we must design experiments that would not require its pre-treatment and ease its use. The applications of rice husk carbon-based nanomaterials are not only limited to the treatment of water pollution; different procedures can be designed in this manner to extend the use of biomass-derived carbon-based nanomaterials for the treatment of air pollution and soil contamination.

In this review, we have summarized the recent development of nanomaterials derived from rice biomass: their versatile synthesis strategies, remarkable properties, and promising application in various disciplines. For a sustainable future, it is crucial to utilize low-valued, abundant, and natural renewable resources for the fabrication of high-value nanomaterials at low cost, find diverse applications in water remediation, and accomplish more efficient cost-effective, convenient, and eco-friendly innovative technologies to overcome environmental issues and expand energy demands. Consequently, exceptional

consideration has been centering toward these materials to address the above issues and make them a prospective contender for the assistance of the humankind.

Author Contributions: Corresponding author, Conceptualization, Project administration and supervision, S.M.; Writing—Original draft and resources and methodology, N.Q.; Writing—Original draft and editing, Z.S.; Validation and visualization, A.S.; Validation and visualization, A.K.; Writing—Review and editing, M.I.; Validation and visualization, F.H. All authors have read and agreed to the published version of the manuscript.

Funding: This research received no external funding.

Data Availability Statement: The data presented are available in the below listed references. Further can be provided on demand from corresponding author.

Conflicts of Interest: Authors declare no conflict of interest.

References

1. Ouyang, J.; Zhou, L.; Liu, Z.; Heng, J.Y.; Chen, W. Biomass-derived activated carbons for the removal of pharmaceutical mircopollutants from wastewater: A review. *Sep. Purif. Technol.* **2020**, *253*, 117536. [CrossRef]
2. Abbas, A.; Mariana, L.T.; Phan, A.N. Biomass-waste derived graphene quantum dots and their applications. *Carbon* **2018**, *140*, 77–99. [CrossRef]
3. Hu, B.; Wang, K.; Wu, L.; Yu, S.H.; Antonietti, M.; Titirici, M.M. Engineering carbon materials from the hydrothermal carbonization process of biomass. *Adv. Mater.* **2010**, *22*, 813–828. [CrossRef] [PubMed]
4. Raja, S.; Mattoso, L.H.; Moreira, F.K. Biomass-Derived Nanomaterials. In *Nanostructured Materials for Energy Related Applications*; Springer: Berlin/Heidelberg, Germany, 2019; pp. 243–270.
5. Wang, Y.; Sun, J.; He, B.; Feng, M. Synthesis and modification of biomass derived carbon dots in ionic liquids and their application: A mini review. *Green Chem. Eng.* **2020**, *1*, 94–108. [CrossRef]
6. Boruah, A.; Saikia, M.; Das, T.; Goswamee, R.L.; Saikia, B.K. Blue-emitting fluorescent carbon quantum dots from waste biomass sources and their application in fluoride ion detection in water. *J. Photochem. Photobiol. B Biol.* **2020**, *209*, 111940. [CrossRef] [PubMed]
7. Wang, Z.; Smith, A.T.; Wang, W.; Sun, L. Versatile nanostructures from rice husk biomass for energy applications. *Angew. Chem. Int. Ed.* **2018**, *57*, 13722–13734. [CrossRef] [PubMed]
8. Wang, Z.; Shen, D.; Wu, C.; Gu, S. State-of-the-art on the production and application of carbon nanomaterials from biomass. *Green Chem.* **2018**, *20*, 5031–5057. [CrossRef]
9. Deng, J.; You, Y.; Sahajwalla, V.; Joshi, R.K. Transforming waste into carbon-based nanomaterials. *Carbon* **2016**, *96*, 105–115. [CrossRef]
10. Mohammadinejad, R.; Karimi, S.; Iravani, S.; Varma, R.S. Plant-derived nanostructures: Types and applications. *Green Chem.* **2016**, *18*, 20–52. [CrossRef]
11. Fathy, N.A.; Basta, A.H.; Lotfy, V.F. Novel trends for synthesis of carbon nanostructures from Agricultural wastes. In *Carbon Nanomaterials for Agri-Food and Environmental Applications*; Elsevier: Amsterdam, The Netherlands, 2020; pp. 59–74.
12. Mukherjee, A.; Majumdar, S.; Servin, A.D.; Pagano, L.; Dhankher, O.P.; White, J.C. Carbon nanomaterials in agriculture: A critical review. *Front. Plant Sci.* **2016**, *7*, 172. [CrossRef]
13. Gu, S.; Zhou, J.; Yu, C.; Luo, Z.; Wang, Q.; Shi, Z. A novel two-staged thermal synthesis method of generating nanosilica from rice husk via pre-pyrolysis combined with calcination. *Ind. Crop. Prod.* **2015**, *65*, 1–6. [CrossRef]
14. Pode, R. Potential applications of rice husk ash waste from rice husk biomass power plant. *Renew. Sustain. Energy Rev.* **2016**, *53*, 1468–1485. [CrossRef]
15. Umeda, J.; Kondoh, K. High-purification of amorphous silica originated from rice husks by combination of polysaccharide hydrolysis and metallic impurities removal. *Ind. Crop. Prod.* **2010**, *32*, 539–544. [CrossRef]
16. Sun, L.; Gong, K. Silicon-based materials from rice husks and their applications. *Ind. Eng. Chem. Res.* **2001**, *40*, 5861–5877. [CrossRef]
17. Masulili, A.; Utomo, W.H.; Syechfani, M. Rice husk biochar for rice based cropping system in acid soil 1. The characteristics of rice husk biochar and its influence on the properties of acid sulfate soils and rice growth in West Kalimantan, Indonesia. *J. Agric. Sci.* **2010**, *2*, 39. [CrossRef]
18. Chen, H.; Wang, W.; Martin, J.C.; Oliphant, A.J.; Doerr, P.A.; Xu, J.F.; DeBorn, K.M.; Chen, C.; Sun, L. Extraction of lignocellulose and synthesis of porous silica nanoparticles from rice husks: A comprehensive utilization of rice husk biomass. *ACS Sustain. Chem. Eng.* **2013**, *1*, 254–259. [CrossRef]
19. Wang, H.; Xu, Z.; Kohandehghan, A.; Li, Z.; Cui, K.; Tan, X.; Stephenson, T.J.; King'Ondu, C.K.; Holt, C.M.; Olsen, B.C. Interconnected carbon nanosheets derived from hemp for ultrafast supercapacitors with high energy. *ACS Nano* **2013**, *7*, 5131–5141. [CrossRef]

20. Muramatsu, H.; Kim, Y.A.; Yang, K.S.; Cruz-Silva, R.; Toda, I.; Yamada, T.; Terrones, M.; Endo, M.; Hayashi, T.; Saitoh, H. Rice husk-derived graphene with nano-sized domains and clean edges. *Small* **2014**, *10*, 2766–2770. [CrossRef]
21. Rhee, I.; Kim, Y.A.; Shin, G.-O.; Kim, J.H.; Muramatsu, H. Compressive strength sensitivity of cement mortar using rice husk-derived graphene with a high specific surface area. *Constr. Build. Mater.* **2015**, *96*, 189–197. [CrossRef]
22. Rhee, I.; Lee, J.-S.; Kim, J.H.; Kim, Y.A. Thermal performance, freeze-and-thaw resistance, and bond strength of cement mortar using rice husk-derived graphene. *Constr. Build. Mater.* **2017**, *146*, 350–359. [CrossRef]
23. Hidalgo, P.; Navia, R.; Hunter, R.; Coronado, G.; Gonzalez, M. Synthesis of carbon nanotubes using biochar as precursor material under microwave irradiation. *J. Environ. Manag.* **2019**, *244*, 83–91. [CrossRef]
24. Debalina, B.; Reddy, R.B.; Vinu, R. Production of carbon nanostructures in biochar, bio-oil and gases from bagasse via microwave assisted pyrolysis using Fe and Co as susceptors. *J. Anal. Appl. Pyrolysis* **2017**, *124*, 310–318. [CrossRef]
25. Wang, Z.; Ogata, H.; Morimoto, S.; Ortiz-Medina, J.; Fujishige, M.; Takeuchi, K.; Muramatsu, H.; Hayashi, T.; Terrones, M.; Hashimoto, Y. Nanocarbons from rice husk by microwave plasma irradiation: From graphene and carbon nanotubes to graphenated carbon nanotube hybrids. *Carbon* **2015**, *94*, 479–484. [CrossRef]
26. Thompson, E.; Danks, A.; Bourgeois, L.; Schnepp, Z. Iron-catalyzed graphitization of biomass. *Green Chem.* **2015**, *17*, 551–556. [CrossRef]
27. Fathy, N.A. Carbon nanotubes synthesis using carbonization of pretreated rice straw through chemical vapor deposition of camphor. *RSC Adv.* **2017**, *7*, 28535–28541. [CrossRef]
28. Qi, H.; Teng, M.; Liu, M.; Liu, S.; Li, J.; Yu, H.; Teng, C.; Huang, Z.; Liu, H.; Shao, Q. Biomass-derived nitrogen-doped carbon quantum dots: Highly selective fluorescent probe for detecting Fe3+ ions and tetracyclines. *J. Colloid Interface Sci.* **2019**, *539*, 332–341. [CrossRef]
29. Yuan, M.; Zhong, R.; Gao, H.; Li, W.; Yun, X.; Liu, J.; Zhao, X.; Zhao, G.; Zhang, F. One-step, green, and economic synthesis of water-soluble photoluminescent carbon dots by hydrothermal treatment of wheat straw, and their bio-applications in labeling, imaging, and sensing. *Appl. Surf. Sci.* **2015**, *355*, 1136–1144. [CrossRef]
30. John, T.S.; Yadav, P.K.; Kumar, D.; Singh, S.K.; Hasan, S.H. Highly fluorescent carbon dots from wheat bran as a novel drug delivery system for bacterial inhibition. *Luminescence* **2020**, *35*, 913–923. [CrossRef] [PubMed]
31. Wang, Z.; Yu, J.; Zhang, X.; Li, N.; Liu, B.; Li, Y.; Wang, Y.; Wang, W.; Li, Y.; Zhang, L. Large-scale and controllable synthesis of graphene quantum dots from rice husk biomass: A comprehensive utilization strategy. *ACS Appl. Mater. Interfaces* **2016**, *8*, 1434–1439. [CrossRef] [PubMed]
32. Kalita, H.; Mohapatra, J.; Pradhan, L.; Mitra, A.; Bahadur, D.; Aslam, M. Efficient synthesis of rice based graphene quantum dots and their fluorescent properties. *RSC Adv.* **2016**, *6*, 23518–23524. [CrossRef]
33. Wang, W.; Wang, Z.; Liu, J.; Peng, Y.; Yu, X.; Wang, W.; Zhang, Z.; Sun, L. One-pot facile synthesis of graphene quantum dots from rice husks for Fe^{3+} sensing. *Ind. Eng. Chem. Res.* **2018**, *57*, 9144–9150. [CrossRef]
34. Mansurov, Z. *Seitzhanova Makpal Azizovna*; University of Naples Federico II: Naples, Italy, 2020.
35. Seitzhanova, M.; Mansurov, Z.; Yeleuov, M.; Roviello, V.; Di Capua, R. The characteristics of graphene obtained from rice husk and graphite. *Eurasian Chem.-Technol. J.* **2019**, *21*, 149–156. [CrossRef]
36. Tohamy, H.-A.S.; Anis, B.; Youssef, M.A.; Abdallah, A.E.; El-Sakhawy, M.; Kamel, S. Preparation of eco-friendly graphene oxide from agricultural wastes for water treatment. *Desalin. Water Treat.* **2020**, *191*, 250–262. [CrossRef]
37. Naik, M.; Debbarma, J.; Saha, M.; Bhargava, A. Graphene oxide nanoflakes from various agrowastes. *Mater. Werkst.* **2020**, *51*, 368–374. [CrossRef]
38. Silva, G.A. Nanotechnology approaches to crossing the blood-brain barrier and drug delivery to the CNS. *BMC Neurosci.* **2008**, *9*, S4. [CrossRef]
39. Rauti, R.; Musto, M.; Bosi, S.; Prato, M.; Ballerini, L. Properties and behavior of carbon nanomaterials when interfacing neuronal cells: How far have we come? *Carbon* **2019**, *143*, 430–446. [CrossRef]
40. Nasir, S.; Hussein, M.Z.; Zainal, Z.; Yusof, N.A. Carbon-based nanomaterials/allotropes: A glimpse of their synthesis, properties and some applications. *Materials* **2018**, *11*, 295. [CrossRef]
41. Magrez, A.; Kasas, S.; Salicio, V.; Pasquier, N.; Seo, J.W.; Celio, M.; Catsicas, S.; Schwaller, B.; Forró, L. Cellular Toxicity of Carbon-Based Nanomaterials. *Nano Lett.* **2006**, *6*, 1121–1125. [CrossRef]
42. Villarreal, C.C.; Pham, T.; Ramnani, P.; Mulchandani, A. Carbon allotropes as sensors for environmental monitoring. *Curr. Opin. Electrochem.* **2017**, *3*, 106–113. [CrossRef]
43. Jiang, J.-W.; Leng, J.; Li, J.; Guo, Z.; Chang, T.; Guo, X.; Zhang, T. Twin graphene: A novel two-dimensional semiconducting carbon allotrope. *Carbon* **2017**, *118*, 370–375. [CrossRef]
44. Siqueira, J.R.; Oliveira, O.N. 9—Carbon-Based Nanomaterials. In *Nanostructures*; Da Róz, A.L., Ferreira, M., de Lima Leite, F., Oliveira, O.N., Eds.; William Andrew Publishing: Norwich, UK, 2017; pp. 233–249. [CrossRef]
45. Tiwari, S.K.; Kumar, V.; Huczko, A.; Oraon, R.; Adhikari, A.D.; Nayak, G. Magical allotropes of carbon: Prospects and applications. *Crit. Rev. Solid State Mater. Sci.* **2016**, *41*, 257–317. [CrossRef]
46. Harrison, B.S.; Atala, A. Carbon nanotube applications for tissue engineering. *Biomaterials* **2007**, *28*, 344–353. [CrossRef] [PubMed]
47. Venkataraman, A.; Amadi, E.V.; Chen, Y.; Papadopoulos, C. Carbon nanotube assembly and integration for applications. *Nanoscale Res. Lett.* **2019**, *14*, 1–47. [CrossRef] [PubMed]

48. Raccichini, R.; Varzi, A.; Passerini, S.; Scrosati, B. The role of graphene for electrochemical energy storage. *Nat. Mater.* **2015**, *14*, 271–279. [CrossRef]
49. Titirici, M.-M.; White, R.J.; Brun, N.; Budarin, V.L.; Su, D.S.; del Monte, F.; Clark, J.H.; MacLachlan, M.J. Sustainable carbon materials. *Chem. Soc. Rev.* **2015**, *44*, 250–290. [CrossRef]
50. Gao, Z.; Zhang, Y.; Song, N.; Li, X. Biomass-derived renewable carbon materials for electrochemical energy storage. *Mater. Res. Lett.* **2017**, *5*, 69–88. [CrossRef]
51. Gao, J.; Zhu, M.; Huang, H.; Liu, Y.; Kang, Z. Advances, challenges and promises of carbon dots. *Inorg. Chem. Front.* **2017**, *4*, 1963–1986. [CrossRef]
52. Allen, M.J.; Tung, V.C.; Kaner, R.B. Honeycomb carbon: A review of graphene. *Chem. Rev.* **2010**, *110*, 132–145. [CrossRef]
53. Choi, W.; Lahiri, I.; Seelaboyina, R.; Kang, Y.S. Synthesis of graphene and its applications: A review. *Crit. Rev. Solid State Mater. Sci.* **2010**, *35*, 52–71. [CrossRef]
54. Cooper, D.R.; D'Anjou, B.; Ghattamaneni, N.; Harack, B.; Hilke, M.; Horth, A.; Majlis, N.; Massicotte, M.; Vandsburger, L.; Whiteway, E. Experimental review of graphene. *Int. Sch. Res. Not.* **2012**, *2012*, 501686. [CrossRef]
55. Wang, X.; Shi, G. An introduction to the chemistry of graphene. *Phys. Chem. Chem. Phys.* **2015**, *17*, 28484–28504. [CrossRef]
56. Homaeigohar, S.; Elbahri, M. Graphene membranes for water desalination. *NPG Asia Mater.* **2017**, *9*, e427. [CrossRef]
57. Tuck, C.O.; Pérez, E.; Horváth, I.T.; Sheldon, R.A.; Poliakoff, M. Valorization of biomass: Deriving more value from waste. *Science* **2012**, *337*, 695–699. [CrossRef]
58. Kumar, S.; Sangwan, P.; Dhankhar, R.M.V.; Bidra, S. Utilization of rice husk and their ash: A review. *Res. J. Chem. Environ. Sci* **2013**, *1*, 126–129.
59. Serra, M.F.; Conconi, M.S.; Gauna, M.R.; Suárez, G.; Aglietti, E.F.; Rendtorff, N. Mullite ($3Al_2O_3{\cdot}2SiO_2$) ceramics obtained by reaction sintering of rice husk ash and alumina, phase evolution, sintering and microstructure. *J. Asian Ceram. Soc.* **2016**, *4*, 61–67. [CrossRef]
60. Ismail, M.S.; Yusof, N.; Yusop, M.Z.M.; Ismail, A.F.; Jaafar, J.; Aziz, F.; Karim, Z.A. Synthesis and characterization of graphene derived from rice husks. *Malays. J. Fundam. Appl. Sci.* **2019**, *15*, 516–521. [CrossRef]
61. Wang, J.; Kaskel, S. KOH activation of carbon-based materials for energy storage. *J. Mater. Chem.* **2012**, *22*, 23710–23725. [CrossRef]
62. Arifin, N.F.T.; Yusof, N.; Ismail, A.F.; Jaafar, J.; Aziz, F.; Salleh, W.N.W. Graphene from waste and bioprecursors synthesis method and its application: A review. *Malays. J. Fundam. Appl. Sci.* **2020**, *16*, 342–350. [CrossRef]
63. Raghavan, N.; Thangavel, S.; Venugopal, G. A short review on preparation of graphene from waste and bioprecursors. *Appl. Mater. Today* **2017**, *7*, 246–254. [CrossRef]
64. Priyanka, M.; Saravanakumar, M. A short review on preparation and application of carbon foam. *IOP Conf. Ser. Mater. Sci. Eng.* **2017**, *263*, 032018. [CrossRef]
65. Singh, P.; Bahadur, J.; Pal, K. One-step one chemical synthesis process of graphene from rice husk for energy storage applications. *Graphene* **2017**, *6*, 61–71. [CrossRef]
66. Uda, M.; Gopinath, S.C.; Hashim, U.; Uda, M.A.; hulwani Ibrahim, N.; Parmin, N.; Halim, N.; Anbu, P. Simple and Green Approach Strategy to Synthesis Graphene Using Rice Straw Ash. *IOP Conf. Ser. Mater. Sci. Eng.* **2020**, *864*, 012181. [CrossRef]
67. Othman, F.E.C.; Ismail, M.S.; Yusof, N.; Samitsu, S.; Yusop, M.Z.; Arifin, N.F.T.; Alias, N.H.; Jaafar, J.; Aziz, F.; Salleh, W.N.W. Methane adsorption by porous graphene derived from rice husk ashes under various stabilization temperatures. *Carbon Lett.* **2020**, *30*, 535–543. [CrossRef]
68. De la Hoz, A.; Diaz-Ortiz, A.; Moreno, A. Microwaves in organic synthesis. Thermal and non-thermal microwave effects. *Chem. Soc. Rev.* **2005**, *34*, 164–178. [CrossRef]
69. Kang, C.; Huang, Y.; Yang, H.; Yan, X.F.; Chen, Z.P. A review of carbon dots produced from biomass wastes. *Nanomaterials* **2020**, *10*, 2316. [CrossRef]
70. Omoriyekomwan, J.E.; Tahmasebi, A.; Dou, J.; Wang, R.; Yu, J. A review on the recent advances in the production of carbon nanotubes and carbon nanofibers via microwave-assisted pyrolysis of biomass. *Fuel Process. Technol.* **2020**, *214*, 106686. [CrossRef]
71. Kumar, M.; Sachdeva, A.; Garg, R.K.; Singh, S. Synthesis and Characterization of Graphene Prepared from Rice Husk by a Simple Microwave Process. *Nano Hybrids Compos.* **2020**, *29*, 74–83. [CrossRef]
72. Hashmi, A.; Singh, A.K.; Jain, B.; Singh, A. Muffle atmosphere promoted fabrication of graphene oxide nanoparticle by agricultural waste. *Fuller. Nanotub. Carbon Nanostruct.* **2020**, *28*, 627–636. [CrossRef]
73. Zhou, H. *Combustible Solid Waste Thermochemical Conversion: A Study of Interactions and Influence Factors*; Springer: Berlin/Heidelberg, Germany, 2017.
74. Shannon, M.A.; Bohn, P.W.; Elimelech, M.; Georgiadis, J.G.; Marinas, B.J.; Mayes, A.M. Science and technology for water purification in the coming decades. *Nanosci. Technol. A Collect. Rev. Nat. J.* **2010**, 337–346. [CrossRef]
75. Elimelech, M.; Phillip, W.A. The future of seawater desalination: Energy, technology, and the environment. *Science* **2011**, *333*, 712–717. [CrossRef]
76. UN Water. *The United Nations World Water Development Report 2014: Water and Energy*; United Nations: Paris, France, 2014.
77. Hegab, H.M.; Zou, L. Graphene oxide-assisted membranes: Fabrication and potential applications in desalination and water purification. *J. Membr. Sci.* **2015**, *484*, 95–106. [CrossRef]
78. Xu, K.; Feng, B.; Zhou, C.; Huang, A. Synthesis of highly stable graphene oxide membranes on polydopamine functionalized supports for seawater desalination. *Chem. Eng. Sci.* **2016**, *146*, 159–165. [CrossRef]

79. Fritzmann, C.; Löwenberg, J.; Wintgens, T.; Melin, T. State-of-the-art of reverse osmosis desalination. *Desalination* **2007**, *216*, 1–76. [CrossRef]
80. Nicolaï, A.; Sumpter, B.G.; Meunier, V. Tunable water desalination across graphene oxide framework membranes. *Phys. Chem. Chem. Phys.* **2014**, *16*, 8646–8654. [CrossRef]
81. Zheng, Z.; Grünker, R.; Feng, X. Synthetic two–dimensional materials: A new paradigm of membranes for ultimate separation. *Adv. Mater.* **2016**, *28*, 6529–6545. [CrossRef]
82. Boretti, A.; Al-Zubaidy, S.; Vaclavikova, M.; Al-Abri, M.; Castelletto, S.; Mikhalovsky, S. Outlook for graphene-based desalination membranes. *NPJ Clean Water* **2018**, *1*, 5. [CrossRef]
83. Han, Y.; Xu, Z.; Gao, C. Ultrathin graphene nanofiltration membrane for water purification. *Adv. Funct. Mater.* **2013**, *23*, 3693–3700. [CrossRef]
84. Thomas, M.; Corry, B.; Hilder, T.A. What have we learnt about the mechanisms of rapid water transport, ion rejection and selectivity in nanopores from molecular simulation? *Small* **2014**, *10*, 1453–1465. [CrossRef]
85. Surwade, S.P.; Smirnov, S.N.; Vlassiouk, I.V.; Unocic, R.R.; Veith, G.M.; Dai, S.; Mahurin, S.M. Water desalination using nanoporous single-layer graphene. *Nat. Nanotechnol.* **2015**, *10*, 459–464. [CrossRef]
86. Wang, Q.; Kalantar-Zadeh, K.K.; Kis, A.A.; Coleman, J.N.; Strano, M.S. Electronics and Optoelectronics of Two-Dimensional Transition Metal Dichalcogenides. *Nat. Nanotechnol.* **2012**, *7*, 699–712. [CrossRef]
87. Lee, K.P.; Arnot, T.C.; Mattia, D. A review of reverse osmosis membrane materials for desalination—Development to date and future potential. *J. Membr. Sci.* **2011**, *370*, 1–22. [CrossRef]
88. Fathizadeh, M.; Tien, H.N.; Khivantsev, K.; Song, Z.; Zhou, F.; Yu, M. Polyamide/nitrogen-doped graphene oxide quantum dots (N-GOQD) thin film nanocomposite reverse osmosis membranes for high flux desalination. *Desalination* **2019**, *451*, 125–132. [CrossRef]
89. McGuinness, N.B.; Garvey, M.; Whelan, A.; John, H.; Zhao, C.; Zhang, G.; Dionysiou, D.D.; Byrne, J.A.; Pillai, S.C. Nanotechnology solutions for global water challenges. In *Water Challenges and Solutions on a Global Scale*; ACS Publications: Washington, DC, USA, 2015; pp. 375–411.
90. Raghav, S.; Painuli, R.; Kumar, D. Threats to Water: Issues and Challenges Related to Ground Water and Drinking Water. In *A New Generation Material Graphene: Applications in Water Technology*; Springer: Cham, Switzerland, 2019; pp. 1–19. [CrossRef]
91. Tatarchuk, T.; Bououdina, M.; Al-Najar, B.; Bitra, R.B. Green and ecofriendly materials for the remediation of inorganic and organic pollutants in water. In *A New Generation Material Graphene: Applications in Water Technology*; Springer: Cham, Switzerland, 2019; pp. 69–110. [CrossRef]
92. Padmaja, K.; Cherukuri, J.; Reddy, M.A. Conventional to cutting edge technologies in Drinking Water Purification–a REVIEW. *Int. J. Innov. Res. Sci. Eng. Technol.* **2014**, *3*, 9375–9385.
93. Aghigh, A.; Alizadeh, V.; Wong, H.Y.; Islam, M.S.; Amin, N.; Zaman, M. Recent advances in utilization of graphene for filtration and desalination of water: A review. *Desalination* **2015**, *365*, 389–397. [CrossRef]
94. Baby Shaikh, R.; Saifullah, B.; Rehman, F.U. Greener method for the removal of toxic metal ions from the wastewater by application of agricultural waste as an adsorbent. *Water* **2018**, *10*, 1316. [CrossRef]
95. Bolisetty, S.; Peydayesh, M.; Mezzenga, R. Sustainable technologies for water purification from heavy metals: Review and analysis. *Chem. Soc. Rev.* **2019**, *48*, 463–487. [CrossRef]
96. Chigo-Anota, E.; Salazar-Villanueva, M.; Hernández-Cocoletzi, H. Electronic Properties of Boron Nitride Oxide Nanoclusters. *J. Nanosci. Nanotechnol.* **2011**, *11*, 5515–5518. [CrossRef]
97. Kumar, P.S.; Ramakrishnan, K.; Kirupha, S.D.; Sivanesan, S. Thermodynamic and kinetic studies of cadmium adsorption from aqueous solution onto rice husk. *Braz. J. Chem. Eng.* **2010**, *27*, 347–355. [CrossRef]
98. Shafiq, M.; Alazba, A.; Amin, M. Removal of heavy metals from wastewater using date palm as a biosorbent: A comparative review. *Sains Malays.* **2018**, *47*, 35–49.
99. Lee, J.-Y.; Chen, C.-H.; Cheng, S.; Li, H.-Y. Adsorption of Pb (II) and Cu (II) metal ions on functionalized large-pore mesoporous silica. *Int. J. Environ. Sci. Technol.* **2016**, *13*, 65–76. [CrossRef]
100. Wang, J.; Chen, B. Adsorption and coadsorption of organic pollutants and a heavy metal by graphene oxide and reduced graphene materials. *Chem. Eng. J.* **2015**, *281*, 379–388. [CrossRef]
101. Economides, M.J.; Wood, D.A. The state of natural gas. *J. Nat. Gas Sci. Eng.* **2009**, *1*, 1–13. [CrossRef]
102. He, Y.; Zhou, W.; Qian, G.; Chen, B. Methane storage in metal–organic frameworks. *Chem. Soc. Rev.* **2014**, *43*, 5657–5678. [CrossRef] [PubMed]
103. Arami-Niya, A.; Daud, W.M.A.W.; Mjalli, F.S.; Abnisa, F.; Shafeeyan, M.S. Production of microporous palm shell based activated carbon for methane adsorption: Modeling and optimization using response surface methodology. *Chem. Eng. Res. Des.* **2012**, *90*, 776–784. [CrossRef]
104. Policicchio, A.; Filosa, R.; Abate, S.; Desiderio, G.; Colavita, E. Activated carbon and metal organic framework as adsorbent for low-pressure methane storage applications: An overview. *J. Porous Mater.* **2017**, *24*, 905–922. [CrossRef]
105. Choi, P.-S.; Jeong, J.-M.; Choi, Y.-K.; Kim, M.-S.; Shin, G.-J.; Park, S.-J. A review: Methane capture by nanoporous carbon materials for automobiles. *Carbon Lett.* **2016**, *17*, 18–28. [CrossRef]

106. Mortazavi, S.; Reyhani, A.; Mirershadi, S. Hydrogen storage properties of multi-walled carbon nanotubes and carbon nano-onions grown on single and bi-catalysts including Fe, Mo, Co and Ni supported by MgO. *Int. J. Hydrog. Energy* **2017**, *42*, 24885–24896. [CrossRef]
107. Tian, Z.; Dong, S. Yttrium dispersion on capped carbon nanotube: Promising materials for hydrogen storage applications. *Int. J. Hydrog. Energy* **2016**, *41*, 1053–1059. [CrossRef]
108. Shiraz, H.G.; Shiraz, M.G. Palladium nanoparticle and decorated carbon nanotube for electrochemical hydrogen storage. *Int. J. Hydrog. Energy* **2017**, *42*, 11528–11533. [CrossRef]
109. Hayashi, J.i.; Kazehaya, A.; Muroyama, K.; Watkinson, A.P. Preparation of activated carbon from lignin by chemical activation. *Carbon* **2000**, *38*, 1873–1878. [CrossRef]
110. Rios, R.B.; Silva, F.W.M.; Torres, A.E.B.; Azevedo, D.C.; Cavalcante, C.L. Adsorption of methane in activated carbons obtained from coconut shells using H 3 PO 4 chemical activation. *Adsorption* **2009**, *15*, 271–277. [CrossRef]
111. Han, M.; Zhao, Q.; Zhu, Z.; Hu, Y.; Tao, Z.; Chen, J. The enhanced hydrogen storage of micro-nanostructured hybrids of Mg (BH 4) 2–carbon nanotubes. *Nanoscale* **2015**, *7*, 18305–18311. [CrossRef]
112. Zhu, Z.; Zheng, Q. Methane adsorption on the graphene sheets, activated carbon and carbon black. *Appl. Therm. Eng.* **2016**, *108*, 605–613. [CrossRef]
113. Durá, G.; Budarin, V.L.; Castro-Osma, J.A.; Shuttleworth, P.S.; Quek, S.C.; Clark, J.H.; North, M. Importance of Micropore–Mesopore Interfaces in Carbon Dioxide Capture by Carbon-Based Materials. *Angew. Chem.* **2016**, *128*, 9319–9323. [CrossRef]
114. Che Othman, F.E.; Yusof, N.; Yub Harun, N.; Bilad, M.R.; Jaafar, J.; Aziz, F.; Wan Salleh, W.N.; Ismail, A.F. Novel activated carbon nanofibers composited with cost-effective graphene-based materials for enhanced adsorption performance toward methane. *Polymers* **2020**, *12*, 2064. [CrossRef]
115. Liu, S.; Zeng, T.H.; Hofmann, M.; Burcombe, E.; Wei, J.; Jiang, R.; Kong, J.; Chen, Y. Antibacterial activity of graphite, graphite oxide, graphene oxide, and reduced graphene oxide: Membrane and oxidative stress. *ACS Nano* **2011**, *5*, 6971–6980. [CrossRef]
116. Chen, J.; Peng, H.; Wang, X.; Shao, F.; Yuan, Z.; Han, H. Graphene oxide exhibits broad-spectrum antimicrobial activity against bacterial phytopathogens and fungal conidia by intertwining and membrane perturbation. *Nanoscale* **2014**, *6*, 1879–1889. [CrossRef]
117. Carpio, I.E.M.; Santos, C.M.; Wei, X.; Rodrigues, D.F. Toxicity of a polymer–graphene oxide composite against bacterial planktonic cells, biofilms, and mammalian cells. *Nanoscale* **2012**, *4*, 4746–4756. [CrossRef]
118. Smith, S.C.; Rodrigues, D.F. Carbon-based nanomaterials for removal of chemical and biological contaminants from water: A review of mechanisms and applications. *Carbon* **2015**, *91*, 122–143. [CrossRef]
119. Hosseinalipour, S.; Jabbari, E.; Madadelahi, M.; Fardad, A. Gas Mixing Simulation in a T-Shape Micro Channel Using The DSMC Method. *Transp. Phenom. Nano Micro Scales* **2014**, *2*, 132–139.
120. Hillert, M.; Lange, N. The structure of graphite filaments. *Z. Für Krist. Cryst. Mater.* **1959**, *111*, 24–34. [CrossRef]
121. Radushkevich, L.V.; Lukyanovich, V.M. The Structure of Carbon Forming in Thermal Decomposition of Carbon Monoxide on an Iron Catalyst. *Russ. J. Phys. Chem.* **1952**, *26*, 88–95.
122. Oberlin, A.; Endo, M.; Koyama, T. Filamentous growth of carbon through benzene decomposition. *J. Cryst. Growth* **1976**, *32*, 335–349. [CrossRef]
123. Iijima, S. Helical microtubules of graphitic carbon. *Nature* **1991**, *354*, 56–58. [CrossRef]
124. Ebbesen, T.W.; Ajayan, P.M. Large-scale synthesis of carbon nanotubes. *Nature* **1992**, *358*, 220–222. [CrossRef]
125. Greil, P. Perspectives of nano-carbon based engineering materials. *Adv. Eng. Mater.* **2015**, *17*, 124–137. [CrossRef]
126. Baughman, R.; Zakhidov, A.; Heer, W. Carbon Nanotubes-The Route Toward Applications. *Science* **2002**, *297*, 787–792. [CrossRef]
127. Liu, W.-W.; Aziz, A.; Chai, S.-P.; Mohamed, A.R.; Tye, C.-T. The effect of carbon precursors (methane, benzene and camphor) on the quality of carbon nanotubes synthesised by the chemical vapour decomposition. *Phys. E Low-Dimens. Syst. Nanostruct.* **2011**, *43*, 1535. [CrossRef]
128. De Volder, M.F.; Tawfick, S.H.; Baughman, R.H.; Hart, A.J. Carbon nanotubes: Present and future commercial applications. *Science* **2013**, *339*, 535–539. [CrossRef] [PubMed]
129. Prasek, J.; Drbohlavova, J.; Chomoucka, J.; Hubalek, J.; Jasek, O.; Adam, V.; Kizek, R. Methods for carbon nanotubes synthesis—Review. *J. Mater. Chem.* **2011**, *21*, 15872–15884. [CrossRef]
130. Dai, H. Carbon Nanotubes: Synthesis, Integration, and Properties. *Acc. Chem. Res.* **2002**, *35*, 1035–1044. [CrossRef]
131. Hong, E.H.; Lee, K.-H.; Oh, S.H.; Park, C.-G. Synthesis of Carbon Nanotubes Using Microwave Radiation. *Adv. Funct. Mater.* **2003**, *13*, 961–966. [CrossRef]
132. Omatola, K.; Onojah, A. Elemental analysis of rice husk ash using X-ray fluorescence technique. *Int. J. Phys. Sci.* **2009**, *4*, 189–193.
133. Thess, A.; Lee, R.; Nikolaev, P.; Dai, H.; Petit, P.; Robert, J.; Xu, C.H.; Lee, Y.H.; Kim, S.-G.; Rinzler, A.; et al. Crystalline Ropes of Metallic Carbon Nanotubes. *Science* **1996**, *273*, 483–487. [CrossRef]
134. Ren, Z.F.; Huang, Z.P.; Xu, J.W.; Wang, J.H.; Bush, P.; Siegal, M.P.; Provencio, P.N. Synthesis of large arrays of well-aligned carbon nanotubes on glass. *Science* **1998**, *282*, 1105–1107. [CrossRef]
135. José-Yacamán, M.; Miki-Yoshida, M.; Rendón, L.; Santiesteban, J.G. Catalytic growth of carbon microtubules with fullerene structure. *Appl. Phys. Lett.* **1993**, *62*, 202. [CrossRef]
136. Cho, W.S.; Hamada, E.; Kondo, Y.; Takayanagi, K. Synthesis of carbon nanotubes from bulk polymer. *Appl. Phys. Lett.* **1996**, *69*, 278–279. [CrossRef]

137. Richter, H.; Hernádi, K.; Caudano, R.; Fonseca, A.; Migeon, H.; Nagy, J.; Schneider, S.; Vandooren, J.; Tiggelen, P.J. Formation of nanotubes in low pressure hydrocarbon flames. *Carbon* **1996**, *34*, 427–429. [CrossRef]
138. Chernozatonskii, L.A.; Kosakovskaja, Z.J.; Fedorov, E.A.; Panov, V.I. New carbon tubelite-ordered film structure of multilayer nanotubes. *Phys. Lett. A* **1995**, *197*, 40–46. [CrossRef]
139. Eatemadi, A.; Daraee, H.; Karimkhanloo, H.; Kouhi, M.; Zarghami, N.; Akbarzadeh, A.; Abasi, M.; Hanifehpour, Y.; Joo, S.W. Carbon nanotubes: Properties, synthesis, purification, and medical applications. *Nanoscale Res. Lett.* **2014**, *9*, 393. [CrossRef] [PubMed]
140. Yan, Y.; Miao, J.; Yang, Z.; Xiao, F.-X.; Yang, H.B.; Liu, B.; Yang, Y. Carbon nanotube catalysts: Recent advances in synthesis, characterization and applications. *Chem. Soc. Rev.* **2015**, *44*, 3295–3346. [CrossRef] [PubMed]
141. Martin, P.M. (Ed.) Chapter 1—Deposition Technologies: An Overview. In *Handbook of Deposition Technologies for Films and Coatings*, 3rd ed.; William Andrew Publishing: Boston, MA, USA, 2010; pp. 1–31. [CrossRef]
142. Alslaibi, T.M.; Abustan, I.; Ahmad, M.A.; Foul, A.A. A review: Production of activated carbon from agricultural byproducts via conventional and microwave heating. *J. Chem. Technol. Biotechnol.* **2013**, *88*, 1183–1190. [CrossRef]
143. Asnawi, M.; Azhari, S.; Hamidon, M.N.; Ismail, I.; Helina, I. Synthesis of carbon nanomaterials from rice husk via microwave oven. *J. Nanomater.* **2018**, *2018*, 2898326. [CrossRef]
144. Lotfy, V.F.; Fathy, N.A.; Basta, A.H. Novel approach for synthesizing different shapes of carbon nanotubes from rice straw residue. *J. Environ. Chem. Eng.* **2018**, *6*, 6263–6274. [CrossRef]
145. Liu, X.; Zhang, S.; Pan, B. Potential of carbon nanotubes in water treatment. *Recent Prog. Carbon Nanotub. Res.* **2012**, *201110*, 51332.
146. Qu, X.; Brame, J.; Li, Q.; Alvarez, P.J. Nanotechnology for a safe and sustainable water supply: Enabling integrated water treatment and reuse. *Acc. Chem. Res.* **2013**, *46*, 834–843. [CrossRef]
147. Chaudhary, S.; Kumar, S.; Kaur, B.; Mehta, S.K. Potential prospects for carbon dots as a fluorescence sensing probe for metal ions. *RSC Adv.* **2016**, *6*, 90526–90536.
148. Upadhyayula, V.K.; Deng, S.; Mitchell, M.C.; Smith, G.B. Application of carbon nanotube technology for removal of contaminants in drinking water: A review. *Sci. Total Environ.* **2009**, *408*, 1–13. [CrossRef]
149. Sarkar, B.; Mandal, S.; Tsang, Y.F.; Vithanage, M.; Biswas, J.K.; Yi, H.; Dou, X.; Ok, Y.S. Sustainable sludge management by removing emerging contaminants from urban wastewater using carbon nanotubes. In *Industrial and Municipal Sludge*; Elsevier: Amsterdam, The Netherlands, 2019; pp. 553–571.
150. Tousova, Z.; Oswald, P.; Slobodnik, J.; Blaha, L.; Muz, M.; Hu, M.; Brack, W.; Krauss, M.; Di Paolo, C.; Tarcai, Z. European demonstration program on the effect-based and chemical identification and monitoring of organic pollutants in European surface waters. *Sci. Total Environ.* **2017**, *601*, 1849–1868. [CrossRef]
151. Sillanpää, M. *Natural Organic Matter in Water: Characterization and Treatment Methods*; Butterworth-Heinemann: Oxford, UK, 2014.
152. Leonard, P.; Hearty, S.; Brennan, J.; Dunne, L.; Quinn, J.; Chakraborty, T.; O'Kennedy, R. Advances in biosensors for detection of pathogens in food and water. *Enzym. Microb. Technol.* **2003**, *32*, 3–13. [CrossRef]
153. De Paolis, F.; Kukkonen, J. Binding of organic pollutants to humic and fulvic acids: Influence of pH and the structure of humic material. *Chemosphere* **1997**, *34*, 1693–1704. [CrossRef]
154. Dizge, N.; Tansel, B. Multiparametric investigation of competitive and noncompetitive sorption characteristics of SMP fractions (carbohydrate and protein) on activated carbon. *J. Hazard. Mater.* **2011**, *185*, 996–1004. [CrossRef]
155. Cheng, W.; Dastgheib, S.A.; Karanfil, T. Adsorption of dissolved natural organic matter by modified activated carbons. *Water Res.* **2005**, *39*, 2281–2290. [CrossRef] [PubMed]
156. Dastgheib, S.A.; Karanfil, T.; Cheng, W. Tailoring activated carbons for enhanced removal of natural organic matter from natural waters. *Carbon* **2004**, *42*, 547–557. [CrossRef]
157. Wang, F.; Yao, J.; Chen, H.; Yi, Z.; Xing, B. Sorption of humic acid to functionalized multi-walled carbon nanotubes. *Environ. Pollut.* **2013**, *180*, 1–6. [CrossRef]
158. Lee, J.; Jeong, S.; Liu, Z. Progress and challenges of carbon nanotube membrane in water treatment. *Crit. Rev. Environ. Sci. Technol.* **2016**, *46*, 999–1046. [CrossRef]
159. Shanmuganathan, S.; Loganathan, P.; Kazner, C.; Johir, M.; Vigneswaran, S. Submerged membrane filtration adsorption hybrid system for the removal of organic micropollutants from a water reclamation plant reverse osmosis concentrate. *Desalination* **2017**, *401*, 134–141. [CrossRef]
160. Xu, L.; Shahid, S.; Shen, J.; Emanuelsson, E.A.C.; Patterson, D.A. A wide range and high resolution one-filtration molecular weight cut-off method for aqueous based nanofiltration and ultrafiltration membranes. *J. Membr. Sci.* **2017**, *525*, 304–311. [CrossRef]
161. Vatanpour, V.; Esmaeili, M.; Farahani, M.H.D.A. Fouling reduction and retention increment of polyethersulfone nanofiltration membranes embedded by amine-functionalized multi-walled carbon nanotubes. *J. Membr. Sci.* **2014**, *466*, 70–81. [CrossRef]
162. Kang, G.-D.; Cao, Y.-M. Development of antifouling reverse osmosis membranes for water treatment: A review. *Water Res.* **2012**, *46*, 584–600. [CrossRef]
163. Ali, S.; Rehman, S.A.U.; Luan, H.-Y.; Farid, M.U.; Huang, H. Challenges and opportunities in functional carbon nanotubes for membrane-based water treatment and desalination. *Sci. Total Environ.* **2019**, *646*, 1126–1139. [CrossRef] [PubMed]
164. Ahmad, J.; Naeem, S.; Ahmad, M.; Usman, A.R.; Al-Wabel, M.I. A critical review on organic micropollutants contamination in wastewater and removal through carbon nanotubes. *J. Environ. Manag.* **2019**, *246*, 214–228. [CrossRef] [PubMed]

165. Yang, K.; Zhu, L.; Xing, B. Adsorption of polycyclic aromatic hydrocarbons by carbon nanomaterials. *Environ. Sci. Technol.* **2006**, *40*, 1855–1861. [CrossRef] [PubMed]
166. Liu, G.; Jin, W.; Xu, N. Graphene-based membranes. *Chem. Soc. Rev.* **2015**, *44*, 5016–5030. [CrossRef]
167. Lin, D.; Xing, B. Adsorption of phenolic compounds by carbon nanotubes: Role of aromaticity and substitution of hydroxyl groups. *Environ. Sci. Technol.* **2008**, *42*, 7254–7259. [CrossRef]
168. Cho, H.-H.; Smith, B.A.; Wnuk, J.D.; Fairbrother, D.H.; Ball, W.P. Influence of surface oxides on the adsorption of naphthalene onto multiwalled carbon nanotubes. *Environ. Sci. Technol.* **2008**, *42*, 2899–2905. [CrossRef]
169. Engel, M.; Chefetz, B. Adsorption and desorption of dissolved organic matter by carbon nanotubes: Effects of solution chemistry. *Environ. Pollut.* **2016**, *213*, 90–98. [CrossRef]
170. Ajmani, G.S.; Goodwin, D.; Marsh, K.; Fairbrother, D.H.; Schwab, K.J.; Jacangelo, J.G.; Huang, H. Modification of low pressure membranes with carbon nanotube layers for fouling control. *Water Res.* **2012**, *46*, 5645–5654. [CrossRef]
171. Yang, X.; Lee, J.; Yuan, L.; Chae, S.-R.; Peterson, V.K.; Minett, A.I.; Yin, Y.; Harris, A.T. Removal of natural organic matter in water using functionalised carbon nanotube buckypaper. *Carbon* **2013**, *59*, 160–166. [CrossRef]
172. Wang, Y.; Huang, H.; Wei, X. Influence of wastewater precoagulation on adsorptive filtration of pharmaceutical and personal care products by carbon nanotube membranes. *Chem. Eng. J.* **2018**, *333*, 66–75. [CrossRef]
173. Wang, S.; Liang, S.; Liang, P.; Zhang, X.; Sun, J.; Wu, S.; Huang, X. In-situ combined dual-layer CNT/PVDF membrane for electrically-enhanced fouling resistance. *J. Membr. Sci.* **2015**, *491*, 37–44. [CrossRef]
174. Wang, Y.; Zhu, J.; Huang, H.; Cho, H.-H. Carbon nanotube composite membranes for microfiltration of pharmaceuticals and personal care products: Capabilities and potential mechanisms. *J. Membr. Sci.* **2015**, *479*, 165–174. [CrossRef]
175. Ye, S.; Zeng, G.; Wu, H.; Zhang, C.; Liang, J.; Dai, J.; Liu, Z.; Xiong, W.; Wan, J.; Xu, P. Co-occurrence and interactions of pollutants, and their impacts on soil remediation—A review. *Crit. Rev. Environ. Sci. Technol.* **2017**, *47*, 1528–1553. [CrossRef]
176. Lapworth, D.; Baran, N.; Stuart, M.; Ward, R. Emerging organic contaminants in groundwater: A review of sources, fate and occurrence. *Environ. Pollut.* **2012**, *163*, 287–303. [CrossRef]
177. Westerhoff, P.; Yoon, Y.; Snyder, S.; Wert, E. Fate of endocrine-disruptor, pharmaceutical, and personal care product chemicals during simulated drinking water treatment processes. *Environ. Sci. Technol.* **2005**, *39*, 6649–6663. [CrossRef]
178. Suárez, S.; Carballa, M.; Omil, F.; Lema, J.M. How are pharmaceutical and personal care products (PPCPs) removed from urban wastewaters? *Rev. Environ. Sci. Bio/Technol.* **2008**, *7*, 125–138. [CrossRef]
179. Valavanidis, A.; Vlachogianni, T.; Triantafillaki, S.; Dassenakis, M.; Androutsos, F.; Scoullos, M. Polycyclic aromatic hydrocarbons in surface seawater and in indigenous mussels (*Mytilus galloprovincialis*) from coastal areas of the Saronikos Gulf (Greece). *Estuar. Coast. Shelf Sci.* **2008**, *79*, 733–739. [CrossRef]
180. Gimeno, R.; Marcé, R.; Borrull, F. Determination of organic contaminants in coastal water. *TrAC Trends Anal. Chem.* **2004**, *23*, 341–350. [CrossRef]
181. Fromme, H.; Küchler, T.; Otto, T.; Pilz, K.; Müller, J.; Wenzel, A. Occurrence of phthalates and bisphenol A and F in the environment. *Water Res.* **2002**, *36*, 1429–1438. [CrossRef]
182. Sánchez-Avila, J.; Meyer, J.; Lacorte, S. Spatial distribution and sources of perfluorochemicals in the NW Mediterranean coastal waters (Catalonia, Spain). *Environ. Pollut.* **2010**, *158*, 2833–2840. [CrossRef]
183. Liu, X.; Wang, M.; Zhang, S.; Pan, B. Application potential of carbon nanotubes in water treatment: A review. *J. Environ. Sci.* **2013**, *25*, 1263–1280. [CrossRef]
184. Ji, L.; Chen, W.; Zheng, S.; Xu, Z.; Zhu, D. Adsorption of sulfonamide antibiotics to multiwalled carbon nanotubes. *Langmuir* **2009**, *25*, 11608–11613. [CrossRef]
185. Zhao, H.; Liu, X.; Cao, Z.; Zhan, Y.; Shi, X.; Yang, Y.; Zhou, J.; Xu, J. Adsorption behavior and mechanism of chloramphenicols, sulfonamides, and non-antibiotic pharmaceuticals on multi-walled carbon nanotubes. *J. Hazard. Mater.* **2016**, *310*, 235–245. [CrossRef]
186. Pyrzynska, K.; Stafiej, A.; Biesaga, M. Sorption behavior of acidic herbicides on carbon nanotubes. *Microchim. Acta* **2007**, *159*, 293–298. [CrossRef]
187. Nam, S.-W.; Choi, D.-J.; Kim, S.-K.; Her, N.; Zoh, K.-D. Adsorption characteristics of selected hydrophilic and hydrophobic micropollutants in water using activated carbon. *J. Hazard. Mater.* **2014**, *270*, 144–152. [CrossRef]
188. Sarkar, B.; Mandal, S.; Tsang, Y.F.; Kumar, P.; Kim, K.-H.; Ok, Y.S. Designer carbon nanotubes for contaminant removal in water and wastewater: A critical review. *Sci. Total Environ.* **2018**, *612*, 561–581. [CrossRef]
189. Straathof, H.M. Investigations on the phytotoxic relevance of volatilization of herbicides. *Meded. Fac. Landbouwwet. Rijksuniv. Gent* **1986**, *51*, 433–438.
190. Anju, A.; Ravi, S.P.; Bechan, S. Water pollution with special reference to pesticide contamination in India. *J. Water Resour. Prot.* **2010**, *2010*, 1793.
191. Rocha, J.-D.R.; Rogers, R.E.; Dichiara, A.B.; Capasse, R.C. Emerging investigators series: Highly effective adsorption of organic aromatic molecules from aqueous environments by electronically sorted single-walled carbon nanotubes. *Environ. Sci. Water Res. Technol.* **2017**, *3*, 203–212. [CrossRef]
192. Huang, Z.; Li, Y.; Chen, W.; Shi, J.; Zhang, N.; Wang, X.; Li, Z.; Gao, L.; Zhang, Y. Modified bentonite adsorption of organic pollutants of dye wastewater. *Mater. Chem. Phys.* **2017**, *202*, 266–276. [CrossRef]

193. Pirkarami, A.; Olya, M.E. Removal of dye from industrial wastewater with an emphasis on improving economic efficiency and degradation mechanism. *J. Saudi Chem. Soc.* **2017**, *21*, S179–S186. [CrossRef]
194. Ghaedi, M.; Khajehsharifi, H.; Yadkuri, A.H.; Roosta, M.; Asghari, A. Oxidized multiwalled carbon nanotubes as efficient adsorbent for bromothymol blue. *Toxicol. Environ. Chem.* **2012**, *94*, 873–883. [CrossRef]
195. Ma, J.; Yu, F.; Zhou, L.; Jin, L.; Yang, M.; Luan, J.; Tang, Y.; Fan, H.; Yuan, Z.; Chen, J. Enhanced adsorptive removal of methyl orange and methylene blue from aqueous solution by alkali-activated multiwalled carbon nanotubes. *ACS Appl. Mater. Interfaces* **2012**, *4*, 5749–5760. [CrossRef] [PubMed]
196. Rajabi, M.; Mahanpoor, K.; Moradi, O. Removal of dye molecules from aqueous solution by carbon nanotubes and carbon nanotube functional groups: Critical review. *RSC Adv.* **2017**, *7*, 47083–47090. [CrossRef]
197. Sadegh, H.; Zare, K.; Maazinejad, B.; Shahryari-Ghoshekandi, R.; Tyagi, I.; Agarwal, S.; Gupta, V.K. Synthesis of MWCNT-COOH-Cysteamine composite and its application for dye removal. *J. Mol. Liq.* **2016**, *215*, 221–228. [CrossRef]
198. Jahangiri-Rad, M.; Nadafi, K.; Mesdaghinia, A.; Nabizadeh, R.; Younesian, M.; Rafiee, M. Sequential study on reactive blue 29 dye removal from aqueous solution by peroxy acid and single wall carbon nanotubes: Experiment and theory. *Iran. J. Environ. Health Sci. Eng.* **2013**, *10*, 5. [CrossRef]
199. Padaki, M.; Murali, R.S.; Abdullah, M.S.; Misdan, N.; Moslehyani, A.; Kassim, M.; Hilal, N.; Ismail, A. Membrane technology enhancement in oil–water separation. A review. *Desalination* **2015**, *357*, 197–207. [CrossRef]
200. Zhu, L.; Chen, M.; Dong, Y.; Tang, C.Y.; Huang, A.; Li, L. A low-cost mullite-titania composite ceramic hollow fiber microfiltration membrane for highly efficient separation of oil-in-water emulsion. *Water Res.* **2016**, *90*, 277–285. [CrossRef]
201. Jame, S.A.; Zhou, Z. Electrochemical carbon nanotube filters for water and wastewater treatment. *Nanotechnol. Rev.* **2016**, *5*, 41–50. [CrossRef]
202. Gu, J.; Xiao, P.; Chen, J.; Liu, F.; Huang, Y.; Li, G.; Zhang, J.; Chen, T. Robust preparation of superhydrophobic polymer/carbon nanotube hybrid membranes for highly effective removal of oils and separation of water-in-oil emulsions. *J. Mater. Chem. A* **2014**, *2*, 15268–15272. [CrossRef]
203. Chen, X.; Hong, L.; Xu, Y.; Ong, Z.W. Ceramic pore channels with inducted carbon nanotubes for removing oil from water. *ACS Appl. Mater. Interfaces* **2012**, *4*, 1909–1918. [CrossRef]
204. Betancourt, W.Q.; Rose, J.B. Drinking water treatment processes for removal of Cryptosporidium and Giardia. *Vet. Parasitol.* **2004**, *126*, 219–234. [CrossRef]
205. Richardson, S.D. Disinfection by-products and other emerging contaminants in drinking water. *TrAC Trends Anal. Chem.* **2003**, *22*, 666–684. [CrossRef]
206. Tian, C.; Liu, R.; Liu, H.; Qu, J. Disinfection by-products formation and precursors transformation during chlorination and chloramination of highly-polluted source water: Significance of ammonia. *Water Res.* **2013**, *47*, 5901–5910. [CrossRef]
207. Hijnen, W.; Suylen, G.; Bahlman, J.; Brouwer-Hanzens, A.; Medema, G. GAC adsorption filters as barriers for viruses, bacteria and protozoan (oo) cysts in water treatment. *Water Res.* **2010**, *44*, 1224–1234. [CrossRef]
208. Zhang, S.; Shao, T.; Karanfil, T. The effects of dissolved natural organic matter on the adsorption of synthetic organic chemicals by activated carbons and carbon nanotubes. *Water Res.* **2011**, *45*, 1378–1386. [CrossRef]
209. Osman, A.I.; Farrell, C.; Ala'a, H.; Harrison, J.; Rooney, D.W. The production and application of carbon nanomaterials from high alkali silicate herbaceous biomass. *Sci. Rep.* **2020**, *10*, 2563. [CrossRef]
210. Yang, J.; Hou, B.; Wang, J.; Tian, B.; Bi, J.; Wang, N.; Li, X.; Huang, X. Nanomaterials for the removal of heavy metals from wastewater. *Nanomaterials* **2019**, *9*, 424. [CrossRef] [PubMed]
211. Srivastava, V.C.; Mall, I.D.; Mishra, I.M. Optimization of parameters for adsorption of metal ions onto rice husk ash using Taguchi's experimental design methodology. *Chem. Eng. J.* **2008**, *140*, 136–144. [CrossRef]
212. Kurniawan, T.A.; Chan, G.Y.; Lo, W.-h.; Babel, S. Comparisons of low-cost adsorbents for treating wastewaters laden with heavy metals. *Sci. Total Environ.* **2006**, *366*, 409–426. [CrossRef]
213. Lu, C.; Su, F. Adsorption of natural organic matter by carbon nanotubes. *Sep. Purif. Technol.* **2007**, *58*, 113–121. [CrossRef]
214. Ren, X.; Chen, C.; Nagatsu, M.; Wang, X. Carbon nanotubes as adsorbents in environmental pollution management: A review. *Chem. Eng. J.* **2011**, *170*, 395–410. [CrossRef]
215. Abbas, A.; Al-Amer, A.M.; Laoui, T.; Al-Marri, M.J.; Nasser, M.S.; Khraisheh, M.; Atieh, M.A. Heavy metal removal from aqueous solution by advanced carbon nanotubes: Critical review of adsorption applications. *Sep. Purif. Technol.* **2016**, *157*, 141–161.
216. Xu, J.; Cao, Z.; Zhang, Y.; Yuan, Z.; Lou, Z.; Xu, X.; Wang, X. A review of functionalized carbon nanotubes and graphene for heavy metal adsorption from water: Preparation, application, and mechanism. *Chemosphere* **2018**, *195*, 351–364. [CrossRef]
217. Yu, X.-Y.; Luo, T.; Zhang, Y.-X.; Jia, Y.; Zhu, B.-J.; Fu, X.-C.; Liu, J.-H.; Huang, X.-J. Adsorption of lead (II) on O_2-plasma-oxidized multiwalled carbon nanotubes: Thermodynamics, kinetics, and desorption. *ACS Appl. Mater. Interfaces* **2011**, *3*, 2585–2593. [CrossRef]
218. Gupta, A.; Vidyarthi, S.; Sankararamakrishnan, N. Enhanced sorption of mercury from compact fluorescent bulbs and contaminated water streams using functionalized multiwalled carbon nanotubes. *J. Hazard. Mater.* **2014**, *274*, 132–144. [CrossRef]
219. Pillay, K.; Cukrowska, E.; Coville, N. Multi-walled carbon nanotubes as adsorbents for the removal of parts per billion levels of hexavalent chromium from aqueous solution. *J. Hazard. Mater.* **2009**, *166*, 1067–1075. [CrossRef]

220. Farid, M.U.; Luan, H.-Y.; Wang, Y.; Huang, H.; An, A.K.; Khan, R.J. Increased adsorption of aqueous zinc species by Ar/O_2 plasma-treated carbon nanotubes immobilized in hollow-fiber ultrafiltration membrane. *Chem. Eng. J.* **2017**, *325*, 239–248. [CrossRef]
221. Ihsanullah; Al-Khaldi, F.A.; Abu-Sharkh, B.; Abulkibash, A.M.; Qureshi, M.I.; Laoui, T.; Atieh, M.A. Effect of acid modification on adsorption of hexavalent chromium (Cr (VI)) from aqueous solution by activated carbon and carbon nanotubes. *Desalination Water Treat.* **2016**, *57*, 7232–7244. [CrossRef]
222. Al Amer, A.M.; Laoui, T.; Abbas, A.; Al-Aqeeli, N.; Patel, F.; Khraisheh, M.; Atieh, M.A.; Hilal, N. Fabrication and antifouling behaviour of a carbon nanotube membrane. *Mater. Des.* **2016**, *89*, 549–558.
223. Bahgat, M.; Farghali, A.; El Rouby, W.; Khedr, M. Synthesis and modification of multi-walled carbon nano-tubes (MWCNTs) for water treatment applications. *J. Anal. Appl. Pyrolysis* **2011**, *92*, 307–313. [CrossRef]
224. Gupta, V.; Agarwal, S.; Saleh, T.A. Chromium removal by combining the magnetic properties of iron oxide with adsorption properties of carbon nanotubes. *Water Res.* **2011**, *45*, 2207–2212. [CrossRef]
225. Lu, C.; Chiu, H. Adsorption of zinc (II) from water with purified carbon nanotubes. *Chem. Eng. Sci.* **2006**, *61*, 1138–1145. [CrossRef]
226. Vuković, G.D.; Marinković, A.D.; Čolić, M.; Ristić, M.Đ.; Aleksić, R.; Perić-Grujić, A.A.; Uskoković, P.S. Removal of cadmium from aqueous solutions by oxidized and ethylenediamine-functionalized multi-walled carbon nanotubes. *Chem. Eng. J.* **2010**, *157*, 238–248. [CrossRef]
227. Li, J.; Chen, S.; Sheng, G.; Hu, J.; Tan, X.; Wang, X. Effect of surfactants on Pb (II) adsorption from aqueous solutions using oxidized multiwall carbon nanotubes. *Chem. Eng. J.* **2011**, *166*, 551–558. [CrossRef]
228. Addo Ntim, S.; Mitra, S. Removal of trace arsenic to meet drinking water standards using iron oxide coated multiwall carbon nanotubes. *J. Chem. Eng. Data* **2011**, *56*, 2077–2083. [CrossRef]
229. Sharma, S.; Bhattacharya, A. Drinking water contamination and treatment techniques. *Appl. Water Sci.* **2017**, *7*, 1043–1067. [CrossRef]
230. Brady-Estévez, A.S.; Kang, S.; Elimelech, M. A single-walled-carbon-nanotube filter for removal of viral and bacterial pathogens. *Small* **2008**, *4*, 481–484. [CrossRef]
231. Deng, S.; Upadhyayula, V.K.; Smith, G.B.; Mitchell, M.C. Adsorption equilibrium and kinetics of microorganisms on single-wall carbon nanotubes. *IEEE Sens. J.* **2008**, *8*, 954–962. [CrossRef]
232. Du, J.; Wang, S.; You, H.; Zhao, X. Understanding the toxicity of carbon nanotubes in the environment is crucial to the control of nanomaterials in producing and processing and the assessment of health risk for human: A review. *Environ. Toxicol. Pharmacol.* **2013**, *36*, 451–462. [CrossRef]
233. Kang, S.; Herzberg, M.; Rodrigues, D.F.; Elimelech, M. Antibacterial effects of carbon nanotubes: Size does matter! *Langmuir* **2008**, *24*, 6409–6413. [CrossRef]
234. Liu, T.; Tang, H.; Cai, X.; Zhao, J.; Li, D.; Li, R.; Sun, X. A study on bactericidal properties of Ag coated carbon nanotubes. *Nucl. Instrum. Methods Phys. Res. Sect. B Beam Interact. Mater. Atoms* **2007**, *264*, 282–286. [CrossRef]
235. Al-Khaldi, F.A.; Abusharkh, B.; Khaled, M.; Atieh, M.A.; Nasser, M.; Saleh, T.A.; Agarwal, S.; Tyagi, I.; Gupta, V.K. Adsorptive removal of cadmium (II) ions from liquid phase using acid modified carbon-based adsorbents. *J. Mol. Liq.* **2015**, *204*, 255–263.
236. Laoui, T.; Al-Amer, A.M.; Khalil, A.B.; Abbas, A.; Khraisheh, M.; Atieh, M.A. Novel anti-microbial membrane for desalination pretreatment: A silver nanoparticle-doped carbon nanotube membrane. *Desalination* **2015**, *376*, 82–93.
237. Ahmed, F.; Santos, C.M.; Mangadlao, J.; Advincula, R.; Rodrigues, D.F. Antimicrobial PVK: SWNT nanocomposite coated membrane for water purification: Performance and toxicity testing. *Water Res.* **2013**, *47*, 3966–3975. [CrossRef]
238. Aslan, S.; Deneufchatel, M.; Hashmi, S.; Li, N.; Pfefferle, L.D.; Elimelech, M.; Pauthe, E.; Van Tassel, P.R. Carbon nanotube-based antimicrobial biomaterials formed via layer-by-layer assembly with polypeptides. *J. Colloid Interface Sci.* **2012**, *388*, 268–273. [CrossRef]
239. Mostafavi, S.; Mehrnia, M.; Rashidi, A. Preparation of nanofilter from carbon nanotubes for application in virus removal from water. *Desalination* **2009**, *238*, 271–280. [CrossRef]
240. Brady-Estévez, A.S.; Nguyen, T.H.; Gutierrez, L.; Elimelech, M. Impact of solution chemistry on viral removal by a single-walled carbon nanotube filter. *Water Res.* **2010**, *44*, 3773–3780. [CrossRef]
241. Vecitis, C.D.; Zodrow, K.R.; Kang, S.; Elimelech, M. Electronic-structure-dependent bacterial cytotoxicity of single-walled carbon nanotubes. *ACS Nano* **2010**, *4*, 5471–5479. [CrossRef]
242. Akhavan, O.; Ghaderi, E. Toxicity of graphene and graphene oxide nanowalls against bacteria. *ACS Nano* **2010**, *4*, 5731–5736. [CrossRef]
243. Lyon, D.Y.; Alvarez, P.J. Fullerene water suspension (nC60) exerts antibacterial effects via ROS-independent protein oxidation. *Environ. Sci. Technol.* **2008**, *42*, 8127–8132. [CrossRef] [PubMed]
244. Chang, X.; Zhai, X.; Sun, S.; Gu, D.; Dong, L.; Yin, Y.; Zhu, Y. MnO2/g-C3N4 nanocomposite with highly enhanced supercapacitor performance. *Nanotechnology* **2017**, *28*, 135705. [CrossRef] [PubMed]
245. Li, Q.; Xu, Y.; Zheng, S.; Guo, X.; Xue, H.; Pang, H. Recent progress in some amorphous materials for supercapacitors. *Small* **2018**, *14*, 1800426. [CrossRef] [PubMed]
246. Thiagarajan, K.; Bavani, T.; Arunachalam, P.; Lee, S.J.; Theerthagiri, J.; Madhavan, J.; Pollet, B.G.; Choi, M.Y. Nanofiber NiMoO4/g-C3N4 composite electrode materials for redox supercapacitor applications. *Nanomaterials* **2020**, *10*, 392. [CrossRef]

247. Sharma, K.; Arora, A.; Tripathi, S.K. Review of supercapacitors: Materials and devices. *J. Energy Storage* **2019**, *21*, 801–825.
248. Banerjee, S.; De, B.; Sinha, P.; Cherusseri, J.; Kar, K.K. Applications of Supercapacitors. In *Handbook of Nanocomposite Supercapacitor Materials I*; Springer: Berlin/Heidelberg, Germany, 2020; pp. 341–350.
249. Vangari, M.; Pryor, T.; Jiang, L. Supercapacitors: Review of materials and fabrication methods. *J. Energy Eng.* **2013**, *139*, 72–79. [CrossRef]
250. Guan, L.; Yu, L.; Chen, G.Z. Capacitive and non-capacitive faradaic charge storage. *Electrochim. Acta* **2016**, *206*, 464–478. [CrossRef]
251. You, B.; Wang, L.; Yao, L.; Yang, J. Three dimensional N-doped graphene–CNT networks for supercapacitor. *Chem. Commun.* **2013**, *49*, 5016–5018. [CrossRef]
252. Huang, Y.; Liang, J.; Chen, Y. An overview of the applications of graphene-based materials in supercapacitors. *Small* **2012**, *8*, 1805–1834. [CrossRef]
253. Jung, S.; Myung, Y.; Kim, B.N.; Kim, I.G.; You, I.-K.; Kim, T. Activated biomass-derived graphene-based carbons for supercapacitors with high energy and power density. *Sci. Rep.* **2018**, *8*, 1–8. [CrossRef]
254. Kumar, R.; Sahoo, S.; Joanni, E.; Singh, R.K.; Maegawa, K.; Tan, W.K.; Kawamura, G.; Kar, K.K.; Matsuda, A. Heteroatom doped graphene engineering for energy storage and conversion. *Mater. Today* **2020**, *39*, 47–65. [CrossRef]
255. Zhang, L.L.; Zhao, X. Carbon-based materials as supercapacitor electrodes. *Chem. Soc. Rev.* **2009**, *38*, 2520–2531. [CrossRef]
256. Barisci, J.N.; Wallace, G.G.; Baughman, R.H. Electrochemical characterization of single-walled carbon nanotube electrodes. *J. Electrochem. Soc.* **2000**, *147*, 4580. [CrossRef]
257. Yu, D.; Qian, Q.; Wei, L.; Jiang, W.; Goh, K.; Wei, J.; Zhang, J.; Chen, Y. Emergence of fiber supercapacitors. *Chem. Soc. Rev.* **2015**, *44*, 647–662. [CrossRef]
258. Niu, C.; Sichel, E.K.; Hoch, R.; Moy, D.; Tennent, H. High power electrochemical capacitors based on carbon nanotube electrodes. *Appl. Phys. Lett.* **1997**, *70*, 1480–1482. [CrossRef]
259. Cherusseri, J.; Sharma, R.; Kar, K.K. Nanotechnology advancements on carbon nanotube/polypyrrole composite electrodes for supercapacitors. In *Handbook of Polymer Nanocomposites. Processing, Performance and Application*; Springer: Berlin/Heidelberg, Germany, 2015; pp. 479–510.
260. Pan, H.; Li, J.; Feng, Y. Carbon nanotubes for supercapacitor. *Nanoscale Res. Lett.* **2010**, *5*, 654–668. [CrossRef]
261. Frackowiak, E.; Metenier, K.; Bertagna, V.; Beguin, F. Supercapacitor electrodes from multiwalled carbon nanotubes. *Appl. Phys. Lett.* **2000**, *77*, 2421–2423. [CrossRef]
262. Gayner, C.; Kar, K.K.; Kim, W. Recent progress and futuristic development of PbSe thermoelectric materials and devices. *Mater. Today Energy* **2018**, *9*, 359–376. [CrossRef]
263. Ahn, H.-J.; Sohn, J.I.; Kim, Y.-S.; Shim, H.-S.; Kim, W.B.; Seong, T.-Y. Electrochemical capacitors fabricated with carbon nanotubes grown within the pores of anodized aluminum oxide templates. *Electrochem. Commun.* **2006**, *8*, 513–516. [CrossRef]
264. Jung, M.; Kim, H.-G.; Lee, J.-K.; Joo, O.-S.; Mho, S.-i. EDLC characteristics of CNTs grown on nanoporous alumina templates. *Electrochim. Acta* **2004**, *50*, 857–862. [CrossRef]
265. Banerjee, S.; Sharma, R.; Kar, K.K. Nanocomposites based on carbon nanomaterials and electronically nonconducting polymers. In *Composite Materials*; Springer: Berlin/Heidelberg, Germany, 2017; pp. 251–280.
266. Li, C.; Wang, D.; Liang, T.; Wang, X.; Wu, J.; Hu, X.; Liang, J. Oxidation of multiwalled carbon nanotubes by air: Benefits for electric double layer capacitors. *Powder Technol.* **2004**, *142*, 175–179. [CrossRef]
267. Hola, K.; Bourlinos, A.B.; Kozak, O.; Berka, K.; Siskova, K.M.; Havrdova, M.; Tucek, J.; Safarova, K.; Otyepka, M.; Giannelis, E.P. Photoluminescence effects of graphitic core size and surface functional groups in carbon dots: COO− induced red-shift emission. *Carbon* **2014**, *70*, 279–286. [CrossRef]
268. Wang, J.; Qiu, J. A review of carbon dots in biological applications. *J. Mater. Sci.* **2016**, *51*, 4728–4738. [CrossRef]
269. Yang, Y.; Wu, D.; Han, S.; Hu, P.; Liu, R. Bottom-up fabrication of photoluminescent carbon dots with uniform morphology via a soft–hard template approach. *Chem. Commun.* **2013**, *49*, 4920–4922. [CrossRef]
270. Zhao, Q.-L.; Zhang, Z.-L.; Huang, B.-H.; Peng, J.; Zhang, M.; Pang, D.-W. Facile preparation of low cytotoxicity fluorescent carbon nanocrystals by electrooxidation of graphite. *Chem. Commun.* **2008**, *41*, 5116–5118. [CrossRef]
271. Duran, N.; Simoes, M.B.; de Moraes, A.; Favaro, W.J.; Seabra, A.B. Nanobiotechnology of carbon dots: A review. *J. Biomed. Nanotechnol.* **2016**, *12*, 1323–1347. [CrossRef]
272. Liang, Q.; Ma, W.; Shi, Y.; Li, Z.; Yang, X. Easy synthesis of highly fluorescent carbon quantum dots from gelatin and their luminescent properties and applications. *Carbon* **2013**, *60*, 421–428. [CrossRef]
273. Zhu, L.; Shen, D.; Wu, C.; Gu, S. State-of-the-Art on the Preparation, Modification, and Application of Biomass-Derived Carbon Quantum Dots. *Ind. Eng. Chem. Res.* **2020**, *59*, 22017–22039. [CrossRef]
274. Liu, R.; Gao, M.; Zhang, J.; Li, Z.; Chen, J.; Liu, P.; Wu, D. An ionic liquid promoted microwave-hydrothermal route towards highly photoluminescent carbon dots for sensitive and selective detection of iron (III). *RSC Adv.* **2015**, *5*, 24205–24209. [CrossRef]
275. Agbor, V.B.; Cicek, N.; Sparling, R.; Berlin, A.; Levin, D.B. Biomass pretreatment: Fundamentals toward application. *Biotechnol. Adv.* **2011**, *29*, 675–685. [CrossRef] [PubMed]
276. Ferreira, R.; Garcia, H.; Sousa, A.F.; Guerreiro, M.; Duarte, F.J.; Freire, C.S.; Calhorda, M.J.; Silvestre, A.J.; Kunz, W.; Rebelo, L.P.N. Unveiling the dual role of the cholinium hexanoate ionic liquid as solvent and catalyst in suberin depolymerisation. *RSC Adv.* **2014**, *4*, 2993–3002. [CrossRef]

277. Mandal, T.K.; Parvin, N. Rapid detection of bacteria by carbon quantum dots. *J. Biomed. Nanotechnol.* **2011**, *7*, 846–848. [CrossRef] [PubMed]
278. Ray, S.; Saha, A.; Jana, N.R.; Sarkar, R. Fluorescent carbon nanoparticles: Synthesis, characterization, and bioimaging application. *J. Phys. Chem. C* **2009**, *113*, 18546–18551. [CrossRef]
279. Choudhury, M.; Nath, S.; Chakdar, D.; Gope, G.; Nath, R. Acetone sensing of ZnO quantum dots embedded in polyvinyl alcohol matrix. *Adv. Sci. Lett.* **2010**, *3*, 6–9. [CrossRef]
280. Thongsai, N.; Tanawannapong, N.; Praneerad, J.; Kladsomboon, S.; Jaiyong, P.; Paoprasert, P. Real-time detection of alcohol vapors and volatile organic compounds via optical electronic nose using carbon dots prepared from rice husk and density functional theory calculation. *Colloids Surf. A Physicochem. Eng. Asp.* **2019**, *560*, 278–287. [CrossRef]
281. Wu, Z.L.; Zhang, P.; Gao, M.X.; Liu, C.F.; Wang, W.; Leng, F.; Huang, C.Z. One-pot hydrothermal synthesis of highly luminescent nitrogen-doped amphoteric carbon dots for bioimaging from Bombyx mori silk–natural proteins. *J. Mater. Chem. B* **2013**, *1*, 2868–2873. [CrossRef]
282. Pal, T.; Mohiyuddin, S.; Packirisamy, G. Facile and green synthesis of multicolor fluorescence carbon dots from curcumin: In vitro and in vivo bioimaging and other applications. *ACS Omega* **2018**, *3*, 831–843. [CrossRef]
283. Abidin, N.H.Z.; Wongso, V.; Hui, K.C.; Cho, K.; Sambudi, N.S.; Ang, W.L.; Saad, B. The effect of functionalization on rice-husks derived carbon quantum dots properties and cadmium removal. *J. Water Process Eng.* **2020**, *38*, 101634. [CrossRef]
284. Naik, J.P.; Sutradhar, P.; Saha, M. Molecular scale rapid synthesis of graphene quantum dots (GQDs). *J. Nanostructure Chem.* **2017**, *7*, 85–89. [CrossRef]
285. Wang, Z.; Liu, J.; Wang, W.; Wei, Z.; Wang, F.; Gong, P.; Wang, J.; Li, N.; Liu, B.; Zhang, Z. Photoluminescent carbon quantum dot grafted silica nanoparticles directly synthesized from rice husk biomass. *J. Mater. Chem. B* **2017**, *5*, 4679–4689. [CrossRef]
286. Wongso, V.; Sambudi, N.; Sufian, S.; Abdullah, B. The effect of pH in the synthesis of carbon quantum dots from rice husk on their photoluminescence properties. *IOP Conf. Ser. Earth Environ. Sci.* **2019**, *268*, 012087. [CrossRef]
287. Shen, J.; Zhu, Y.; Yang, X.; Li, C. Graphene quantum dots: Emergent nanolights for bioimaging, sensors, catalysis and photovoltaic devices. *Chem. Commun.* **2012**, *48*, 3686–3699. [CrossRef]
288. Zhang, Z.; Zhang, J.; Chen, N.; Qu, L. Graphene quantum dots: An emerging material for energy-related applications and beyond. *Energy Environ. Sci.* **2012**, *5*, 8869–8890. [CrossRef]
289. Li, K.; Zhao, X.; Wei, G.; Su, Z. Recent advances in the cancer bioimaging with graphene quantum dots. *Curr. Med. Chem.* **2018**, *25*, 2876–2893. [CrossRef]
290. Feng, L.-L.; Wu, Y.-X.; Zhang, D.-L.; Hu, X.-X.; Zhang, J.; Wang, P.; Song, Z.-L.; Zhang, X.-B.; Tan, W. Near infrared graphene quantum dots-based two-photon nanoprobe for direct bioimaging of endogenous ascorbic acid in living cells. *Anal. Chem.* **2017**, *89*, 4077–4084. [CrossRef]
291. Ananthanarayanan, A.; Wang, Y.; Routh, P.; Sk, M.A.; Than, A.; Lin, M.; Zhang, J.; Chen, J.; Sun, H.; Chen, P. Nitrogen and phosphorus co-doped graphene quantum dots: Synthesis from adenosine triphosphate, optical properties, and cellular imaging. *Nanoscale* **2015**, *7*, 8159–8165. [CrossRef]
292. Roy, P.; Periasamy, A.P.; Chuang, C.; Liou, Y.-R.; Chen, Y.-F.; Joly, J.; Liang, C.-T.; Chang, H.-T. Plant leaf-derived graphene quantum dots and applications for white LEDs. *New J. Chem.* **2014**, *38*, 4946–4951. [CrossRef]
293. Rahbari, R.; Sheahan, T.; Modes, V.; Collier, P.; Macfarlane, C.; Badge, R.M. A novel L1 retrotransposon marker for HeLa cell line identification. *Biotechniques* **2009**, *46*, 277–284. [CrossRef] [PubMed]
294. Ngu, P.Z.Z.; Chia, S.P.P.; Fong, J.F.Y.; Ng, S.M. Synthesis of carbon nanoparticles from waste rice husk used for the optical sensing of metal ions. *New Carbon Mater.* **2016**, *31*, 135–143. [CrossRef]
295. Liu, Y.; Deng, M.; Zhu, T.; Tang, X.; Han, S.; Huang, W.; Shi, Y.; Liu, A. The synthesis of water-dispersible zinc doped AgInS2 quantum dots and their application in Cu2+ detection. *J. Lumin.* **2017**, *192*, 547–554. [CrossRef]
296. Kahrizi, P.; Mohseni-Shahri, F.S.; Moeinpour, F. Adsorptive removal of cadmium from aqueous solutions using $NiFe_2O_4$/hydroxyapatite/graphene quantum dots as a novel nano-adsorbent. *J. Nanostructure Chem.* **2018**, *8*, 441–452. [CrossRef]
297. Wang, Z.; Long, P.; Feng, Y.; Qin, C.; Feng, W. Surface passivation of carbon dots with ethylene glycol and their high-sensitivity to Fe^{3+}. *RSC Adv.* **2017**, *7*, 2810–2816. [CrossRef]
298. Abdelsalam, H.; Teleb, N.; Yahia, I.; Zahran, H.; Elhaes, H.; Ibrahim, M. First principles study of the adsorption of hydrated heavy metals on graphene quantum dots. *J. Phys. Chem. Solids* **2019**, *130*, 32–40. [CrossRef]
299. Qiao, X.; Huang, W.; Bian, Y. Effective removal of cadmium ions from a simulated gastrointestinal fluid by Lentinus edodes. *Int. J. Environ. Res. Public Health* **2014**, *11*, 12486–12498. [CrossRef]
300. Shtepliuk, I.; Caffrey, N.M.; Iakimov, T.; Khranovskyy, V.; Abrikosov, I.A.; Yakimova, R. On the interaction of toxic Heavy Metals (Cd, Hg, Pb) with graphene quantum dots and infinite graphene. *Sci. Rep.* **2017**, *7*, 1–17. [CrossRef]
301. Zhao, L.; Wang, Y.; Zhao, X.; Deng, Y.; Xia, Y. Facile synthesis of nitrogen-doped carbon quantum dots with chitosan for fluorescent detection of Fe^{3+}. *Polymers* **2019**, *11*, 1731. [CrossRef]
302. Yang, T.; Li, Y.-K.; Chen, M.-L.; Wang, J.-H. Supported carbon dots decorated with metallothionein for selective cadmium adsorption and removal. *Chin. Chem. Lett.* **2015**, *26*, 1496–1501. [CrossRef]
303. Liu, B.R.; Li, J.-F.; Lu, S.-W.; Lee, H.-J.; Huang, Y.-W.; Shannon, K.B.; Aronstam, R.S. Cellular internalization of quantum dots noncovalently conjugated with arginine-rich cell-penetrating peptides. *J. Nanosci. Nanotechnol.* **2010**, *10*, 6534–6543. [CrossRef]

304. Ryman-Rasmussen, J.P.; Riviere, J.E.; Monteiro-Riviere, N.A. Variables influencing interactions of untargeted quantum dot nanoparticles with skin cells and identification of biochemical modulators. *Nano Lett.* **2007**, *7*, 1344–1348. [CrossRef]
305. Liu, H.Y.; Vu, T.Q. Identification of quantum dot bioconjugates and cellular protein co-localization by hybrid gel blotting. *Nano Lett.* **2007**, *7*, 1044–1049. [CrossRef]
306. Gratieri, T.; Schaefer, U.F.; Jing, L.; Gao, M.; Kostka, K.-H.; Lopez, R.F.; Schneider, M. Penetration of quantum dot particles through human skin. *J. Biomed. Nanotechnol.* **2010**, *6*, 586–595. [CrossRef]
307. Mortensen, L.J.; Ravichandran, S.; Zheng, H.; DeLouise, L.A. Progress and challenges in quantifying skin permeability to nanoparticles using a quantum dot model. *J. Biomed. Nanotechnol.* **2010**, *6*, 596–604. [CrossRef]
308. Zheng, H.; Chen, G.; DeLouise, L.A.; Lou, Z. Detection of the cancer marker CD146 expression in melanoma cells with semiconductor quantum dot label. *J. Biomed. Nanotechnol.* **2010**, *6*, 303–311. [CrossRef]
309. Zhang, S.; Li, J.; Zeng, M.; Xu, J.; Wang, X.; Hu, W. Polymer nanodots of graphitic carbon nitride as effective fluorescent probes for the detection of Fe^{3+} and Cu^{2+} ions. *Nanoscale* **2014**, *6*, 4157–4162. [CrossRef]
310. Feng, Y.; Zhong, D.; Miao, H.; Yang, X. Carbon dots derived from rose flowers for tetracycline sensing. *Talanta* **2015**, *140*, 128–133. [CrossRef]
311. Canhoto, O.; Pinzari, F.; Fanelli, C.; Magan, N. Application of electronic nose technology for the detection of fungal contamination in library paper. *Int. Biodeterior. Biodegrad.* **2004**, *54*, 303–309. [CrossRef]
312. Thaler, E.R.; Kennedy, D.W.; Hanson, C.W. Medical applications of electronic nose technology: Review of current status. *Am. J. Rhinol.* **2001**, *15*, 291–295. [CrossRef]
313. Schaller, E.; Bosset, J.O.; Escher, F. 'Electronic noses' and their application to food. *LWT-Food Sci. Technol.* **1998**, *31*, 305–316. [CrossRef]
314. Zhang, J.; Yu, S.-H. Carbon dots: Large-scale synthesis, sensing and bioimaging. *Mater. Today* **2016**, *19*, 382–393. [CrossRef]